



UFBA

UNIVERSIDADE FEDERAL DA BAHIA
ESCOLA POLITÉCNICA
PROGRAMA DE PÓS GRADUAÇÃO EM
ENGENHARIA INDUSTRIAL - PEI

DOUTORADO EM ENGENHARIA INDUSTRIAL

LUCAS NAO HORIUCHI

DEVELOPMENT OF SUSTAINABLE HYBRID
POLY (BUTYLENE SUCCINATE) ECO-
COMPOSITE FOR AGRICULTURAL
PACKAGING APPLICATIONS





UNIVERSIDADE FEDERAL DA BAHIA
ESCOLA POLITÉCNICA
PROGRAMA DE PÓS-GRADUAÇÃO EM ENGENHARIA INDUSTRIAL

**DEVELOPMENT OF SUSTAINABLE HYBRID POLY (BUTYLENE
SUCCINATE) ECO-COMPOSITE FOR AGRICULTURAL PACKAGING
APPLICATIONS**

LUCAS NAO HORIUCHI

Salvador

2025

LUCAS NAO HORIUCHI

**DEVELOPMENT OF SUSTAINABLE HYBRID POLY (BUTYLENE
SUCCINATE) ECO-COMPOSITE FOR AGRICULTURAL PACKAGING
APPLICATIONS**

Tese apresentada ao Programa de Pós-graduação em Engenharia Industrial, da Escola Politécnica, Universidade Federal da Bahia, como requisito para obtenção do grau de Doutor em Engenharia Industrial.

Orientadora: Profa. Dra. Rosana Lopes Lima Fialho

Coorientadora: Profa. Dra. Joyce Batista Azevedo

Salvador

2025

H811 Horiuchi, Lucas Nao.

Development of sustainable hybrid poly (butylene succinate) eco-composite for agricultural packaging applications / Lucas Nao Horiuchi. – Salvador, 2025.

119f.: il. color.

Orientadora: Profa. Dra. Rosana Lopes Lima Fialho.

Coorientadora: Prof. Dra. Joyce Batista Azevedo.

Tese (doutorado) – Curso de Pós-Graduação em Engenharia Industrial, Escola Politécnica, Universidade Federal da Bahia, 2025.

1. Poli(butileno succinato). 2. Canabrava - fibra. 3. Lignina. 4. Sepiolita. 5. Embalagens. I. Fialho, Rosana Lopes Lima. II. Azevedo, Joyce Batista. III. Universidade Federal da Bahia. IV. Título.

CDD: 688.8


Ficha catalográfica elaborada pela Biblioteca Bernadete
Sinay Neves, Escola Politécnica – UFBA.

**“DEVELOPMENT OF SUSTAINABLE HYBRID POLY (BUTYLENE SUCCINATE)
ECO-COMPOSITE FOR AGRICULTURAL PACKAGING APPLICATIONS”.**


LUCAS NAO HORIUCHI

Tese submetida ao corpo docente do programa de pós-graduação em Engenharia Industrial da Universidade Federal da Bahia como parte dos requisitos necessários para a obtenção do grau de doutor em Engenharia Industrial.


Examinada por:

Documento assinado digitalmente
 **ROSANA LOPES LIMA FIALHO**
Data: 26/08/2025 16:31:27-0300
Verifique em <https://validar.iti.gov.br>


Prof^a. Dr^a. Rosana Lopes Lima Fialho _____
Doutora em Engenharia Química pela Universidade Federal do Rio de Janeiro, Brasil,
1998

Documento assinado digitalmente
 **JOYCE BATISTA AZEVEDO**
Data: 26/08/2025 12:35:15-0300
Verifique em <https://validar.iti.gov.br>


Prof^a. Dr^a Joyce Batista Azevedo _____
Doutora em Ciência e Engenharia de Materiais pela Universidade Federal de Campina
Grande, Brasil, 2013

Documento assinado digitalmente
 **JANIA BETANIA ALVES DA SILVA**
Data: 25/08/2025 14:23:50-0300
Verifique em <https://validar.iti.gov.br>


Prof^a. Dr^a. Jânia Betania Alves da Silva _____
Doutora em Engenharia Química pela Universidade Federal da Bahia, Brasil, 2013

Documento assinado digitalmente
 **LUCIANO PISANU**
Data: 26/08/2025 13:47:11-0300
Verifique em <https://validar.iti.gov.br>

Prof. Dr. Luciano Pisanu _____
Doutor em Engenharia Industrial pela Universidade Federal da Bahia, Brasil, 2018

Documento assinado digitalmente
 **MARCELO MASSAYOSHI UEKI**
Data: 25/08/2025 09:04:08-0300
Verifique em <https://validar.iti.gov.br>

Prof. Dr. Marcelo Massayoshi Ueki _____
Doutor em Ciência e Engenharia de Materiais pela Universidade Federal de São Carlos,
Brasil, 2003

Documento assinado digitalmente
 **RENATA BARBOSA**
Data: 23/08/2025 19:15:37-0300
Verifique em <https://validar.iti.gov.br>

Prof^a. Dr^a. Renata Barbosa _____
Doutora em Engenharia de Processos pela Universidade Federal de Campina Grande,
Brasil, 2009

Salvador, BA - Brasil
agosto/2025

I dedicate this work to

Shoichi Horiuchi (*in memoriam*) and Michiko Horiuchi, my father and mother.

And to Luana and Gabriel Horiuchi, my wife and son.

“Knowledge is not what you know, but what you do
with what you know.”

Aldous Huxley

Acknowledgments

I am grateful to all those who contributed to the completion of this doctoral work.

I would like to thank my advisor, professor Rosana Fialho, who accepted the challenge of supervising me, even without knowing me personally and during the pandemic.

I also thank Professor Joyce Azevedo, my co-advisor, with whom I have worked before and who supported, advised and guided me.

To the Postgraduate Program in Industrial Engineering (PEI) at UFBA, for the infrastructure, academic quality, friendliness of the professors, researchers, technical and administrative staff, especially, Professor Elaine, Tatiane, Edilson, Valdinei, Roberta and Cris.

To Mitsubishi Chemical Co, on behalf of Waldir, Carol and Haroldo, for the generous donation of PBS resin, for the valuable discussions on the research topics, and for the opportunity to participate in Feiplastic 2023.

To Selma (from ABECIM, Associação Beneficente Educacional e Cultural de Ilha de Maré) for her kindness and supply of Canabrava fiber.

To Professor Raquel Barbosa, Professor César Vicerias and Professor Fátima Garcia-Villen, for their support in conducting the experiments in Spain, as well as their guidance. And a special thanks to Professor Raquel for her valuable advice on research paper submission.

To my colleagues at Senai Cimatec (Pollyana, Marcela, Pisanu, Erick, Badaró, Talyta, Igor, Adriano, and Marco) who assisted me with analyses and technical discussions.

To my friends, Professor Ueki and Professor Zora (UFS), for their availability and support in the production (injection) of test specimens for testing.

To Professor Renata Barbosa and Fábio Delano (UFPI), for the tests and discussions on biodegradability.

To my friends and colleagues Rita Marinho, Luis Jorge, Albani, Rodrigo, Vini, Mariana, Paulo for their support and encouragement, and especially to Ana Paula Gonçalves for the tips on creating graphs, technical and analytical discussions.

To my parents (Shoichi and Michiko) who once dreamed of coming to Brazil and starting a family here, while staying true to their values, respect for others, and spirit of friendship—principles I carry with me and have sought to reflect throughout this work. And the last, for my wife (Luana) and son (Gabriel) for their constant encouragement and inspiration.

To all my family, near or far, who have always encouraged me.

Sincere thanks to everyone who, in one way or another, helped make this enriching experience a meaningful part of my personal and professional growth.

This work was carried out with the support of the “Coordenação de Aperfeiçoamento de Pessoal de Nível Superior” – Brazil (CAPES) – financing code 001.

Abstract

The growing concern over plastic pollution, particularly from non-biodegradable packaging materials used in agriculture, has driven the search for sustainable alternatives. Poly(butylene succinate) (PBS) is a promising bio-based aliphatic polyester due to its biodegradability and compatibility with conventional processing techniques. However, its high cost still limits its use in low-value applications such as seedling trays and agricultural packaging. In this context, the present study aimed to develop cost-effective, high-performance PBS-based hybrid eco-composites reinforced with Canabrava natural fiber (*Gynerium sagittatum*) (Cana), kraft lignin, and sepiolite or montmorillonite clay and epoxidized soybean oil. The goal was to reduce the overall cost, enhance functional properties, and provide an environmentally responsible alternative material to conventional non-biodegradable thermoplastics. Canabrava fiber, an underutilized lignocellulosic residue from Brazilian handicraft production, was used as sustainable reinforcement and processed by simple mechanical methods without chemical treatments. Lignin, a byproduct of the pulp and paper industry, was incorporated to improve thermal stability, melt flow, and biodegradability control. Sepiolite, a natural fibrous clay with high surface area, was added to improve thermal and mechanical performance. Epoxidized soybean oil (ESB) was also evaluated as a compatibilizer and plasticizer to mitigate the brittleness typically observed in fiber-reinforced biopolymers. The research was conducted in two experimental phases. In the first, PBS/Cana composites containing lignin and clays (sepiolite or montmorillonite) were formulated and characterized through mechanical, thermal, and structural analyses (FTIR, XRD, SEM). In the second phase, a design of experiments (DOE) approach was applied to optimize formulations by evaluating the individual and synergistic effects of lignin, sepiolite, and ESB on properties such as melt flow rate, stiffness, toughness, and soil biodegradability. The results showed that Canabrava fiber significantly increased PBS stiffness and yield strength, while lignin improved melt flow and thermal stability. Sepiolite enhanced dispersion and interfacial interaction with the polymer matrix, resulting in improved mechanical performance. Although epoxidized soybean oil (ESB) was primarily incorporated to enhance fiber-polymer compatibility and secondarily to improve ductility, its contribution to increased ductility was not significant, attributed to its limited solubility in PBS. Optimized formulations showed a good balance between mechanical performance, biodegradation behavior, and cost. The developed composites exhibited competitive technical properties compared to fossil-based polyolefins, while offering a fully biodegradable and renewable alternative. This work advances eco-composite technology by integrating low-cost biomass residues and natural additives into biopolymers, aligning with circular economy principles and sustainable development goals. The properties achieved by the bio composite are comparable to those of polyolefin resins, making it a promising candidate for applications in agriculture, for example.

Keywords:

Poly(butylene succinate); Eco-composites; Canabrava fiber; Sepiolite; Lignin; Epoxidized soybean oil.

Resumo

A crescente preocupação com a poluição plástica, especialmente proveniente de materiais de embalagem não biodegradáveis utilizados na agricultura, tem impulsionado a busca por alternativas sustentáveis. O poli(butileno succinato) (PBS) é um poliéster alifático de base renovável promissor devido à sua biodegradabilidade, compatibilidade com técnicas convencionais de processamento. No entanto, seu elevado custo ainda limita aplicações em produtos de menor valor agregado, como bandejas para mudas e embalagens agrícolas. Neste contexto, o presente estudo teve como objetivo desenvolver eco compósitos híbridos de PBS com desempenho técnico e custo reduzido, reforçados com fibra natural de Canabrava (*Gynerium sagittatum*) (Cana), lignina *kraft*, argila sepiolita ou montmorilonita e óleo de soja epoxidado. A proposta foi diminuir o custo final do material, melhorar suas propriedades funcionais e oferecer uma alternativa ambientalmente responsável aos polímeros convencionais não-biodegradáveis. A fibra de Canabrava, um resíduo lignocelulósico subutilizado proveniente do artesanato em comunidades brasileiras, foi empregada como reforço sustentável e processada por métodos mecânicos simples, sem tratamentos químicos. A lignina, subproduto da indústria de celulose, foi incorporada para melhorar a estabilidade térmica, a fluidez do fundido e o controle da biodegradação. A sepiolita, argila fibrosa natural com alta área superficial, foi usada para reforçar o compósito e aprimorar seu desempenho térmico e mecânico. Também foi avaliado o uso de óleo de soja epoxidado (ESB) como plastificante e compatibilizante, a fim de reduzir a fragilidade típica de biopolímeros reforçados com fibras. A pesquisa foi conduzida em duas fases experimentais. Na primeira, compósitos de PBS/Cana contendo lignina e argilas (sepiolita e montmorilonita) foram formulados e caracterizados por análises mecânicas, térmicas e estruturais (FTIR, DRX, MEV). Na segunda fase, aplicou-se planejamento experimental (DOE) para otimização das formulações, avaliando os efeitos individuais e combinados de lignina, sepiolita e ESB sobre propriedades como fluidez, rigidez, tenacidade e biodegradabilidade em solo. Os resultados mostraram que a adição de fibra de Canabrava aumentou significativamente a rigidez e a resistência ao escoamento do PBS, enquanto a lignina melhorou a fluidez e a estabilidade térmica. A sepiolita favoreceu a dispersão e a interação interfacial com a matriz polimérica, resultando em melhores propriedades mecânicas. Embora o óleo de soja epoxidado (ESB) tenha sido incorporado principalmente para melhorar a compatibilidade fibra-polímero e, secundariamente, para aumentar a ductilidade, sua contribuição para uma maior ductilidade não foi significativa, atribuída à sua limitada solubilidade no PBS. As formulações otimizadas apresentaram bom equilíbrio entre desempenho mecânico, perfil de biodegradação e custo. Os compósitos desenvolvidos mostraram desempenho técnico competitivo frente a resinas de origem fóssil como poliolefinas, oferecendo uma alternativa renovável e biodegradável. Este trabalho avança na tecnologia de eco compósitos ao integrar resíduos de biomassa e aditivos naturais a biopolímeros, alinhando-se à economia circular e aos objetivos de desenvolvimento sustentável. As propriedades alcançadas pelo biocompósito são comparáveis às das resinas poliolefinas, tornando-o um candidato promissor para aplicações na agricultura, por exemplo.

Palavras chaves: Poli(butileno succinato); Eco-compósito; Fibra de Canabrava; Lignina; Sepiolita; Óleo de soja epoxidado.

List of figures

Figure 1: Molecular structure of PBS.....	24
Figure 2: Synthesis reaction of PBS from SA and BDO (Miao and Hamad, 2013).....	24
Figure 3: Schematic representation of the reactions of epoxy and maleic anhydride groups in PBS/natural fiber composites. Adapted of (Liminana et al., 2018)*.....	31
Figure 4: Graphical abstract of the first article presented at Applied Clay Science.....	35
Figure 5: FT-IR spectrum of (A) PBS-MMT composites; (B) PBS-SEP composites. (C) and (D) shows that a shoulder appeared at $1602\text{-}1608\text{ cm}^{-1}$ in the composites.....	45
Figure 6: Tensile test curves for Neat PBS and composites.	46
Figure 7: Flexural test curves (each curve is an average of 5 samples tested).	49
Figure 8: (A) Thermogravimetric Analysis (TGA), and (B) Differential Thermogravimetric (DTG) Analysis.	50
Figure 9. Comprehensive DSC Analysis of PBS Composites: (A) Full Thermal Profiles; (B) Detailed View of the Melting Temperature Region; (C) Detailed View of Crystallization Region.	52
Figure 10: XRD diagrams of (A) MMT, PBS and composite; (B) SEP, PBS and composite.....	54
Figure 11: SEM images and EDS and microanalysis of composites. (A) PBS/Cana. (B) PBS/Cana/Lig. (C) PBS/Cana/Lig/MMT2.5. (D) PBS/Cana/Lig/SEP2.5. (E) EDS microanalysis for PBS/Cana/Lig/MMT2.5. (F) EDS microanalysis for PBS/Cana/Lig/SEP2.5.	55
Figure 12: Optical microscope image of Cana fiber. A) 1x magnification; B) 50x magnification.	57
Figure 13: EDS mapping image for PBS/Cana/Lig/MMT2.5.....	57
Figure 14: Graphical abstract of second article published at Journal of Applied Polymer Science.....	58
Figure 15: Granulated samples of composite formulations. *2PBS-00 = Neat PBS. **2PBS-12 = PBS/CANA (30 wt.%).	72
Figure 16: (A) Cube plot and (B) Main effects plot of MFR (190°C, 2.16 kg).....	75
Figure 17: Biodegradation test in soil after 30 and 90 days, for Neat PBS and for composite (2PBS-09 = DOE 0 0 0). (A) Weight loss graphics. (B) Surface image of samples before and after biodegradation test.	77

Figure 18: FT-IR spectrum of (A) PBS and raw materials; (B) PBS, SEP and composites. Composites spectra show a shoulder at 1602-1608 cm^{-1} denoting good interaction SEP-PBS.....	79
Figure 19: Tensile test results. (A) Surface plot of Young's modulus. (B) Cube plot of tensile strength. (C) Cube plot of tensile yield. (D) Tensile test curve of Neat PBS and composites.	82
Figure 20: (A) Surface plot of Flexural modulus, (B) Cube plot of flexural strain, and (C) Flexural test curves.....	85
Figure 21: Main effects plot of LIG-SEP-ESB for (A) impact strength and (B) Shore D.	87
Figure 22: (A) Thermogravimetric Analysis (TGA), (B) Differential Thermogravimetric (DTG), (C) Main effects plot on $T_{WL5\%}$, (D) Cube plot of $T_{WL90\%}$ for PBS composites.	89
Figure 23: DSC analysis results of PBS composites: (A) Full thermal profiles; (B) Detailed view of crystallization region; (C) Detailed view of the melting temperature region; (D) Cube plot for degree of crystallinity (X_c); (E) Cube plot for melting temperature.	94
Figure 24: (A) XRD diagrams and (B) Density of SEP and PBS composites. Note: Tukey statistical test, mean value with same letters do not differ at the 5% significance level. The letters are in descending order of mean values. Number of replicates, $n=5$..	96
Figure 25: SEM images and EDS analysis of PBS composites.	99
Figure 26: Schematic of the reactions of epoxy group of ESB and hydroxyl groups of PBS and cellulose (applicable for CANA fiber). Adapted from Liminana, et al., 2018*.	100

List of Tables

Table 1: Thermal properties of PBS and other aliphatic polyesters (Miao and Hamad, 2013).....	24
Table 2: Formulation of bio-composites.....	40
Table 3: MFR results of PBS and composites.	43
Table 4: Tensile parameters results.....	46
Table 5: Impact resistance and hardness Shore D results.....	48
Table 6 Flexural parameters resulted of tests.	49
Table 7: Degradation results parameters of TGA analysis.	50
Table 8: parameters result of DSC analysis.....	53
Table 9: DOE formulation of PBS bio-composites.	65
Table 10: Tensile test results.....	80
Table 11: Flexural test, impact resistance and hardness Shore D results.	83
Table 12: Degradation results of TGA analysis.....	90
Table 13: parameters result of DSC analysis.....	94
Table 14: interlayer space (<i>d-value</i>) and interlayer space variation (Δd) for SEP reflections planes, in SEP and composites.	96

List of Acronyms and Abbreviations

ρ_f -Density of fluid (g/cm³)
 ΔH_m -Melting enthalpy of polymer (J.g⁻¹)
 ρ_s -Density of the samples (g/cm³)
 ΔH_m° - Enthalpy of fusion of polymer 100% crystalline (J.g⁻¹)
ANOVA-Analysis of Variance statistical test
ASTM- American Society for Testing and Materials
BDO-1,4-Butanediol
CANA or **Cana**-Canabrava (*Gynerium sagittatum*) natural fiber
DOE-Design of experiment
DSC-Differential scanning calorimetry
DTG-Differential thermogravimetry
EP440L-Braskem's polypropylene resin
ESB_Epoxydized soybean oil
FT-IR-Fourier transformed infrared
ISO-International Standard Organization
LIG or **Lig**-Lignin
 M_0 - Initial mass value (g)
 M_f - Final mass value (g)
MFR-Melt flow rate (or melt flow index)
MMT- Montmorillonite
PBS – Poly (butylene succinate)
PTT MCC **Biochem**- Bio-PBS producer, joint venture PTT (Thailand) and Mitsubishi Chemical Co.
SA- Succinic acid
SEM-EDS-Scanning electron microscopy – energy dispersive spectroscopy
SEM-Scanning electron microscopy
SEP- Sepiolite
 T_c -Temperature of crystallization (°C)
 T_d -Temperature at peak of mass loss (°C)
TGA-Thermogravimetric analysis
 T_g -Temperature of glass transition (°C)
 T_{max} -Temperature of maximum mass loss (°C)
 T_m -Crystalline melting temperature (°C)
Tukey-test: Statistical method used to compare of means
 $T_{WL5\%}$ -Temperature of mass loss of 5 wt.% (°C)
 $T_{WL50\%}$ -Temperature of mass loss of 50 wt.% (°C)
 $T_{WL90\%}$ -Temperature of mass loss of 90 wt.% (°C)
WL%-Weight loss in percentage (%)
 W_{PBS} – Weight fraction of PBS in the composite
 X_c -Degree of crystallinity (%)
XRD-X ray diffraction

Summary

CHAPTER 1	18
1.0 INTRODUCTION	18
1.1 OBJECTIVE	22
1.1.1 OVERALL OBJECTIVE	22
1.1.2 SPECIFIC OBJECTIVE	22
CHAPTER 2	23
2.0 REVIEW	23
2.1 Poly(butylene succinate) (PBS)	23
2.2 Cellulose biomass-based composites	26
2.3 Canabrava natural fiber (CANA)	26
2.4 Lignin (LIG)	28
2.5 Mineral Clay	28
2.6 Epoxidized soybean oil (ESB)	29
2.7 PBS eco-composite and application in agricultural packaging	32
2.8 Final considerations	33
CHAPTER 3	35
3.0 RESEARCH PAPER 1: “Eco-friendly composite materials of Polybutylene Succinate with clay minerals, lignin and canabrava fiber”	35
3.1 INTRODUCTION	35
3.2 EXPERIMENTAL	38
3.2.1 Materials	38
3.2.2 Preparation of hybrid bio-composites	39
3.2.3 Characterization	40
3.2.3.1 <i>Mechanical Properties</i>	40
3.2.3.2 <i>Melting Flow Rate</i>	41
3.2.3.3 <i>Fourier Transform Infrared Spectroscopy (FT-IR)</i>	41
3.2.3.4 <i>Thermal Analysis</i>	41
3.2.3.5 <i>X-Ray Diffraction (XRD)</i>	42
3.2.3.6 <i>Scanning Electron Microscopy (SEM-EDS)</i>	42
3.2.3.7 <i>Statistical Analysis</i>	42
3.3 RESULTS AND DISCUSSION	43
3.3.1 Melt Flow Rate (MFR)	43
3.3.2 Fourier Transformed Infrared spectroscopy (FT-IR)	44
3.3.3 Mechanical characterization	45

3.3.4	Thermal analysis	49
3.3.5	X-Ray Diffraction (XRD)	53
3.3.6	Morphology Analysis	54
3.4	CONCLUSIONS.....	56
CHAPTER 4.....		58
4.0	RESEARCH PAPER 2:	58
4.1	INTRODUCTION	59
4.2	MATERIALS AND METHODS	64
4.2.1	Materials.....	64
4.2.2	Design of experiments (DOE)	65
4.2.3	Preparation of hybrid bio-composites	66
4.2.4	Characterization	67
4.2.4.1	<i>Melting Flow Rate (MFR)</i>	67
4.2.4.2	<i>Soil biodegradation test</i>	67
4.2.4.3	<i>Mechanical Properties</i>	68
4.2.4.4	<i>Fourier Transform Infrared Spectroscopy (FT-IR)</i>	69
4.2.4.5	<i>Thermal Analysis</i>	69
4.2.4.6	<i>X-Ray Diffraction (XRD)</i>	70
4.2.4.7	<i>Density analysis</i>	71
4.2.4.8	<i>Scanning Electron Microscopy (SEM-EDS)</i>	71
4.2.4.9	<i>Statistical Analysis</i>	71
4.3	RESULTS	72
4.3.1	Melt Flow Rate (MFR).....	73
4.3.2	Soil Biodegradation test.....	75
4.3.3	Fourier Transform Infrared spectroscopy (FT-IR).....	78
4.3.4	Mechanical characterization.....	79
4.3.5	Thermal analysis	88
4.3.6	X-Ray Diffraction (XRD)	95
4.3.7	Density	97
4.3.8	Morphology Analysis	97
4.4	CONCLUSION.....	100
CHAPTER 5.....		103
5.0	FINAL CONSIDERATION	103
5.1	CONCLUSIONS.....	103
5.2	RECOMMENDATIONS FOR FUTURE WORKS.....	104
CHAPTER 6.....		106

6.0	REFERENCES.....	106
	<i>Appendix</i>	115

1.0 INTRODUCTION

The widespread use of conventional plastics has led to significant environmental challenges, particularly in agriculture, where materials such as polypropylene and polyethylene are commonly used in packaging and seedling trays (IBF, 2023). Although these fossil-based polymers perform effectively, they contribute to persistent plastic waste due to limited reuse, recycling difficulties, and slow degradation in natural environments. In response to this growing ecological concern and in alignment with global efforts toward sustainable and circular material solutions, there is increasing demand for eco-friendly alternatives derived from renewable resources, produced with lower energy inputs, and exhibiting reduced environmental impact (OECD, 2022).

Poly(butylene succinate) (PBS) is one of the most promising candidates in this context. PBS is a biodegradable aliphatic polyester that can be synthesized from renewable resources and offers mechanical and thermal properties comparable to polyolefins (Sisti et al., 2016; Kuenz et al., 2020; PTT MCC Biochem, 2023). Additionally, PBS is compatible with standard processing techniques such as extrusion and injection molding (Zakharova et al., 2015; Platnieks et al., 2020). However, its broader commercial adoption remains limited by intrinsic drawbacks, including low stiffness (Someya et al., 2003), poor gas barrier performance, and, most critically, high production cost (Zhang et al., 2019). Addressing these limitations is essential to unlocking the full potential of PBS in several applications, especially in agriculture applications.

Motivated by the need for the development of sustainable, high-performance biocomposites based on renewable, low-cost, and biodegradable components, this thesis adopts the research concept known as eco-composite (Behera et al., 2024), also referred as green composites (Pattnaik et al., 2024a, 2024b) or aligned with green chemistry (Pattnaik et al., 2025) principles, in which composite materials components (matrix, reinforcement and other additives) are derived from environmentally friendly and renewable sources. Within this framework, biocomposites are developed using bio-based PBS and natural fibers that would otherwise be discarded as waste. These fibers are processed through simple mechanical methods, such as crushing and sieving, thereby avoiding the complex chemical or energy-intensive procedures typically required for

producing nano cellulosic material like cellulose nanocrystal (CNC) or cellulose nanofibril (CNF), or micro fibrillated cellulose (MFC) (Joy et al., 2017; Sun et al., 2018; Nabels-Sneiders et al., 2023). Although such nanostructures exhibit outstanding properties, this study prioritizes an eco-composite approach focused on lower environmental impact and resource efficiency. The use of natural fiber waste, abundant in tropical regions such as Brazil, aligns with the principles of sustainability and promotes low-impact material development.

Specifically, the research explores the development and optimization of hybrid PBS-based eco-composites reinforced with Canabrava (*Gynerium sagittatum*) natural fiber (with simple mechanical crushing and sieving, without chemical treatment), mineral clays, and kraft lignin. This work also seeks to valorize locally available biomass residues and naturally occurring minerals into functional additives to enhance the physical, thermal, mechanical, and biodegradation properties of PBS.

Canabrava (Cana) is traditionally used in the artisanal production of baskets and decorative items in Brazilian communities, resulting in substantial fiber waste discarded and collected by local waste services (Coradin et al., 2011). Incorporating this waste into eco-composites not only mitigates disposal issues but also generates socioeconomic benefits by creating new income opportunities for local families. Lignin, a byproduct of the pulp and paper industry, contributes to thermal stability, antioxidant and antimicrobial functionality, and improved melt processability of the composites (Domínguez-Robles et al., 2020; Shah et al., 2023; Ewurum and McDonald, 2025). Sepiolite, a naturally occurring fibrous clay mineral, offers high surface area and microporosity, acting as a structural reinforcement and potential flame retardant (Chikh et al., 2016; Huo et al., 2017; Farshchi and Ostad, 2020; García-Villén et al., 2020).

To address the issue of low fiber–polymer interfacial adhesion and to improve elongation at break and impact strength, the use of epoxidized soybean oil (ESB) was proposed in the final part of this thesis, as its beneficial effects as a compatibilizer and ductility enhancer have been reported in some studies (Zhao et al., 2012; Sahoo et al., 2013; Liminana et al., 2018; Turco et al., 2024).

By combining these components, this research is focused on systematically developing, processing, and characterizing a fully biodegradable hybrid PBS-based eco-composite reinforced with Cana, lignin, sepiolite and epoxidized soybean oil, suitable for

use in agricultural applications, especially seedling trays and tubes – products currently dominated by petrochemical-based polymers, such as polypropylene resin. The formulations are designed to meet the performance required for injection molded packaging for agricultural use. The study investigates how each component affects processing behavior, mechanical properties, biodegradability, and thermal stability, including analyses at the molecular and morphological level. Comparisons are made with conventional polypropylene-based products to assess commercial feasibility. Ultimately, these alternatives seek to meet functional performance requirements while offering a more sustainable end-of-life scenario.

To achieve these objectives, the research is structured into two major experimental studies, each published as a scientific article in high-impact, peer-reviewed journals classified as Qualis A1 by CAPES, reflecting the rigor and reproducibility expected in materials science research.

1) **APPLIED CLAY SCIENCE (2025)**: Published by: **Elsevier BV**. ISSN of this journal is **1691317**. CiteScore: **10.3**. Journal Impact Factor (JIF): **5.8**, 5-year-Journal Impact Factor: **5.4**. SCImago Journal Rank (SJR): **0.985**. Quartile: **Q1**. CAPES: **Qualis A1** (Engenharias III). Indexed in: **Scopus, Web of Science** (SCIE- Science Citation Index Expanded) and **UGC Care**.

2) **JOURNAL OF APPLIED POLYMER SCIENCE (2025)**: Published by **John Wiley & Sons Inc.** ISSN of this journal is **00218995 and 10974628**. CiteScore: **5.8**. JIF: **2.8**. 5-year-JIF: **3.0**. SJR **0.549**. Quartile: **Q2**. CAPES: **Qualis A1** (Engenharias III). Indexed in: **Scopus, Web of Science** (SCIE- Science Citation Index Expanded) and **UGC Care**.

The first study focuses on the development and evaluation of PBS composites containing Cana fiber, lignin, and two clay minerals (montmorillonite or sepiolite), with mechanical (tensile, flexural, impact), thermal (TGA, DSC), and structural (SEM, FTIR, XRD) characterizations. This phase provides foundational understanding of how natural additives influence melt flow, crystallization, interfacial adhesion, and mechanical reinforcement.

In the second study, a formulation strategy is adopted using a design of experiments (DOE) methodology. Here, the influence of varying concentrations of lignin, sepiolite, and epoxidized soybean oil (ESB) is investigated. ESB is introduced as a

compatibilizer and plasticizer to address the typical brittleness and processability issues associated with high-fiber content biocomposites. The DOE framework enables the evaluation of synergistic and antagonistic effects among additives on key properties such as melt flow rate, biodegradability in soil, flexural modulus, tensile strength, elongation at break, and thermal resistance. Optimized formulations are benchmarked against EP440L (Braskem S.A., 2018) polypropylene resin, a widely used fossil-based polymer in agriculture packaging, providing direct comparisons regarding performance and sustainability.

Beyond technical development, this thesis also considers broader socio-environmental aspects. By sourcing Cana from local communities and lignin from regional pulp industries, the research fosters regional bioeconomy and contributes to circular resource use. The substitution of petrochemical plastics by biodegradable composites in agriculture settings supports the global efforts to reduce plastic pollution and carbon emission.

This doctoral thesis is organized into six chapters. **Chapter 1** introduces the motivation, context, and objectives of the research. **Chapter 2** presents a literature review of PBS, natural fiber composites, lignin, and mineral filler in biopolymeric systems. **Chapter 3** and **Chapter 4** correspond to the main experimental studies structured as scientific articles published. **Chapter 5** summarizes the main findings and provides final conclusions and recommendations for future research and potential industrial applications. **Chapter 6** contains all bibliographic references.

In summary, this work proposes the development of a hybrid eco-composite based on bio-PBS and high residue content of crushed, milled and sieved canabrava fiber, incorporating additional natural components—such as lignin, epoxidized soybean oil, and mineral clay—to tailor the material properties and reduce overall production costs. To this end, a comprehensive strategy was used with DOE to evaluate the effect of each component aiming to overcome the limitations of PBS through the integration of abundant, renewable, and low-cost materials. The results contribute not only to material innovation in biodegradable composites, but also to the broader field of sustainable polymer engineering. The bio-based composites developed here present a scalable and practical solution for the reduction of plastic waste—particularly in agricultural applications—and can represent a step forward in the transition to a circular and low-impact materials economy.

1.1 OBJECTIVE

1.1.1 OVERALL OBJECTIVE

Development of hybrid eco-composite of poly (butylene succinate), canabrava natural fiber waste, mineral clay, lignin and epoxidized soybean oil, for agriculture package applications.

1.1.2 SPECIFIC OBJECTIVE

- Develop and characterize eco-friendly PBS composites incorporating Canabrava natural fiber, lignin, and inorganic fillers (specifically montmorillonite and sepiolite clays) and epoxidized soybean oil, to establish foundational understanding of their mechanical, thermal, and rheological behaviors.
- Systematically evaluate the individual and synergistic effects of Canabrava fiber, lignin, montmorillonite or sepiolite and epoxidized soybean oil on the melt flow, crystallization kinetics, interfacial adhesion, and mechanical reinforcement (tensile, flexural, and impact properties) of the PBS matrix.
- Investigate the influence of varying concentrations of lignin, sepiolite, and epoxidized soybean oil (ESB) through a Design of Experiments (DOE) methodology,
- Analyze the composite formulations for enhanced melt flow rate, soil biodegradability, and balanced mechanical performance (flexural modulus, tensile strength, and elongation at break).
- Analyze the interactions and their implications for the overall performance and structure (via FTIR, XRD, SEM) of the developed PBS hybrid composites.
- Verify the intrinsic biodegradation capacity of the developed composites under relevant environmental conditions.
- Compare the performance of optimized PBS hybrid composite formulations with commercial polypropylene resins (e.g., PP EP440L) to assess their technical viability and sustainability as alternatives for agricultural packaging applications.

2.0 REVIEW

2.1 Poly(butylene succinate) (PBS)

Poly(butylene succinate) (PBS) is a linear aliphatic polyester obtained by the polycondensation of succinic acid (SA) or dimethyl succinate with 1,4-butanediol (BDO), by ring-opening polymerization or by enzymatic polymerization (Sisti et al., 2016; Platnieks et al., 2020). Both chemicals can be bio-based (renewable source) or fossil-based (petroleum derived). It has a melting temperature (T_m) of 110°C and a glass transition temperature (T_g) of -36°C (Qi et al., 2019). The initial synthesis of PBS was carried out by Charothers in 1931 from his pioneering work including other aliphatic polyesters. However, due to its low molecular weight (less than 5,000 g/mol), the PBS obtained at the time had little strength and was brittle, showing little commercial interest. Since the 1990s, with the use of new catalysts and reaction agents, and the inclusion of more steps in the polymerization process, it has been possible to obtain PBS with a higher molecular weight (M_w from 40,000 to 1,000,000 g/mol), allowing improvements in thermomechanical properties and ensuring good processability (Sisti et al., 2016). In addition, copolymerization with other dicarboxylic acids and diols can have their properties adjusted, substantially increasing their applications, which range from films for coating in agriculture, fishing lines, films, bags, bottles and food packaging. The properties of PBS have been compared with polyolefins, but its higher price still represents a challenge to be overcome (Moon et al., 2011; Li et al., 2024). With additional research, it is possible to develop new applications in the areas of engineering, automotive components, electrical and aerospace industries with greater added value, in addition to its ecological character and economic advantages (Miao and Hamad, 2019; De Luca et al., 2025).

The molecular structure of PBS is shown in **Figure 1** and the synthesis reaction is shown in **Figure 2** below:

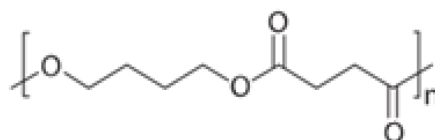


Figure 1: Molecular structure of PBS.

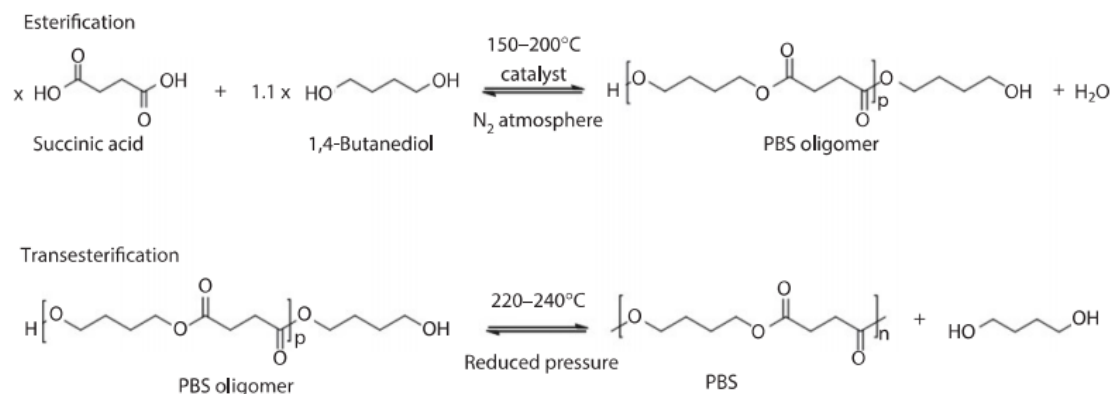


Figure 2: Synthesis reaction of PBS from SA and BDO (Miao and Hamad, 2013).

PBS is a polyester with a high relative degree of crystallinity (35 to 45%) and has a higher melting temperature compared to other aliphatic polyesters such as polyethylene succinate (PES), polyethylene adipate (PEA), and polybutylene adipate (PBA), making it important in applications for use in higher temperatures. **Table 1** shows the main thermal properties of aliphatic polyesters (Miao and Hamad, 2013).

Table 1: Thermal properties of PBS and other aliphatic polyesters (Miao and Hamad, 2013).

Polyester	T_D^a (°C)	T_g (°C)	T_m (°C)	X_C^b (%)
PBS	399	-31	114	62
PES	410	-12	104	40
PBA	391	-61	60	39
PEA	380	-46	48	n.d.
PCL	402	-66	60	75–80

^a Maximum degradation rate temperature analyzed by TGA in N₂.

^b Calculated through DSC measurements.

Compared to other biodegradable polymers, PBS has superior mechanical properties and allows processing using conventional techniques (melt processing) used in thermoplastics (Wang et al., 2018). Compared to thermoplastics such as PP and LDPE, PBS has good biodegradability and processability, tensile strength and elongation to break comparable to those of other polymers. However, PBS has limitations such as low rigidity, low melt strength and melt viscosity, low gas barrier and low crystallization rate, which means that techniques such as copolymerization (Qi et al., 2019), polymer blends and composites with different fillers, fibers and nanofillers are used (Miao and Hamad, 2013; Sisti et al., 2016; Li et al., 2017; A. Nazrin et al., 2020).

Regarding biodegradation, Huang et al., 2018 found through his study (Huang et al., 2018) that PBS/sugarcane rind fiber composites with a maximum of 5 wt.% of fiber presented a maximum mass loss rate of 19.2% in 100 days buried under soil in dumbbell shaped samples. Phua et al., 2012 performed biodegradation tests through the evolution of carbon dioxide (CO₂) and mass loss after 10 to 180 days under conditions of 30°±2°C and 60-70% relative humidity in dumbbell samples, finding that the mass loss rate increases up to 90 days, after which it stabilizes, for both pure PBS and PBS/MMT composites (Phua et al., 2012). Kim et al., 2006 associated the greater biodegradation of the PBS/rice husk flour bio composite due to the greater attack of microorganisms on the bio-flour, and also found that the molecular weight of PBS decreased in the soil burial test (confirmed by FTIR-ATR, due to hydrolysis of the ester bonds in the PBS main chain), which can be attributed to the hydrolysis of the aliphatic ester linkage and the changed low molecular weight materials (Kim et al., 2006; Muranaka et al., 2025).

In certain applications, controlling the biodegradation of PBS is particularly important. Accordingly, studies have investigated the biodegradation of aliphatic polyesters in relation to factors such as chemical stereoregularity, molecular chain flexibility, crystallinity, and surface wettability (Mizuno et al., 2015). In this sense, the gel content and the degree of cross-linking can be controlled through reactive extrusion with control of peroxide concentration and temperature to control the biodegradability of PBS (Wu et al., 2019).

PBS has good reprocessability, showing little degradation and low loss of mechanical properties even after the third processing at 140°C. Immersion in water and exposure to temperature showed an increase in physical degradation caused by hydrolysis and accompanied by a reduction in molecular weight (Kanemura et al., 2012). Some

researchers found that PBS has relatively low tensile toughness loss after 2 reprocessing, from 418.7 KJ/m² to 366.71 KJ/m² (-12.4%) (Yan et al., 2025).

2.2 Cellulose biomass-based composites

Composites based on cellulose biomass have become one of the most widely used reinforcement materials in the preparation of composites, due to their natural origin, biodegradability, and relatively cheapness, which are usually discarded as waste from agricultural and reforestation industries. The structure of cellulose fiber offers low density, high specific strength, rigidity, and is non-toxic to humans and nature (Sharma et al., 2025).

The low cost of natural fibers, especially in the form of a by-product, which would normally be discarded, generating waste and disposal costs, now can create a great opportunity to take advantage of these materials due to the possibility of using them in the production of biocomposites with polymers, especially biopolymers (bio-based and/or biodegradable polymers) which are still expensive and can be reduced in cost with the incorporation of these fibers and still maintain their biodegradable properties (Platnieks et al., 2020; Behera et al., 2024; Pattnaik et al., 2025).

2.3 Canabrava natural fiber (CANA)

Natural fibers can be derived or prepared from various sources such as sisal, cotton, sugarcane bagasse, coconut and others (Silva et al., 2020). Plant fibers, which serve as reinforcement in thermoplastic composites, are lignocellulosic materials (consisting of cellulose, hemicellulose and lignin). Cellulose contains both amorphous and crystalline regions. Crystalline cellulose is typically obtained through the acid hydrolysis of cellulose, a process that effectively removes its amorphous regions, which consist primarily of lignin. Lignocellulosic materials can be incorporated into thermoplastic composites in various forms, including natural fibers (raw or modified), particles and powders, or as nanostructures such as cellulose nanocrystals (CNC), cellulose nanofibrils (CNF), and micro fibrillated cellulose (MFC) (Joy et al., 2017; Sun et al., 2018; Nabels-Sneiders et al., 2023). A primary challenge in natural fiber-reinforced composites stems from the inherent incompatibility between hydrophilic cellulose fibers and hydrophobic polyolefin polymer matrices, such as polypropylene and polyethylene.

To address this issue, compatibilizing agents like silanes, isocyanates, and maleic anhydride-grafted copolymers are commonly employed (Zulkifli et al., 2015).

Among these natural resources, Canabrava (*Gynerium Sagittatum*) is a native tropical grass found in south America mainly in Brazil, Peru, Bolivia and Colombia. The CANA is mainly used in handcraft to produce several kinds, shape and size of basket by native population such as indigenous or maroon community. According to Lopez et al., 2025, between 50 % and 60% of the CANA plant collected is wasted after extracting the fiber for crafting, resulting in byproducts such as leaves, stems, roots, and inflorescences discarded into fields (Lopez et al., 2025). Although natural, these residues can impact on the environment, as it is discarded and of little value, which ends up in waste or landfills. The chemical characterization of CANA presents 24.18% of lignin, 38.95% of cellulose, comparable to bamboo (*Guadua Angustifolia*) with 19.72% of lignin and 59.77% of cellulose content. There are studies on the use of CANA (*Gynerium sagittatum*) waste for sustainable processing of sheets or panels compacted with thermosetting polyurethane resin. (Osorio et al., 2018), and production of artisanal paper from *Gynerium sagittatum* residues (Lopez et al., 2025).

CANA fiber is a natural, abundant, easy to extract and treat, can be used as low-cost waste from handcraft production in some Brazilian communities (Coradin et al., 2011) is an interesting option to be used to obtain a bio-composite. Untreated CANA fiber contains 91.6% of structural components and 8.43% of non-structural components such as waxes, fats, proteins, pectin and other impurities (Franca et al., 2019). CANA has more cellulose content compared to other natural fibers such as sugarcane (38-45% of cellulose, 23-26% of hemicellulose, and 19-25% of lignin), but less than rami fiber (68-76% of cellulose) or cotton (90-95% of cellulose). The high cellulose content is important for nano fibril cellulose obtention. Cellulose and hemicellulose are structural components, although with greater affinity for water due to hydrophilic hydroxyl (-OH) groups, they can improve mechanical properties such as stiffness and strength of composites (Platnieks et al., 2020).

2.4 Lignin (LIG)

Lignin is the amorphous component forming the matrix that embeds cellulose and hemicellulose in plant cells. It is produced in large quantities as a by-product of the pulp and paper industry, yet only about 2% is utilized in value-added applications, with the remainder typically incinerated as industrial fuel (Sahoo et al., 2013). Structurally, lignin is a three-dimensional amorphous biopolymer composed of aliphatic and aromatic units with high molecular weight, consisting primarily of phenylpropane units substituted with hydroxyl and methoxy groups. Its composition varies with plant species, stem diameter, and plant age, and may include low-molecular-weight organic compounds such as fats, waxes, fatty acids, tannins, gums, sugars, starches, resins, dyes, steryl esters, sterols, terpenoids, and other phenolic substances (Abu Ghalia and Dahman, 2017). Lignin exhibits thermal degradation within the temperature range of 250°C to 500°C, indicating its relative thermal stability. Polymer blends and composites incorporating lignin have demonstrated improvements in thermal stability, antioxidant and antibacterial activity, as well as mechanical performance (Domínguez-Robles et al., 2020). Moreover, lignin can act as a dispersing agent for cellulose nano whiskers, contributing to the sustainability of the composite by utilizing natural cellulose-based fibers. Lignin extraction is typically performed by impurity removal in NaOH solution, followed by bleaching with 1% NaClO₂ to eliminate residual lignin from the fibrils (Rosa et al., 2008).

2.5 Mineral Clay

The addition of clays or nano clays can enhance mechanical properties of thermoplastic composites, such as increasing the elastic modulus while maintaining or improving tensile strength and reducing elongation at break, as well as improving thermal and flame resistance (Rashid et al., 2021). In particular, sepiolite (SEP) nanoclay forms layered structures with internal channels known as zeolite tunnels, providing advantageous features such as microporosity and a high specific surface area. Due to its unique morphology, SEP is considered an effective reinforcing agent (García-Quiles et al., 2019). Sepiolite is a type of natural clay composed of magnesium silicate, with the theoretical formula $\text{Si}_{12}\text{O}_{30}\text{Mg}_8(\text{OH})_4 \cdot (\text{H}_2\text{O})_4 \cdot 8\text{H}_2\text{O}$ and is widely recognized for having the highest adsorptive capacity among natural clays due to its high specific surface area, resulting from its porous structure (Zhong et al., 2016)). This clay has been reported to enhance the mechanical strength of composites (Huo et al., 2017; Bahrami et al., 2020).

Additionally, some studies have reported the use of SEP as a flame retardant for PBS (Xiao et al., 2021). SEP clay has shown good dispersibility within the PBS matrix due to specific interactions between the components, leading to enhanced storage and loss moduli (Chikh et al., 2016). Olivato et al. (2017) examined the effect of SEP on polyester-based biocomposites and observed improvements in both the crystallization behavior and dynamic mechanical properties (Olivato et al., 2017). For instance, Farshchi et al. (2020), in their study on SEP as a nanofiller in high-density polyethylene (HDPE), reported notable enhancements, including a reduction in melt flow rate (MFR), a slight decrease in density, and increases in Vicat softening temperature, hardness, melting temperature, and degree of crystallinity (Farshchi and Ostad, 2020). Given the limited number of studies specifically addressing the use of SEP in PBS systems, this represents a promising opportunity for investigation.

Montmorillonite (MMT), a common clay belonging to the smectite group of hosts–guest minerals, is widely used due to its swelling and adsorption capabilities, as well as its ability to improve mechanical strength, stiffness, thermal stability, conductivity, and gas barrier properties of thermoplastic composite materials (García-Quiles et al., 2019). The swelling behavior of MMT allows for its exfoliation, transforming its stacked agglomerated structure into separated nanosheets. During exfoliation, transition metals such as iron, vanadium, and even lanthanides, which are often present in natural MMT, can be released, thereby increasing the specific surface area and generating a greater number of activated sites (Zhong et al., 2016). The incorporation of nanoclay such as montmorillonite (MMT), often organically modified to enhance compatibility with polymeric matrices (OMMT), in combination with reinforcing fibers—such as carbon, glass, basalt, and, more recently and innovatively, lignocellulosic plant fibers including hemp, coconut, flax, and jute—can significantly enhance mechanical properties. Particularly tensile and impact strength improvements are largely dependent on the ability to alter crack propagation dynamics, which is achieved through proper dispersion and, more critically, by intercalation or exfoliation of the nanoclay within the polymer matrix (Chidambara Kuttalam et al., 2021).

2.6 Epoxidized soybean oil (ESB)

Initial analyses revealed that the PBS–CANA fiber composite exhibited fiber–matrix debonding, as evidenced by scanning electron microscopy (SEM) images of

impact-fractured surfaces (Figure 11), indicating poor interfacial adhesion and limited toughness. To address these limitations, the study investigated the use of compatibilizers—preferably of natural origin—to enhance interfacial bonding while preserving the composite's overall sustainability

In fact, a significant challenge in polymer-natural fiber composites is the lack of fiber-matrix interfacial adhesion, which often leads to a reduction in mechanical properties, particularly toughness. This issue arises from the inherent disparity between the hydrophilic nature of cellulose fibers and the hydrophobic character of most polymer matrices. The abundant hydroxyl groups on natural fiber surfaces impart a high affinity for water molecules, leading to facile moisture absorption, which contrasts with the hydrophobic nature of many synthetic polymers (Zhao et al., 2012; Liminana et al., 2018; Ayu et al., 2020; Rafiqah et al., 2021).

Consequently, when natural fibers are incorporated into a polymer matrix, this incompatibility can result in poor interfacial bonding, leading to fiber-matrix debonding under stress. This phenomenon is frequently observed in impact-fractured specimens through scanning electron microscopy (SEM) analysis. To mitigate this, some researchers chemically treat the fibers to react with or remove surface hydroxyl groups. However, these methods can be costly and involve aggressive chemicals. Alternatively, commercial compatibilizing agents, often graft polymers, are employed, although they tend to be expensive. Furthermore, certain studies have explored the use of plasticizers to enhance fiber-polymer interaction, effectively acting as compatibilizing agents. Examples include renewable plasticizer such as castor oil (De Oliveira Santos et al., 2014), linseed oil (epoxidized) (Liminana et al., 2018), soybean oil (epoxidized) (Zhao et al., 2012; De Oliveira Santos et al., 2014; Liminana et al., 2018; Rafiqah et al., 2021). While primarily recognized as plasticizers, these materials have also been reported by some authors to act as compatibilizers, improving fiber-polymer interfacial adhesion, thereby enhancing the impact resistance and increasing the elongation at break of composites (Sahoo et al., 2013; Liminana et al., 2018; Turco et al., 2024).

Specifically, epoxidized soybean oil (ESB) is derived from soybean oil—an abundant, inexpensive, and readily available renewable feedstock—making it an attractive option for sustainable material development. Vegetable oils such as soybean oil contain unsaturation in their molecular structure, which serve as reactive sites for the introduction of functional groups, such as epoxide moieties. Epoxides are highly reactive due to the

ring strain inherent in their three-membered cyclic structure; this strain is relieved through nucleophilic attack on the electrophilic carbon of the C–O bond, resulting in ring opening. This pronounced reactivity makes epoxides valuable intermediates for various chemical modifications. The epoxidation of vegetable oils is typically carried out using oxidizing agents such as hydrogen peroxide or peracetic acid (De Oliveira Santos et al., 2014). ESB is well established as a bio-based plasticizer, non-toxic alternative for phthalates, and it also functions as a co-stabilizer by improving the thermal stability of polymeric systems (Turco et al., 2024). Epoxidized soybean oil (ESB) has recently been reported as an effective plasticizer for biodegradable polymers, including poly(butylene succinate) (PBS). In addition to its plasticizing effect, ESB can also function as a compatibilizing agent between lignocellulosic fibers and polymer matrices (Liminana et al., 2018). **Figure 3** illustrates the mechanism proposed by Liminana et al. (2018) regarding how these plasticizers act as compatibilizing agents.

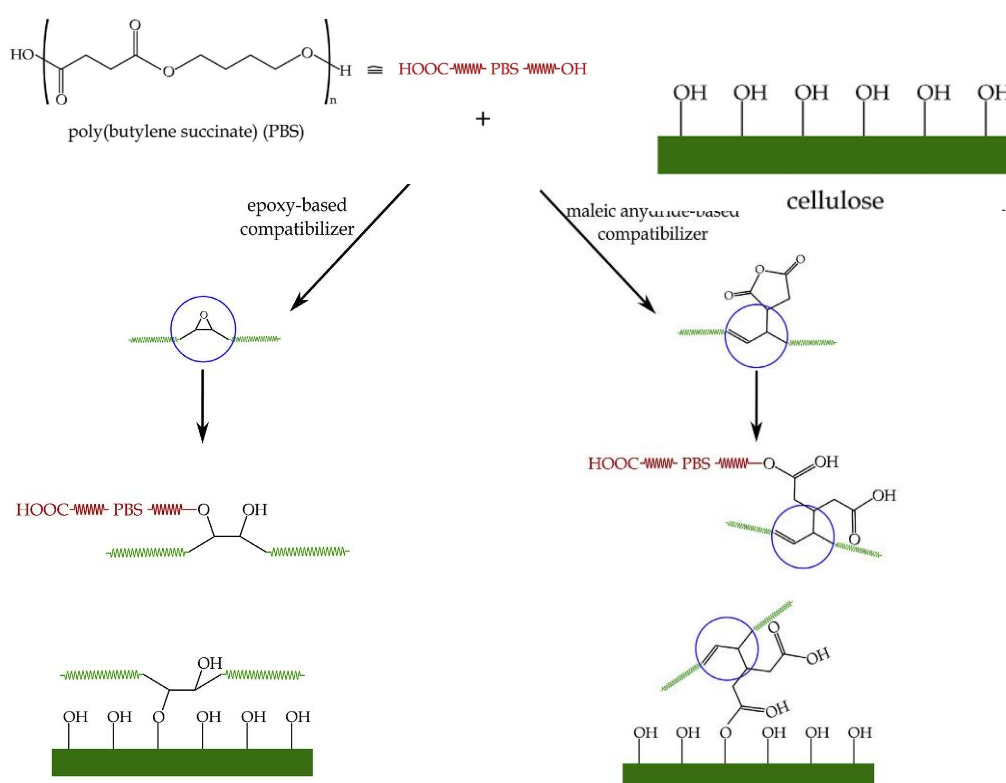


Figure 3: Schematic representation of the reactions of epoxy and maleic anhydride groups in PBS/natural fiber composites. Adapted of (Liminana et al., 2018)*.

* Permission to use the figure was granted through Rightslink by Elsevier and Copyright Clearance Center. License #6027321050107

2.7 PBS eco-composite and application in agricultural packaging

The concept of green composites (Pattnaik et al., 2024a, 2024b), green chemistry (Pattnaik et al., 2025), or eco-composites (Behera et al., 2024) refers to composite materials in which the matrix (polymer) and the reinforcement (fiber or filler) are derived from renewable, biodegradable, or environmentally friendly sources. The primary goals are to reduce environmental impact, promote biodegradability, and utilize waste or sustainable raw materials, offering a sustainable solution to overcome the inherent limitations of biopolymers, such as low stiffness and high cost, by incorporating natural waste that would otherwise be discarded. Additionally, low environmental impact during production, use, and disposal is also desirable, often resulting in biodegradable or compostable materials. Environmentally friendly production involves processes that consume less energy and chemicals or avoid chemicals altogether. In this context, incorporating nanocellulose into biopolymers may also be classified as eco-composites, particularly when derived from natural fiber waste. However, the production of nanocellulose (such as CNC, CNF, MFC) typically requires intensive processing, including mechanical size reduction (crushing and grinding), chemical treatments, extensive washing, physical processing (high shear/high speeds homogenizer, such as Ultra-Turrax), and drying methods (thermal drying, freeze-drying, vaporization), which increase the environmental impact (Joy et al., 2017; Sun et al., 2018; Miao and Hamad, 2019; A. Nazrin et al., 2020; Nabels-Sneiders et al., 2023). As an alternative, natural fiber waste can be processed through simpler methods, such as crushing, grinding, and sieving, to obtain fibers of few millimeters in length, suitable for use in biopolymer composites. Moreover, these natural fiber wastes are often abundantly available, sometimes representing a disposal problem or incurring additional disposal costs (Sharma et al., 2025). In this study, Canabrava residue was processed solely through mechanical crushing and sieving, without the use of direct chemical treatments, which present an advantage for the sustainable production of the bio-composite.

In this context, PBS biocomposites exhibit biodegradability, making them a viable alternative to petroleum-based and non-biodegradable packaging, thereby helping to reduce environmental impact (Rafiqah et al., 2021). In particular, the use of plastic tubes and trays ensures higher quality in seedling production compared to polyethylene plastic bags. Unlike bags, which lack internal grooves to guide the plant root development, causing the roots to coil and increasing the risk of plant lodging after transplantation,

tubes are designed with various sizes, conical shapes, and internal ribs that promote root development and direct growth toward the bottom opening. Tubes are commonly used for the production of seedlings of African mahogany, coffee, açai, sugarcane, cocoa, black pepper, native and fruit species, eucalyptus, and pine (IBF, 2023). Due to their ease of handling, tubes allow for greater automation throughout the seedling production process, from filling to shipment for planting (IBF, 2023).

Typically, the tubes are manufactured from UV-stabilized polypropylene, sometimes incorporating ethylene-propylene-diene terpolymer (EPDM) for enhanced performance (IBF, 2023). The literature reports on the use of Braskem's EP 440L polypropylene resin, a heterophasic copolymer with medium flow rate, specifically designed for injection molding processes, in the manufacturing of these tubes (Nascimento et al., 2020). According to the manufacturer, this resin has a melt flow index of 6.0 g/10 min (at 230°C / 2.16 kg), flexural modulus of 1050 MPa, yield strength of 24 MPa, yield elongation of 6%, Rockwell hardness of 60 (R scale), Izod impact resistance at 23°C without break (75 J/m at -20°C), and a heat deflection temperature of 85°C (under 0.455 MPa) (Braskem S.A., 2018).

2.8 Final considerations

The comprehensive review of existing literature underscores the critical need for sustainable material solutions, particularly for single-use applications in agriculture, where conventional plastics contribute significantly to environmental burden. Biodegradable polymers, notably poly(butylene succinate) (PBS), emerge as highly promising candidates due to their inherent biodegradability and desirable mechanical properties. However, their broader commercial viability remains challenged by limitations such as cost, stiffness, and interfacial adhesion issues when combined with natural reinforcements.

The literature highlights the potential of lignocellulosic fibers as renewable and abundant reinforcements, alongside various natural additives like lignin and mineral clays (e.g., sepiolite), in enhancing the performance and reducing the environmental footprint of biocomposites. While individual contributions of these components have been explored, a significant gap persists in the systematic understanding and optimization of

hybrid multi-component PBS-based eco-composites that simultaneously leverage the synergistic benefits of diverse natural fillers and compatibilizers. Notably, despite its abundance as a local biomass residue, the application of Canabrava fiber in high-performance or more technical composite applications remains largely unexplored in the existing literature, which primarily focuses on its traditional or simpler uses. This highlights an opportunity for research to effectively valorize such underutilized resources. Moreover, there is a distinct need for research that focuses on achieving a balanced set of properties crucial for demanding applications like agricultural packaging, while ensuring economic feasibility without relying on complex, energy-intensive material processing.

This review therefore establishes a clear foundation for the subsequent experimental work, emphasizing the necessity for an integrated approach that addresses the multifaceted challenges of bio composite development. By synthesizing insights from studies on matrix-filler interactions, compatibilization strategies, and the properties of individual components, the path is set for developing novel, high-performance, and truly sustainable eco-composites designed to meet specific industrial requirements while fostering a circular economy.

CHAPTER 3

This chapter is part of a research paper entitled “Eco-friendly composite materials of polybutylene succinate with clay minerals, lignin and canabrava fiber” published in the Applied Clay Science (Elsevier), Vol. 262, 15 December 2024, 107606, (<https://doi.org/10.1016/j.clay.2024.107606>).

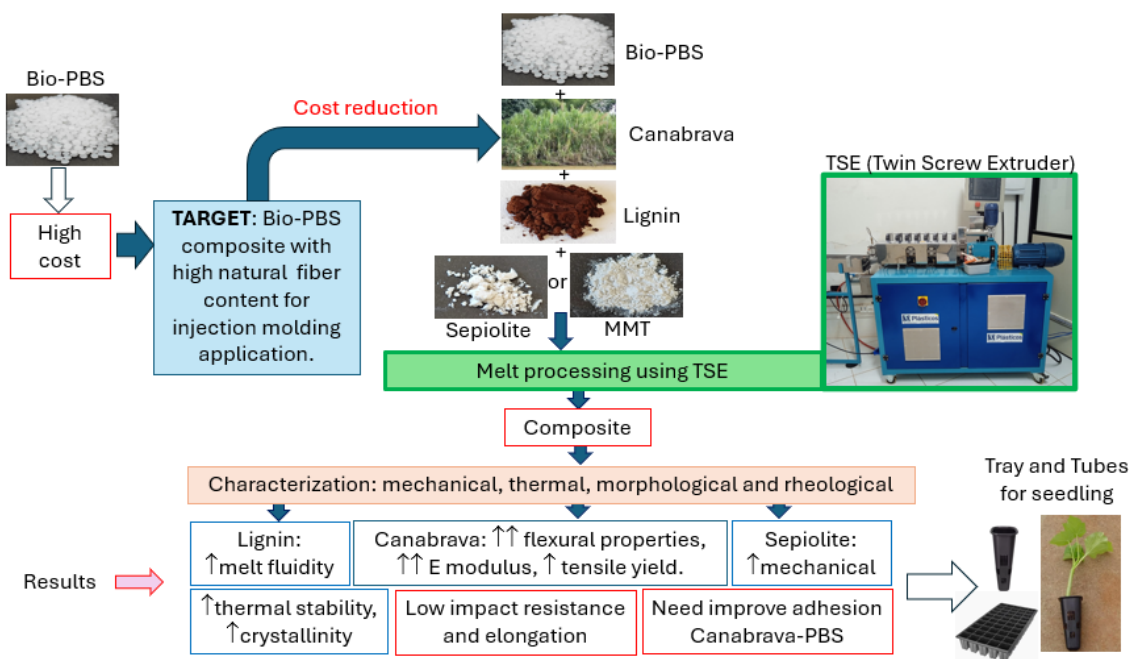


Figure 4: Graphical abstract of the first article presented at Applied Clay Science.

3.0 RESEARCH PAPER 1: “Eco-friendly composite materials of Polybutylene Succinate with clay minerals, lignin and canabrava fiber”

3.1 INTRODUCTION

Polybutylene Succinate (PBS) is acknowledged as a biodegradable and sustainable polymer, primarily due to its capability to be produced from renewable sources. This feature distinguishes it as a viable alternative to petroleum-derived polymers, as evidenced by some authors (Bozell and Petersen, 2010; Kuenz et al., 2020; Barletta et al., 2022). As an aliphatic polyester, PBS is synthesized through the polycondensation of succinic acid with 1,4-butanediol using ring-opening polymerization or enzymatic polymerization methods. This process endows PBS with properties

comparable to those of low-density polyethylene and polypropylene, such as a melting temperature of 110°C and a glass transition temperature of -36°C (Li et al., 2017), coupled with the significant advantage of biodegradability (IBF, 2023).

Overall, the versatility of PBS arises from its biodegradability, compatibility with other polymers and the possibility of using renewable sources for its production (obtention of PBS monomers). Regardless of whether they originate from bio-renewable or fossil sources, these monomers confer desirable mechanical properties to PBS while maintaining compatibility with conventional processing techniques such as extrusion and injection. The development of compostable plastics, exemplified by PBS, which degrade into natural components like water, carbon dioxide, and biomass, has propelled the use of this material in a variety of fields, from biological packaging to the textile sector (PTT MCC Biochem, 2023). However, it still shows some limitations such as low mechanical strength and modulus (stiffness) (Someya et al., 2003), unsatisfactory gas barrier properties, slow crystallization rate, high flammability, and high costs that limit its application in other areas (Zhang et al., 2019).

To overcome these challenges, various strategies have been explored, including copolymerization techniques, polymer blends, and the incorporation of different types of reinforcements, as natural fiber in natural state or modified as cellulose nano fibril (CNF) or cellulose nanocrystal (CNC) or micro fibrillated cellulose (MFC) (Joy et al., 2017). In this regard, it is of utmost importance to appropriately select the reinforcing ingredients to maintain PBS environmental friendliness. To do so, nanofillers (Joy et al., 2017) and natural fibers (Mochane et al., 2021) such as sisal, cotton, sugarcane bagasse, and bamboo, among others, have been successfully employed (Aaliya et al., 2021; Mochane et al., 2021). In particular, canabrava (Cana) (*Gynerium sagittatum*) stands out as a natural fiber with promising potential for sustainable PBS composite production. Primarily derived as waste from basketry and crafts made by local communities in Brazil, Cana exemplifies the concept of complete resource utilization. Its versatility extends to fodder and cellulose production, making it a standout model of sustainability (Coradin et al., 2011).

However, the addition of natural fibers usually increases the melt viscosity of the polymer, which can compromise injection molding capability. The introduction of Lig, isolated from the cellulose matrix complex, as a lubricant during melt processing, has emerged as an innovative solution to this challenge, increasing the melt flow rate and,

consequently, facilitating injection processing. Moreover, the integration of lignin (Lig) into polymer composites not only improves thermal stability but also enhances their antioxidant and antibacterial properties, in addition to reinforcing mechanical integrity. This incorporation marks a significant advancement in the pursuit of environmental sustainability of composites (Shah et al., 2023).

Further PBS improvements can be achieved by other additives such as natural inorganic ingredients. The incorporation of clay minerals such as sepiolite (SEP) and montmorillonite (MMT) emerges as an innovative and effective approach in material engineering, particularly in enhancing polymeric composites like PBS. SEP, characterized by its unique fibrous structure with internal mesoporous channels, exhibits significant microporosity and an extensive specific surface area. This peculiar morphology not only facilitates the interaction with the polymer and fibers but also contributes to an increase in mechanical strength and composite density (leading to higher viscosities and viscoelastic properties), in addition to acting as a flame retardant (García-Quiles et al., 2019).

MMT stands out for its unique properties of cation exchange capacity, adsorption, and swelling. This clay mineral, known for intercalating water molecules and metallic cations between its layers, has also the ability to “intercalate” polymer fibers between its layers (under the appropriate conditions), thus tuning the polymer properties and, ultimately, leading to exfoliation, which increases the specific surface area and exposes active sites for chemical reactions and physical interactions with polymeric matrices. The presence of cations such as iron, vanadium, and lanthanides, which can be released or exchanged, enriches the catalytic, mechanical, and barrier properties of composites. These characteristics not only facilitate the integration and dispersion of the mineral into composites but also enhance stiffness, thermal stability, conductivity, and gas barrier properties, making MMT an indispensable additive for the development of advanced and efficient composite materials, as evidenced by previous research (Zhong et al., 2016; García-Quiles et al., 2019)

The strategic addition of clay minerals, such as SEP and MMT, to PBS composites marks notable progress in the manufacture of advanced and sustainable materials. This combination enriches PBS, concurrently improving its mechanical, thermal, flame resistance, and barrier properties, thereby overcoming previous challenges related to stiffness, permeability, and thermal stability. This advancement could potentially expand

the applications of PBS in other demanding sectors, emphasizing innovation and sustainability in the creation of new materials. Studies such as those demonstrate this efficacy, highlighting the significant potential for the engineering of more efficient and environmentally responsible materials (Zhong et al., 2016; García-Quiles et al., 2019; Rashid et al., 2021).

Traditionally, packaging materials used for agricultural purposes are manufactured in anti-UV photo stabilized polypropylene, often incorporating ethylene-propylene terpolymer (EPDM) (IBF, 2023). These non-biodegradable polymers, typically used only once due to cost and logistical challenges, contribute significantly to environmental pollution. This highlights the urgent need for more sustainable alternatives to reduce the environmental impact. Thus, the aim of this study is to develop a biodegradable composite material with a significant content of Cana natural fiber, aiming at cost reduction compared to pure PBS. This material will be used in the manufacture of PBS tubes and trays designed for agricultural planting (this study does not intend to work with nanocellulose at this time). To do so, PBS properties and performance will be tuned by natural additives such as Cana, Lig, SEP and MMT. The resultant bio-composite alternatives aim to offer an environmentally friendly solution to the current use of non-biodegradable plastic bags and tubes in seedling agriculture. Tubes have technical advantages over bags due to their innovative design that incorporates grooves to effectively guide the growth of plant roots and thus prevent destabilization during transplantation.

3.2 EXPERIMENTAL

3.2.1 Materials

The bio-PBS was provided by PTT-MCC Biochem, with melt flow rate (MFR) value of 22 g/10min (190°C, 2.16 kg), melting temperature of 115°C, glass transition temperature of -36°C, and density of 1.26 g/cm³ (PTT MCC Biochem, 2023). Lig (kraft) was kindly gifted by a brazilian cellulose company. The Cana fiber was obtained as a residue from handcraft production by a local community in Salvador, Bahia, Brazil (Ilha de Maré). This residue was in the form of long strips of 1 to 2 m in length, and was crushed using a TRE40MA crusher (Tramontina S.A., Carlos Barbosa, Brazil) in order to reduce the size to a few centimeters. And then it was blended in a LQL8BIVMF60N5 blender

(BIMG Ltda, Brusque, Brazil), and sieved to obtain fibers with a mean length of 3.18 ± 1.90 mm and a width of 0.45 ± 0.23 mm, calculated using optical microscope and the software ImageJ, analyzing more than one thousand fibers, and the image of Cana fiber by optical microscopy is available in the Supplementary Material SM1 (**Figure 12** at the end of this chapter). The MMT K10 (Sigma-Aldrich Co., St Louis, USA) with a surface area of 220 to 270 m²/g and SEP type PS9 (Pangel S9, Tolsa S.A., Madrid, Spain) of high purity, specific surface area (BET, N₂) of 344 m²/g and total pore volume of 0.4476 cm³. Both clays were used with no modification.

The results of PBS composites analysis were compared to Braskem's EP440L polypropylene resin, which is a heterophasic copolymer of medium fluidity and indicated for the injection molding process, for the manufacture of tubes for agriculture. According to the manufacturer, the EP440L has a flow rate of 6.0 g/10min (at 230°C / 2.16 kg), flexural modulus of 1050 MPa, flow resistance of 24 MPa, flow elongation of 6%, Rockwell hardness 60 (R scale), Izod impact resistance at 23°C without rupture (at -20°C of 75 J/m), thermal deflection temperature of 85°C (at 0.455 MPa) (Braskem S.A., 2018).

3.2.2 Preparation of hybrid bio-composites

All materials were dried in a stove to extract moisture and prevent PBS hydro-degradation (Abderrahim et al., 2015; Muthuraj et al., 2015) that is potentiated by water and high temperature during extrusion processing. The optimum drying conditions were defined by considering the producer datasheet (PTT MCC Biochem, 2023). Briefly, PBS was dried at 80°C for 5 hours in an oven. The materials were extruded in a twin-screw extruder, model DR.16.AX (AX Plásticos Máquinas Técnicas Ltda, Diadema, Brasil), co-rotating, screw diameter (D) of 16 mm and relation length/diameter (L/D) of 40, using a temperature profile of 120/135/140/160/165/170/175/165°C and screw speed of 120 rpm. The literature (Wang et al., 2019; Possari et al., 2021) refers to the temperature of PBS processing around 150°C. The extruded filament was granulated using a granulator with rotating blades coupled to the extruder (AX Plásticos Máquinas Técnicas Ltda, Diadema, Brazil), and they were dried for 8 hours at 80°C to remove moisture.

The formulations of bio-composites are shown in **Table 2**. The percentage of Cana fiber was 30 wt.% for PBS only and for other formulations were 25 wt.% of Cana with 5 wt.% of Lig. These percentages were defined based on pre-tests, which found that more than 30 wt.% of Cana made extrusion difficult to control. MMT and SEP were added over

the PBS/Cana/Lig mixture at 1.17% (codified as MMT1 or SEP1) and 1.72% w/w (codified as MMT2.5 or SEP2.5) with respect to PBS content in each mixture.

Table 2: Formulation of bio-composites.

Sample ID	% (w/w)			
	PBS	Cana	Lig	Clay
Neat PBS (extruded)	100	0	0	0
PBS/Cana	70.0	30.0	0	0
PBS/Cana/Lig	70.0	25.0	5.0	0
PBS/Cana/Lig/MMT1	69.2	24.7	4.9	1.2
PBS/Cana/Lig/MMT2.5	68.8	24.6	4.9	1.7
PBS/Cana/Lig/SEP1	69.2	24.7	4.9	1.2
PBS/Cana/Lig/SEP2.5	68.8	24.6	4.9	1.7

For the mechanical characterization, the granulated samples were molded in ISO format test specimen (ISO 527-1, 2012), using an injection molding machine, with temperature profile 150/160/170/180°C, holding pressure of 700 bar, for 12 seconds, injection pressure of 800 bar and flow rate of 40 cm³/s. For thermal tests, scanning electron microscopy (SEM) and melt flow tests, granulated samples were used.

3.2.3 Characterization

3.2.3.1 Mechanical Properties

The tensile test was carried out in a universal testing machine EMIC DL-2000 (Instron Brasil Scientific Equipment Ltda, São Paulo, Brazil), with 9 kN load cell, according to the ISO 527-1 (ISO 527-1, 2012) standard with atmosphere of 23 ± 2°C and 50 ± 10% relative humidity. Specimen size 1A, gauge length of 50 mm and speed of 5 mm/min. Young's modulus, yield stress (0,2% offset method), yield elongation, tensile strength and elongation at break were obtained to study tensile properties, using at least five specimens for each sample.

The flexural properties were also measured using a universal testing machine EMIC DL-2000, with 9 kN load cell (Instron Brasil Scientific Equipment Ltda, São Paulo, Brazil), speed 2 mm/min, maximum displacement of 20 mm, according to the ISO

178:2019 standards (ISO 178, 2019), length of span between supports 64 mm. The parameters analyzed were flexural modulus, and flexural strength.

The Izod impact test was performed according to ISO 180 (ISO 180, 2019), at 23°C, in an EMIC impact instrument, samples notched (2 mm deep) in a notch sample making machine, model X1S-V (Philpolymer Engineering Thermoplastics Inc, São Roque, Brazil). The hardness SHORE D were measured using Bareiss HPE II Shore D (Bareiss Prüfgerätebau GmbH, Oberdischingen, Germany). The mechanical properties of the composites were also compared to EP-440L polypropylene resin (PP) used to produce tubes for seeding for agriculture.

3.2.3.2 Melting Flow Rate

The behavior of molten composites was evaluated by melting flow rate analysis (MFR) using a plastometer (Maqtest Ltda, Franca, Brazil), according to ISO 1133 part I (ISO 1133-1, 2011), at 190°C and 2.16 kg.

3.2.3.3 Fourier Transform Infrared Spectroscopy (FT-IR)

The FT-IR spectra of the samples were obtained to evaluate changes in the chemical structure of the composite constituents. For this purpose, a Thermo Scientific FT-IR spectrometer, model Nicolet iS10 (Massachusetts, EUA), in ATR mode, wavenumber range 4000-400 cm⁻¹, diamond crystal, flat tip, ambient temperature and sample in powder or pellet form was used.

3.2.3.4 Thermal Analysis

The melt and crystallization of PBS and composites was measured by differential scanning calorimetry (DSC), model Q10 (TA Instruments, New Castle, USA), using about 5 mg of sample in a sealed aluminum pan, under N₂ flow (50.0 mL/min). The samples were first heated from 30 °C to 180 °C and kept for 3 min to remove previous thermal history, then cooled to 30 °C and reheated to 180°C and cooled to 30°C, with a heating/cooling rate of 10°C/min. The second scan was recorded for data analysis. The degree of crystallinity (*X_c*) of PBS was calculated following **Equation 1**.

$$X_c (\%) = \frac{\Delta H_m}{\Delta H_m^0 \times W_{PBS}} \times 100 \quad (\text{Equation 1})$$

where X_C is the degree of crystallinity of PBS, ΔH_m° is the enthalpy of fusion of 100% crystalline PBS (200 J.g⁻¹) (Lule et al., 2020), ΔH_m is the melting enthalpy of the PBS composites obtained by integral of melting peak of PBS on DSC curve, and W_{PBS} is the weight fraction of PBS in the composites.

The thermal stability was evaluated by thermo-gravimetry analysis (TGA) in a model Thermal Analysis System TGA/DSC 3+ (Mettler Toledo, Columbus, USA), the samples were heated from room temperature (28°C) to 950°C, heating rate of 10°C /min, air flow of 50 mL/min.

3.2.3.5 X-Ray Diffraction (XRD)

The structure of PBS and composite components were investigated by XRD analysis, especially regarding to the change in the d -value of the crystalline planes of the clay lamellae, which is indicative of dispersion of the clays due to the exfoliation in PBS. The samples were grounded and sieved in mesh 100 to obtain a fine powder. The analysis was carried out in XRD-6000 diffractometer (Shimadzu, Kyoto-Japan), scan range from 2° to 45° and 2.0°/min (scanning rate), source Cu tube and radiation wavelength (λ) of 0.154056 nm.

3.2.3.6 Scanning Electron Microscopy (SEM–EDS)

The fractured surface of the impact test specimens of the composite samples were characterized through Jeol JSM-5800 LV scanning electron microscopy (SEM), equipped with an Energy Dispersive X-ray Microanalysis system (EDS), (JEOL Ltd, Tokio, Japan), with accelerating voltage of 3 to 20 kV, in order to analyze the morphology and adhesion of the polymer matrix to the fibers. EDS detectors were used to study elemental and mapping composition of composites (clay, Lig, and natural fibers).

3.2.3.7 Statistical Analysis

The data were submitted to the Tukey test to verify significant differences between the averages using Statistica 7.1 (StatSoft, Inc., Tulsa, Oklahoma, USA). Mean values followed by the same letters in the same column do not differ at the 5% significance level (Tukey, $p < 0.05$). The letters are in descending order of mean values. This procedure aims to ascertain the presence or absence of significant heterogeneity in the sample means.

3.3 RESULTS AND DISCUSSION

3.3.1 Melt Flow Rate (MFR)

MFR values determined for each bio-composite are gathered in **Table 3**, that shows the mean value and deviation bar for 10 replicated analyses. The incorporation of Cana fiber led to a reduction in MFR compared to neat PBS, due to a restriction in the fiber's fluidity. In other words, Cana fibers limited the MFR, and no reliable value was obtained. However, the addition of Lig increased the MFR, though not sufficiently to reach the original MFR value of neat PBS. In any case, these results demonstrate the lubricating effect of Lig in the melting state of PBS, reducing the viscosity value, thus counteracting the fluidity problems of PBS/Cana.

At first sight, the addition of clay minerals (MMT and SEP) had minimum influence in the melt viscosity (**Table 3**). Results seemed to indicate that smaller clay percentages (PBS/Cana/Lig/MMT1 and PBS/Cana/Lig/SEP1) tend to increase the MFR values with respect to their counterparts using 1.72% of clay mineral. Despite this trend, the statistical analysis did not show significant differences between PBS/Cana/Lig/MMT1 nor PBS/Cana/Lig/MMT2.5 with respect to PBS/Cana/Lig ($p\text{-value} > 0.05$ and $F < F_{\text{critical}}$). On the contrary, the ANOVA test for PBS/Cana/Lig/SEP (both samples, with 1.17% and 1.72% wt of sepiolite) compared to the PBS/Cana/Lig sample, revealed significant differences ($p\text{-value} < 0.05$ and $F > F_{\text{critical}}$) in the mean MFR values, indicating that SEP increased the MFR compared to the sample without clay.

High melt fluidity is important for processability, especially for the injection molding process (Possari et al., 2021). For comparison, the polypropylene EP440L resin has an MFR of 6.0 g/10min (230°C/2.16kg), despite the lower test temperature for PBS (190°C), which still presented higher MFR values than polypropylene EP440L.

Table 3: MFR results of PBS and composites.

Samples	MFR (g/10 min)
Neat PBS	35.5 ± 0.7^a
PBS/Cana	0.0^d
PBS/Cana/Lig	15.6 ± 0.9^c
PBS/Cana/Lig/MMT1	16.8 ± 1.0^c
PBS/Cana/Lig/MMT2.5	15.6 ± 1.3^c
PBS/Cana/Lig/SEP1	24.5 ± 1.0^b
PBS/Cana/Lig/SEP2.5	16.9 ± 1.1^c

Note 1: Tukey statistical test, mean value with same superscript letters do not differ at the 5% significance level. The letters are in descending order of mean values. Number of replicates n=10. Note 2: PBS/Cana had an MFR result equal to zero.

3.3.2 Fourier Transformed Infrared spectroscopy (FT-IR)

The FT-IR spectrum obtained allows analyzing the chemical structure of composite components and their interactions. **Figure 5A** shows that Cana has a band around 3400–3200 cm^{-1} attributed to hydrogen bonded –OH stretching vibration (Liu et al., 2009), or due free water (moisture) presence (Zhang and Zhang, 2016). MMT are recognized at the overlapping bands of 1042 cm^{-1} (Si-O), 880 cm^{-1} (Al-O-H), and 800 cm^{-1} (Al-Mg-O-H) (Phua et al., 2011). Sepiolite has bands in 3616 cm^{-1} corresponding to the OH stretching vibrations from $\text{Mg}_3\text{O-H}$, in 1656 cm^{-1} due vibrational distortion of water inside the structure, 980, 1010 and 1206 cm^{-1} attributed to Si-O bonds within silica tetrahedra (Chikh et al., 2016). PBS has bands around 1710 cm^{-1} related to the C=O stretching vibration of ester group (Zhang and Zhang, 2016; Zhu et al., 2017), in 1330 cm^{-1} and 2945 cm^{-1} were assigned to the symmetric and asymmetric deformational vibrations of $-\text{CH}_2-$ groups and in 1144–1152 cm^{-1} due the $-\text{C-O-C}-$ stretching in the ester linkages (Phua et al., 2011). As shown in **Figure 5A** to **5D** the position of 1714 cm^{-1} band in neat PBS remained unchanged in the composites, but a slight shoulder appeared at 1602–1608 cm^{-1} upon the addition of both clays, this corresponding to the hydrogen-bonded carbonyl groups (Chikh et al., 2016), indicating the existence of interactions between clays and PBS.

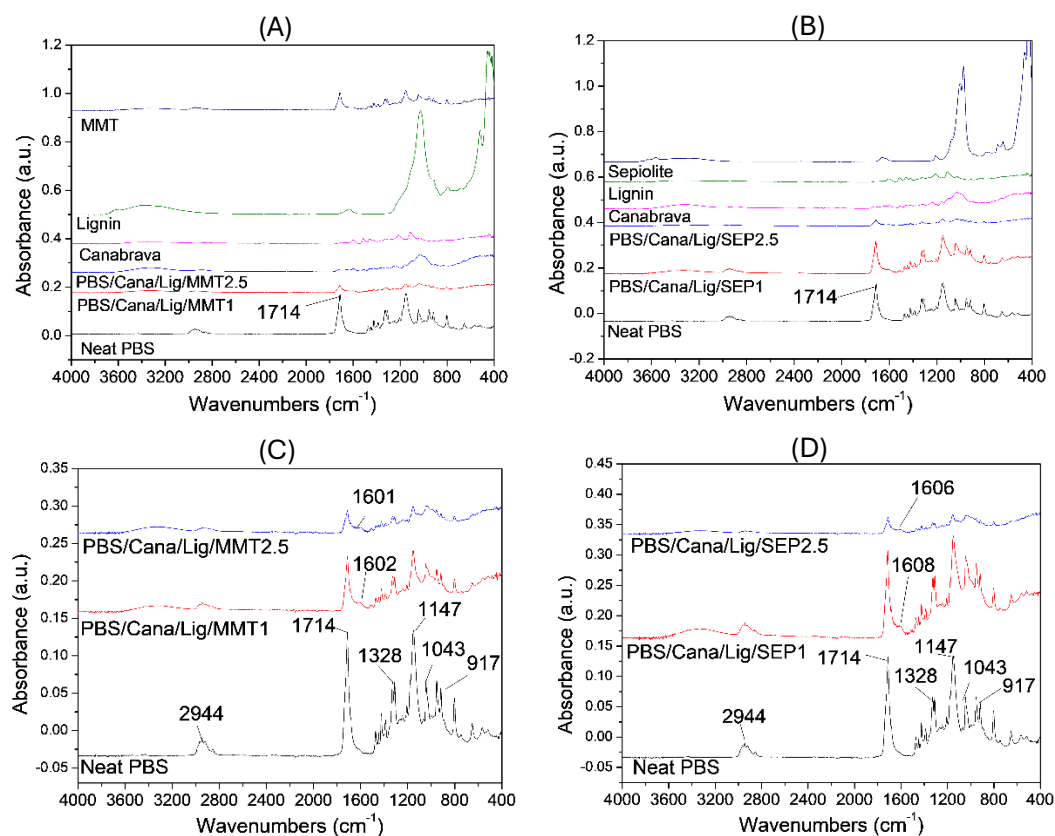


Figure 5: FT-IR spectrum of (A) PBS-MMT composites; (B) PBS-SEP composites. (C) and (D) shows that a shoulder appeared at 1602-1608 cm^{-1} in the composites.

3.3.3 Mechanical characterization

The tensile test curves (**Figure 6**) of the hybrid bio-composite show an increase in Young's modulus and yield stress (**Table 4**) observed with the addition of Cana, as expected, as natural fibers in general have reinforcing capacity, which is why they are used in composites. Lig further contributes to the enhancement of the composite's yield strength. However, MMT seems to exert no significant effect on tensile stress and yield stress (ANOVA showing no significant difference in mean value). On the other hand, the hybrid composite with the presence of SEP slightly increases the tensile strength, tensile yield and Young's modulus values with respect to PBS/Cana/Lig and PBS/Cana (**Table 4**). This indicates better interaction of SEP with PBS, perhaps being favored over MMT due to its greater surface area and its morphology composed of a fibrous structure with micropores and needle-like morphology with silanol groups (Si-OH) on its surface (Huo et al., 2017), resulting in better interaction between inorganic fiber and organic polymer

matrix and improvement in these properties. In all composites, the elongation at break decreased compared to neat PBS (**Table 4**). These results are probably due to the significant Cana fiber content (30 wt.%), which already promotes a high increase in the PBS/Cana modulus compared to pure PBS (+350%) and in the yield stress (+162%), which may have masked or overlapped the effect of the clays. Someya et al. 2003, for example, obtained an increase from 700 MPa to 1000 MPa using 3 wt.% of modified MMT in PBS (Someya et al., 2003), and in the present study the increase obtained with the use of Cana was from 666 MPa to 2350 MPa. The EP440L resin exhibits a yield strength of 24 MPa and a yield elongation of 6%. According to the present results, the yield strength of pure PBS (11 MPa) is lower than that of EP440L. Nevertheless, the addition of Cana fiber, Lig, and ultimately SEP, elevates these values to a maximum of 21.7 MPa, thus being closer to EP440L.

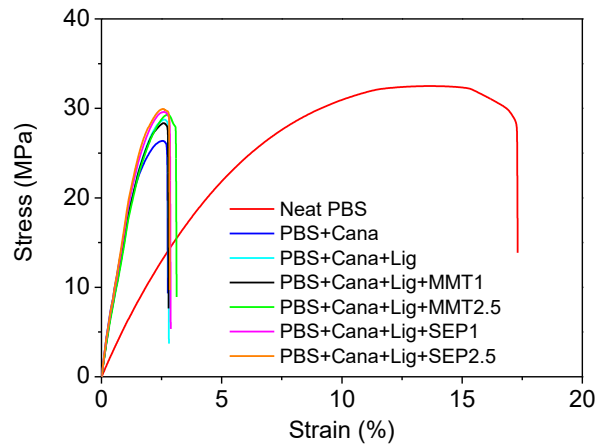


Figure 6: Tensile test curves for Neat PBS and composites.

Table 4: Tensile parameters results.

Samples	Young's Modulus (MPa)	Yield Stress (MPa)	Yield elongation (%)	Tensile strength (MPa)	Elongation at break (%)
Neat PBS	666 ± 9.0 ^c	11.0 ± 0.5 ^d	1.85 ± 0.06 ^a	33.7 ± 0.6 ^a	16.83±2.38 ^a
PBS/Cana	2350 ± 51.4 ^a	17.7 ± 0.6 ^c	0.95 ± 0.02 ^c	26.8 ± 0.3 ^d	2.53 ± 0.10 ^b
PBS/Cana/Lig	2119 ± 30.1 ^c	20.3±0.5 ^{a,b}	1.16 ± 0.03 ^b	29.2 ± 0.3 ^{b,c}	2.53 ± 0.03 ^b
PBS/Cana/Lig/MMT1	2026 ± 25.7 ^d	20.0±0.6 ^b	1.18 ± 0.05 ^b	28.9 ± 0.5 ^{c,d}	2.61 ± 0.19 ^b
PBS/Cana/Lig/MMT2.5	1966 ±22.1 ^d	19.5 ± 0.6 ^{b,c}	1.19 ± 0.02 ^b	29.4 ± 0.2 ^{b,c}	2.93 ± 0.25 ^b
PBS/Cana/Lig/SEP1	2210 ± 29.6 ^b	20.8 ± 0.6 ^{a,b}	1.15 ± 0.03 ^b	30.1 ± 0.4 ^{b,c}	2.65 ± 0.08 ^b
PBS/Cana/Lig/SEP2.5	2309 ± 28.6 ^a	21.7 ± 0.7 ^a	1.14 ± 0.08 ^b	31.3 ± 1.0 ^b	2.59 ± 0.14 ^b

Note: Tukey statistical test, mean value with same superscript letters in the same column do not differ at the 5% significance level. The letters are in ascending order of mean values. Mean values ± s.d. (n = 5).

Neat PBS yield elongation was 1.85%, although the inclusion of Cana resulted in a decrease to 0.95. Generally, the addition of natural fiber negatively affects the mechanical properties of composite, reducing ductility and in some cases the strength, because composites are strongly dependent on fiber content, compatibility, interfacial adhesion, that can cause formation of aggregates, voids in the composite structure, and little bonding between filler and polymer (Platnieks et al., 2020), this is in agreement with the results obtained here with the incorporating of up to 30 wt.% fiber, which leads to a reduction of elongation capacity in the composites compared to the neat PBS. The incorporation of Lig partially offsets the reduction in deformation, whereas clays appear to have negligible impact (**Table 5**). In terms of yield elongation, neat PBS exhibit lower values than EP440L (its yield elongation being 6%). Contrary to the yield tension, the introduction of Cana and Lig do not approach elongation values closer to EP440L.

The impact resistance of the composite decreases with the addition of Cana when compared to neat PBS, and the inclusion of Lig further reduces impact resistance. Some authors only show the tensile properties results and do not show impact resistance results for PBS-MMT composites (Ojijo and Ray, 2014; Tian et al., 2016) , and other shows that impact strength was reduced with addition of 2 wt.% of MMT (unmodified) in PBS (Phua et al., 2011), which the impact strength reduced from 8.78 kJ/m² to 8.3 kJ/m². In particular case, the decrease in impact strength of the composites could be attributed to the significant Cana fiber content (>30 wt.%), which could have led to difficulties in incorporation into PBS and poor fiber-polymer interfacial adhesion. The addition of clay minerals (MMT or SEP) did not influence this parameter, as illustrated in (**Table 5**). The large amount of Cana fiber may be overriding the impact resistance results with the use of other additives (Lig and clays), without any improvements being observed. In fact, the ANOVA test indicates no significant difference in impact resistance between the PBS/Cana/Lig samples with and without the clays. These findings suggest that Lig does not function as a plasticizer—which would typically increase both melt flow rate (MFR) and impact resistance—but as a lubricant. The EP440L resin remained intact under impact at 23°C, showing no signs of rupture. In general composites with natural fiber show brittle tensile behavior, caused by the formation of aggregates, voids in the composite's structure, and weak bonding between filler and polymer, furthermore, pure thermoplastic represents a continuous material, while composites present two phases, inherently

presenting some discontinuities, which can lead to the initiation of crack propagation (Frollini et al., 2013).

Table 5: Impact resistance and hardness Shore D results.

Samples	Impact Resistance (KJ/m ²)	Hardness Shore D
Neat PBS	19.4 ± 0.3 ^a	67.6 ± 0.3 ^c
PBS/Cana	16.5 ± 0.5 ^b	70.7 ± 1.2 ^{a, b}
PBS/Cana/Lig	15.6 ± 0.3 ^{b, c}	69.6 ± 0.6 ^{a, b, c}
PBS/Cana/Lig/MMT1	15.2 ± 0.2 ^{b, c}	70.6 ± 1.2 ^b
PBS/Cana/Lig/MMT2.5	15.1 ± 0.2 ^{b, c}	70.5 ± 1.2 ^{a, b}
PBS/Cana/Lig/SEP1	14.6 ± 0.2 ^c	68.9 ± 0.7 ^{a, c}
PBS/Cana/Lig/SEP2.5	14.7 ± 0.3 ^c	70.3 ± 1.4 ^{a, b}

Note: Tukey statistical test, mean value with same superscript letters in the same column do not differ at the 5% significance level. The letters are in descending order of mean values. Mean values ± s.d. (n = 5).

The hardness of PBS composites increased by the use of the main additives (Cana and Lig). According to results, it is possible to hypothesize that the ingredient responsible for hardness increase is Cana, the highest value reported for PBS/Cana. Moreover, Cana is present in all composites, explaining why the hardness Shore D values remained higher than neat PBS. Lig and clays have little or no effect on hardness (**Table 5**).

Flexural tests are important for the application, its results gathered in **Figure 7** and **Table 6**, which show the average curves of each sample. The flexural modulus is a critical parameter for material application. As demonstrated by the data, the flexural modulus and flexural strength (**Table 6**) increase across all composite formulations when compared to neat PBS. The inclusion of Lig is observed to decrease the flexural modulus relative to composites containing Cana. Clays exert a minor influence, slightly enhancing the flexural modulus and strength. The flexural modulus of pure PBS was 664 MPa, lower than the 1050 MPa of the EP440L resin, indicating reduced flexural stiffness. However, the biocomposites exhibit flexural modulus values ranging from 2275 MPa (PBS/Cana/Lig/MMT1) to 2462 MPa (PBS/Cana/Lig/SEP2.5), exceeding that of EP440L. This suggests the potential for reducing the flexural modulus through additives such as plasticizers, which could improve impact resistance and yield elongation values, currently lower than those of EP440L.

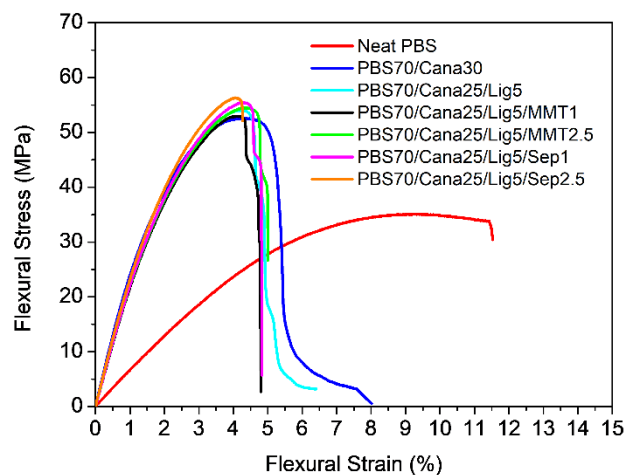


Figure 7: Flexural test curves (each curve is an average of 5 samples tested).

Table 6 Flexural parameters results.

Samples	Flexural Strength (MPa)	Flexural Modulus (MPa)
Neat PBS	35.2 ± 1.4^d	664 ± 38^d
PBS/Cana	52.7 ± 0.6^a	2588 ± 19^c
PBS/Cana/Lig	54.2 ± 1.0^c	$2333 \pm 53^{b,c}$
PBS/Cana/Lig/MMT1	53.4 ± 1.1^c	2275 ± 36^c
PBS/Cana/Lig/MMT2.5	54.6 ± 0.2^c	$2322 \pm 59^{a,b,c}$
PBS/Cana/Lig/SEP1	55.7 ± 1.1^c	$2334 \pm 45^{a,b}$
PBS/Cana/Lig/SEP2.5	56.6 ± 0.5^b	2462 ± 26^a

Note: Tukey statistical test, mean value with same superscript letters in the same column do not differ at the 5% significance level. The letters are in ascending order of mean values. Mean values \pm s.d. (n = 5).

3.3.4 Thermal analysis

The thermal stability of polymer materials influences their flame retardancy and thermal degradation characteristics. Consequently, analyzing thermal stability is an effective method for evaluating these properties. According to literature (Frollini et al., 2013; Liminana et al., 2018), degradation of a lignocellulosic filler takes place in four different stages: water removal (50-60 °C), hemicellulose degradation (300-320 °C), cellulose degradation (345-365 °C) and, finally, Lig degradation ($T > 400$ °C). The weight loss around 180.0 °C is ascribed to dehydration of chemically bonded water and hydroxyl groups in Lig, resulting in a mass loss of about 5%. A minor shoulder at about 285.5 °C (**Figure 8B**) is attributed to the partial decomposition of carboxylic and anhydride groups and the decomposition of the residual hemicellulose in kraft Lig, with mass loss about

6.7%. The maximum Lig mass loss occurs between 290 °C and 600 °C which corresponds to the pyrolysis of Lig (Yan et al., 2021). Lig degradation generates water, methanol, CO, and CO₂ (Liminana et al., 2018). According to the literature, the degradation of PBS occurs as chain degradation, exhibits a single stage degradation (single DTG peak) and starts at approximately 280-300°C, with a peak at 410°C, and the decomposition is almost complete at 430-440°C (mass loss >90 wt%) (Frollini et al., 2013). The TGA thermograms in **Figure 8A** show that mass loss starts in around 240 °C and the values of temperature of mass loss of 5 wt% ($T_{WL5\%}$), 50wt% ($T_{WL50\%}$), 90%wt ($T_{WL90\%}$), maximum mass loss (T_{max}), temperature at peak of mass loss rate (T_d) of PBS and composites are presented in **Table 7**. The temperature at peak (T_d) of mass degradation can be found in DTG analysis (**Figure 8B**).

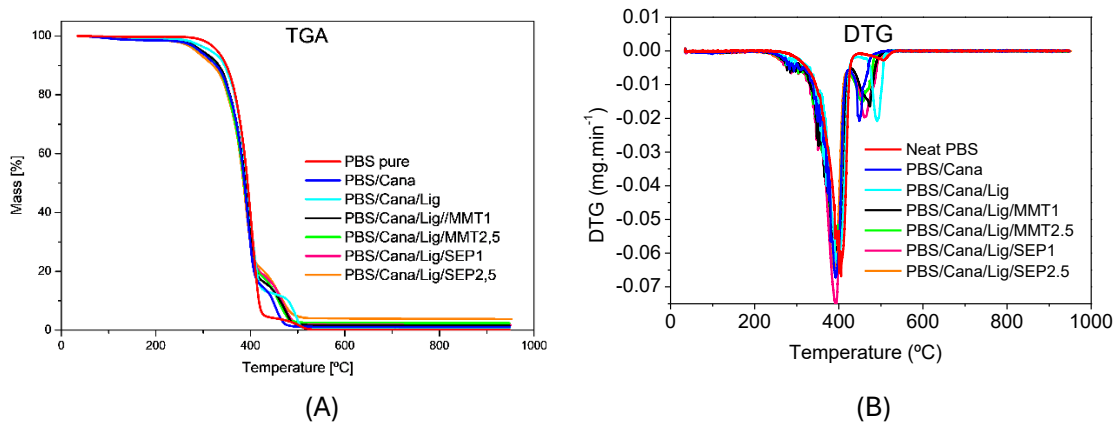


Figure 8: (A) Thermogravimetric Analysis (TGA), and (B) Differential Thermogravimetric (DTG) Analysis.

Table 7: Degradation results parameters of TGA analysis.

Sample	$T_{WL5\%}$ (°C)	$T_{WL50\%}$ (°C)	$T_{WL90\%}$ (°C)	T_{max} (°C)	T_d (peak) (°C)	Residual Mass (%)
Neat PBS	329.7	394.2	418.2	424.3	402.6	0.14
PBS/Cana	292.0	387.5	447.8	470.9	392.8	1.06
PBS/Cana/Lig	315.6	393.2	479.9	507.8	395.5	0.63
PBS/Cana/Lig/MMT1	297.2	389.3	463.0	489.6	391.6	1.51
PBS/Cana/Lig/MMT2.5	291.8	386.7	459.4	483.7	390.5	2.36
PBS/Cana/Lig/SEP1	291.5	386.9	466.4	492.2	393.2	1.77
PBS/Cana/Lig/SEP2.5	284.4	385.1	468.7	493.3	389.1	3.77

As can be seen in **Table 7**, $T_{WL5\%}$ and $T_{WL50\%}$ of PBS/Cana and PBS/Cana/Lig were smaller than neat PBS, somewhat expected since Cana and Lig are organic compounds

that usually degrade at lower temperatures than neat PBS. Moreover, the addition of clay particles to these composites further reduces $T_{WL5\%}$ and $T_{WL50\%}$ with respect to neat PBS. MMT and SEP are inorganic minerals whose thermal events are mainly due to water loss (free water, bound water) from 30-500°C and dehydroxylation from 500°C (SEP) and 600°C (MMT) (García-Quiles et al., 2019; García-Villén et al., 2019, 2020). In all cases, the weight loss experienced by clay during these events is minimum (2-7%, depending on the environmental conditions in which they were preserved until use). The evaporation of water bound to clay structures can be explaining the decrease in $T_{WL5\%}$ and $T_{WL50\%}$. A decrease in degradation temperature of the organic compounds (Cana and Lig) can also be feasible, since the presence of clay particles can “disperse” organic molecules in the composite structure, making them more susceptible to thermal degradation.

The $T_{WL90\%}$ increased with Cana, Lig and clays addition, from 418.2°C for neat PBS to around 460~470°C for the rest of the composites. The T_{max} has a more significant increase in composites (around 490°C) compared with neat PBS (424.3°C). More into detail, SEP is slightly better in terms of thermal stability compared with MMT because the T_{max} of SEP composites are around 492~493°C, while MMT ones are around 483~489°C. By the same token $T_{WL90\%}$ values of SEP are higher than MMT composites (466~468°C for SEP and 459~463°C for MMT). The residual mass result obtained by TGA analysis seems consistent with the content of the materials. Neat PBS presented a very low residual (0.14%). The addition of Cana fiber (30 wt.%) resulted in a residual of 1.06%, indicating a low ash content. The residual of the PBS/Cana/Lig sample had a slight decrease (0.63%), perhaps it is due to the smaller amount of Cana that was replaced by the Lig mass. An increase in the residual is observed in the other samples due to the addition of clays.

The DSC curves (**Figure 9A**) show two main peaks, one endothermic peak at 115.0°C (for neat PBS) that can be attributed to a crystalline melting transformation (T_m) and other peak (exothermic) at 72.7°C (for neat PBS), corresponding to crystallization of PBS. The T_m values of PBS (around 115°C) did not change with the addition of Cana, Lig and clays (**Figure 9B** and **Table 8**), but SEP caused the appearance of a small peak at 103-104°C, while for neat PBS and other composites appear a shoulder (near 110°C). Several authors (Liang et al., 2009; Liminana et al., 2018; Arabeche et al., 2022) reported that PBS can present three peaks (T_{m1} , T_{m2} and T_{m3}), the main and higher temperature T_m peak (T_{m1}) is not related to the crystallization of previous cooling process and attributed to the recrystallization of the partially melted crystals during heating process (melting–

recrystallization–remelting process). The others small T_m peaks (T_{m2} and T_{m3}) are possibly attributed to the melting of original crystals with different crystalline lamella distribution with different thermal stabilities. The appearance of the T_{m3} peak when SEP is added to PBS is a strong indication of good SEP-PBS interaction, since T_{m3} peak is attributed to the formation of original crystals in the interfacial region between the clay and the polymer (Arabeche et al., 2022), while the melting temperature T_{m1} remains unchanged. This can denote a good dispersion of SEP and its ability to crystallize at its interface. PBS has a low crystallization temperature (72.7°C) (**Figure 9C** and **Table 8**) but the peak shifted to a higher temperature with the addition of Cana, Lig and MMT (around 78°C), and increased further with the addition of SEP (around 86 °C), indicating that the crystallization rate of PBS was enhanced with the addition of these, especially SEP. The increase in PBS crystallization can be attributed to the effect of fillers such natural fiber and clays have on the nucleation of crystallization (Liang et al., 2009).

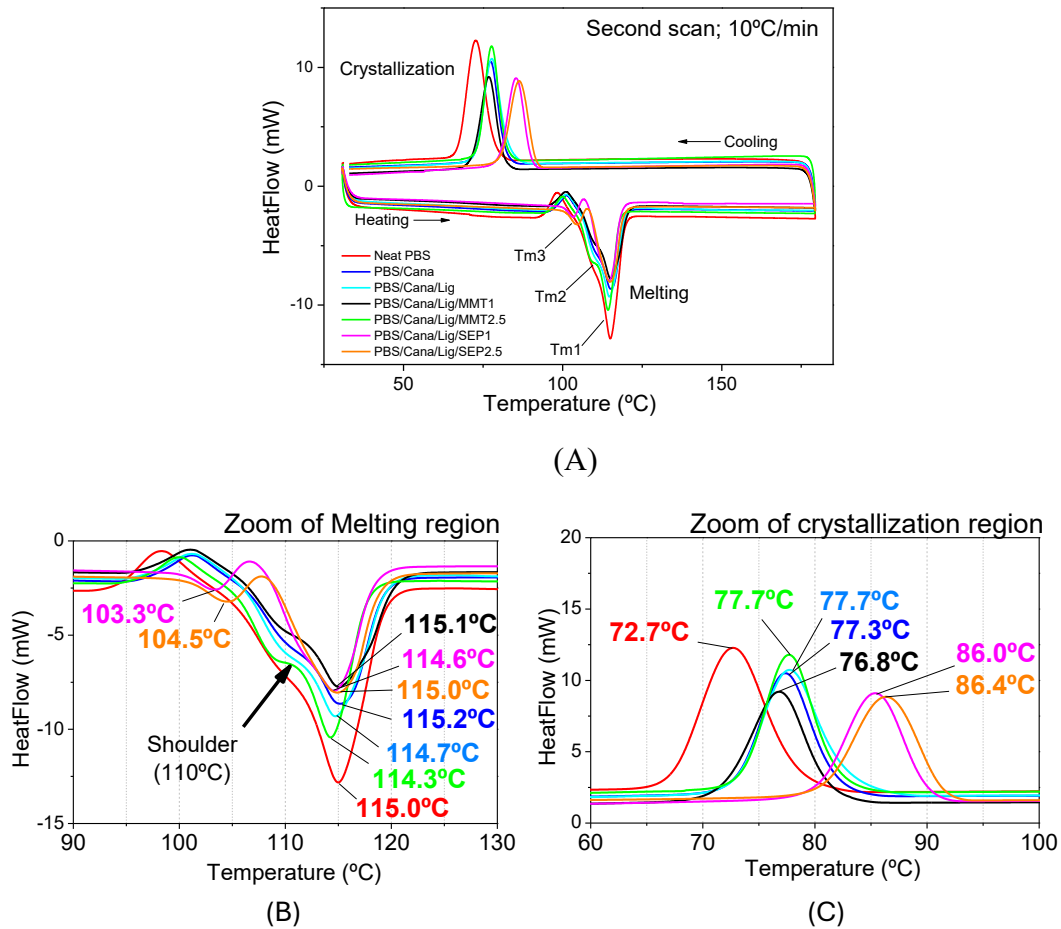


Figure 9. Comprehensive DSC Analysis of PBS Composites: (A) Full Thermal Profiles; (B) Detailed View of the Melting Temperature Region; (C) Detailed View of Crystallization Region.

Table 8: parameters result of DSC analysis.

Sample	T_c (°C)	T_m (°C)	ΔH_m (J/g)	X_c (%)
Neat PBS	72.7	115.0	67.17	33.6%
PBS/Cana	77.3	115.2	54.48	38.9%
PBS/Cana/Lig	77.7	114.7	55.30	39.5%
PBS/Cana/Lig/MMT1	76.8	115.1	52.08	37.6%
PBS/Cana/Lig/MMT2.5	77.7	114.3	54.57	39.5%
PBS/Cana/Lig/Sep1	86.0	114.6	56.55	40.9%
PBS/Cana/Lig/Sep2.5	86.4	115.0	53.05	38.4%

The melting enthalpy (ΔH_m) and degree of crystallinity (X_c) increased with the addition of Cana, Lig, and clays (**Table 8**), possibly enhanced by the nucleation effect of these components. Some studies found that the degree of crystallinity of PBS increases with the content of cellulose filler, achieving 35% crystallinity with 30% of natural fiber (Liang et al., 2009).

3.3.5 X-Ray Diffraction (XRD)

The XRD diagrams of clays, neat PBS and composites are shown in **Figure 10A** (with MMT) and **Figure 10B** (with SEP). Native sepiolite has characteristics reflections are in the planes (1 1 0), (0 4 0) and (4 0 0) at $2\theta = 7.2^\circ$, 19.6° , 26.5° , respectively (Nikolic et al., 2017). MMT exhibits a broad reflection at $2\theta = 6.08^\circ$, corresponding to the 0 0 1 basal reflection with a d_{001} -value of 1.45 nm (Phua et al., 2011).

Analyzing XRD diagrams, MMT presents a reflection for (0 0 1) plan at $2\theta = 5.3^\circ$ corresponding to a d-value of 1.67 nm, calculated using Bragg condition, $n\lambda = 2.d.\sin(\theta)$, but the composite did not present that plane (0 0 1) (**Figure 10A**). Some authors (Someya et al., 2003; Chen et al., 2015; Soares et al., 2017) show that the absence of this reflection in the composite, strongly indicates a exfoliation of the clay, especially below 5 wt.% of MMT. This is an indicative of achievement of MMT exfoliation in PBS/Cana/Lig/MMT2.5 composites, but it was not confirmed by improvements in other properties (mechanical for example), perhaps due to the large dosage of Cana fiber, which ended up overlapping its effect.

Related to SEP, the reflection 2θ for (1 1 0) plan in the composite, changed a little (7.3° to 7.1°), this represents a d_{001} -value varying from 1.210 nm to 1.244 nm ($\Delta d = 0.034$

nm), and the approximate width of the extended molecular chain of PBS is about 0.4 – 0.6 nm (Someya et al., 2003), then Δd is lower than the width of the PBS, indicating that PBS did not intercalated into SEP interlayer space.

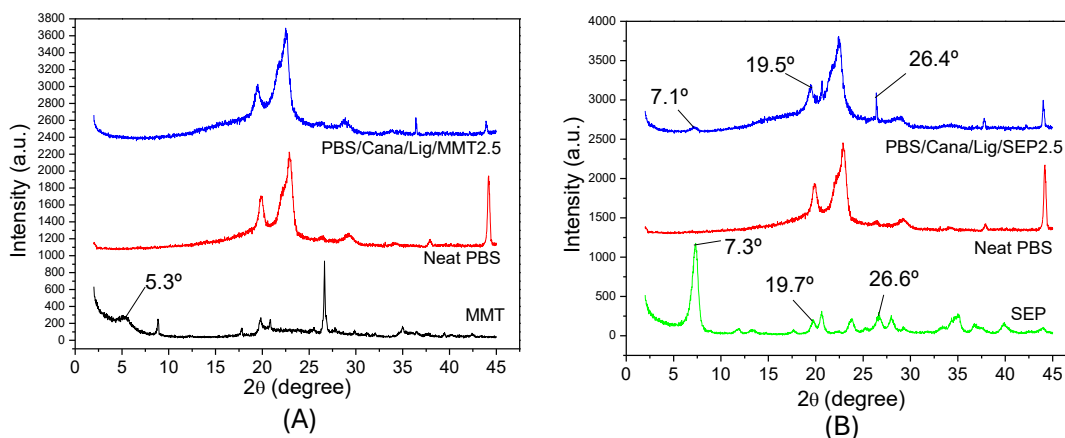


Figure 10: XRD diagrams of (A) MMT, PBS and composite; (B) SEP, PBS and composite.

3.3.6 Morphology Analysis

The morphology of the samples after break (at Izod impact test) were studied by SEM. PBS/Cana composites (**Figure 11A**) show the presence of Cana fibers embedded in the PBS matrix. It is possible to observe in some images (**Figures 11A, C and D**) that the Cana fibers detach from the polymer matrix, indicating a certain lack of fiber-matrix adhesion, resulting in low impact resistance. As explained previously, this may be due to the high percentage of Cana fiber used (up to 30 wt.%), which may have led to its poor incorporation into the PBS. In addition, the low natural fiber-polymer interaction is already widely reported in the literature due to the hydrophilic character of cellulose in natural fibers that contain hydroxyl groups and the hydrophobic character of polymers (Miao and Hamad, 2013), causing a certain incompatibility that can be minimized by using various methods to improve this interaction, such as the use of compatibilizing agents, functionalization, chemical treatment of the fibers (Platnieks et al., 2020). PBS/Cana/Lig/MMT2.5 composite images are gathered in **Figure 11C**, whereas **Figure 11D** corresponds to PBS/Cana/Lig/SEP2.5. As happened with the rest of the samples, Cana fibers are visible after the impact test. Although clay mineral particles are not distinguishable by this SEM analysis, EDS analysis (**Figure 11E and F**) proved their presence by the detection of Si and Mg, and sulfur is supposed to be from Lig. The distribution of these elements (Si, Mg, Al, S) in the composite can be seen by EDS map

image of PBS/Cana/Lig/MMT2.5 sample, is available in **Supplementary Material 2 (Figure 13)**, which presents a good dispersion of the clay in the PBS matrix due to the good shear mixing promoted by the twin screw extruder processing. Nevertheless, by taking a closer look at the PBS textural aspect, a more compact PBS matrix can be detected in samples with clays when compared to PBS/Cana and PBS/Cana/Lig. These morphologies are somewhat coherent with impact test results, indicating that the addition of MMT and SEP reduced the impact resistance of the composites, even if no statistically significant differences were found.

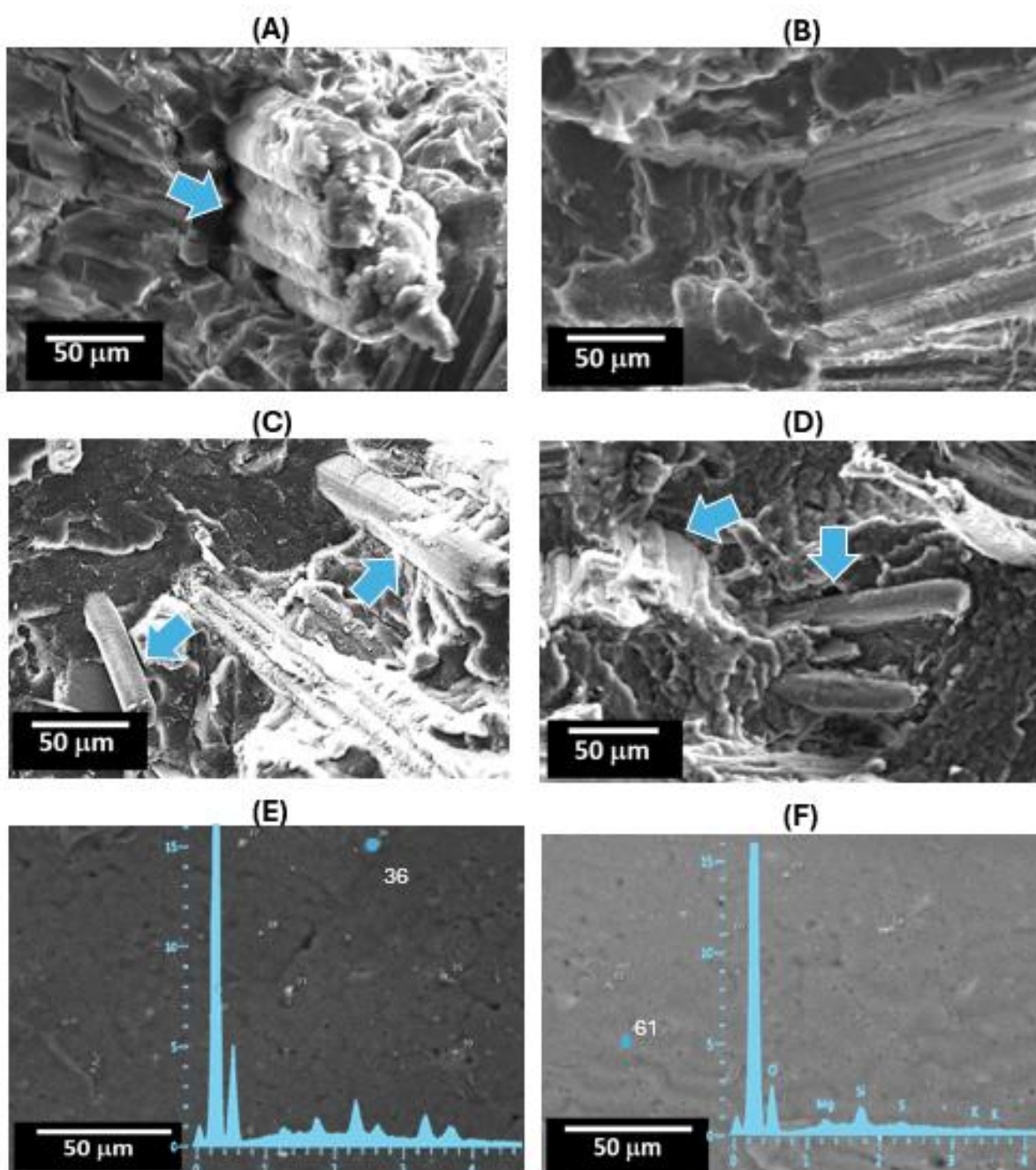


Figure 11: SEM images and EDS and microanalysis of composites. (A) PBS/Cana. (B) PBS/Cana/Lig. (C) PBS/Cana/Lig/MMT2.5. (D) PBS/Cana/Lig/SEP2.5. (E) EDS

microanalysis for PBS/Cana/Lig/MMT2.5. (F) EDS microanalysis for PBS/Cana/Lig/SEP2.5.

3.4 CONCLUSIONS

In the present study, naturally occurring residues and natural clay minerals are combined and proposed as functional ingredients of biodegradable composites for agricultural use. Polybutylene succinate (PBS) was chosen as the main polymer due to its biodegradability, although its properties require further enhancement with the use of other environmentally friendly ingredients, such as canabrava (Cana), Lignin (Lig), montmorillonite (MMT) and sepiolite (SEP). Polypropylene resin EP440L was used as a reference standard due to its common application in seedling production. The addition of 30% Cana reduced the melt flow rate (MFR) of the PBS composite; however, this effect was partially mitigated by the lubricating effect of Lig and SEP, resulting in an MFR similar to that of EP440L. Cana and SEP significantly increased the stiffness and flexural strength of the composites. Thermal analyses revealed an increase in crystallization and thermal stability, with sepiolite outperforming montmorillonite. Although the impact resistance of the composites decreased, the results indicate that the incorporation of PBS with Cana, Lig, and natural clays enhances the composite properties, thereby improving their efficacy and environmental sustainability for agricultural use, particularly in seedling cultivation processes.

Supplementary Material (SM1):

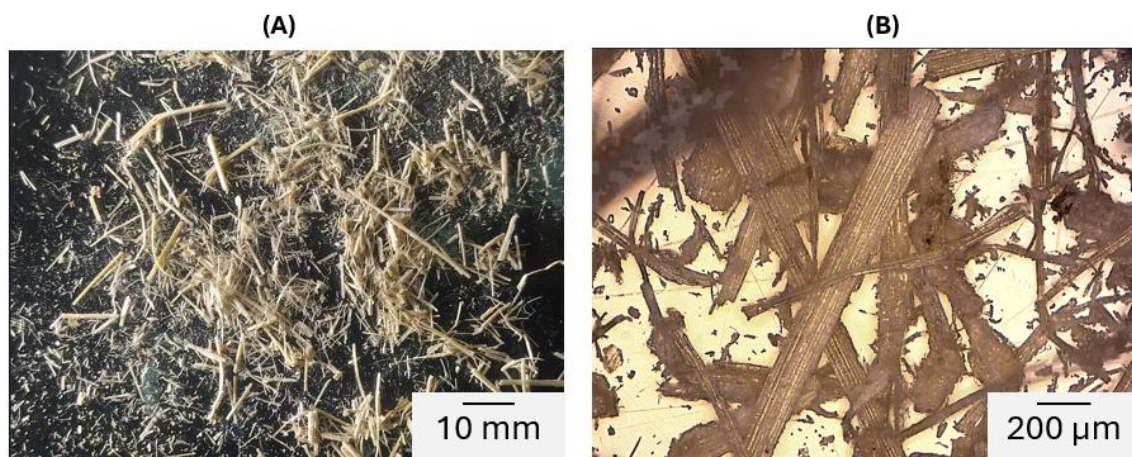


Figure 12: Optical microscope image of Cana fiber. A) 1x magnification; B) 50x magnification.

Supplementary Material (SM2):

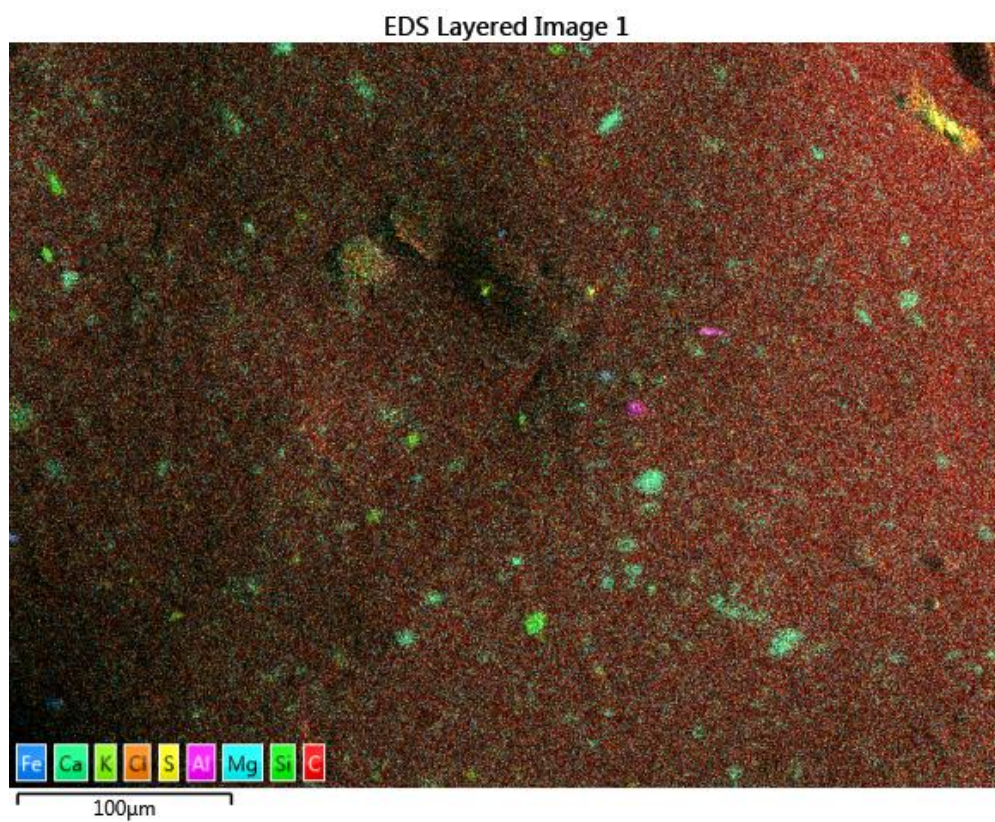


Figure 13: EDS mapping image for PBS/Cana/Lig/MMT2.5.

CHAPTER 4

This chapter is part of a research paper entitled “**Advanced biodegradable materials: the development of PBS hybrid composites reinforced with natural fibers, lignin, and sepiolite for sustainable applications**” published in the *Journal of Applied Polymer Science (Wiley VCH)*, submitted on 14th April 2025 and accepted for publication on 20th June 2025. DOI 10.1002app.20251219.

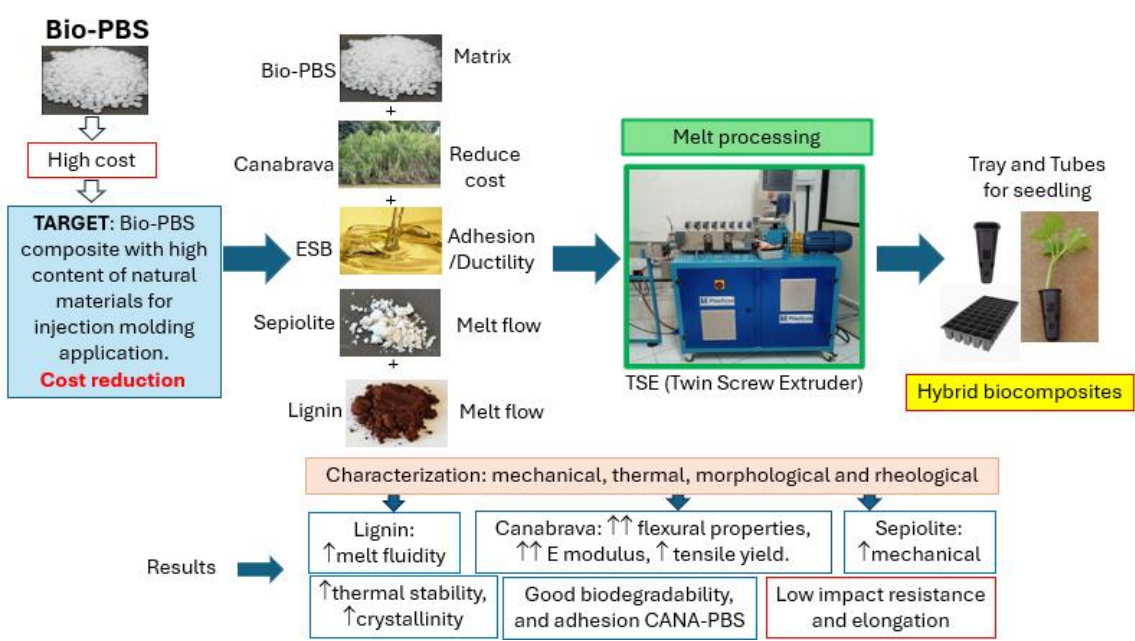


Figure 14: Graphical abstract of second article published at Journal of Applied Polymer Science.

4.0 RESEARCH PAPER 2:

Article title: “Advanced biodegradable materials: the development of PBS hybrid composites reinforced with natural fibers, lignin, and sepiolite for sustainable applications”.

4.1 INTRODUCTION

The rapid growth of the plastics industry has significantly benefited the global economy, but its expansion has outpaced efforts to manage its environmental impact. Increasing plastic production and consumption contribute to critical challenges, including pollution, resource depletion, economic burdens, and climate change. Furthermore, the heavy reliance on fossil-based plastics results in a high carbon footprint, intensifying environmental harm throughout the plastic lifecycle. Single-use plastics in packaging are a major driver of global plastic pollution. Specifically for agricultural applications, plastic waste management poses a recycling challenge due to logistical and cost-related barriers. For example, plastic seeding trays are commonly made from polypropylene (PP), a non-biodegradable fossil-based resin (IBF, 2023).

Addressing these issues requires innovative solutions and a transition toward a circular economy (OECD, 2022), such as the use of biopolymers, which offer a promising alternative as they are partially or entirely derived from biomass and can decompose under composting conditions or, in some cases, naturally. Their biodegradability and lower greenhouse gas emissions make them a key component of a more sustainable plastic economy (Bozell and Petersen, 2010). In this context, polybutylene succinate (PBS), emerges as a promising alternative, as it is bio-based (produced from renewable sources) and biodegradable (PTT MCC Biochem, 2023). PBS is an aliphatic polyester obtained through the polycondensation of succinic acid and 1,4-butanediol (Kuenz et al., 2020). PBS possesses good mechanical, thermal, and physical properties (Sisti et al., 2016), comparable to fossil-based polyolefins such as polyethylene (PE) and polypropylene (PP), making it a suitable candidate for packaging and injection-molded applications. However, the widespread application of PBS is limited by its high production cost and

some intrinsic property constraints, such as low stiffness, slow crystallization rate, and limited gas barrier performance (Barletta et al., 2022).

To face these challenges and enable the use of PBS in higher-value applications where customers perceive its value, ongoing research explores various techniques involving cellulose-derived products, such as cellulose nanofibril (CNF), cellulose nanocrystal (CNC) or cellulose microcrystal (MFC) composites (Joy et al., 2017; Sun et al., 2018; Nabels-Sneiders et al., 2023). These nanocomposites are particularly promising due to their origin from cellulose, a natural and renewable raw material and the ability to achieve significant property enhancements with only a small addition of nanocomponent. However, their production requires a series of complex chemical and mechanical treatments (Platnieks et al., 2021).

In this context, eco-friendly biocomposites (Behera et al., 2024; Pattnaik et al., 2024a), also known as green chemistry (Pattnaik et al., 2025) or green composites (Pattnaik et al., 2024a, 2024b) present a sustainable solution to address the limitations of biopolymers, such as low stiffness and high cost, while simultaneously incorporating natural waste materials that would otherwise be discarded. Thus reinforcing PBS with low-cost natural materials such as natural fibers, lignin, and mineral clay can improve these limited properties of PBS and is a promising strategy (Sisti et al., 2016). Canabrava (CANA) fiber (*Gynerium Sagittatum*) is natural, abundant, easy to extract and treat, can be used as low-cost waste from handcraft production in some Brazilian communities (Coradin et al., 2011) is an interesting option to be incorporated into PBS to obtain a biocomposite. Untreated CANA fiber contains 91.6% of structural components (59.83% of cellulose, 20.67% of hemicellulose, 11.07% of lignin) and 8.43% of non-structural components such as waxes, fats, proteins, pectin and other impurities (Franca et al., 2019). CANA has more cellulose content compared to other natural fibers such as sugarcane (38-

45% of cellulose, 23-26% of hemicellulose, and 19-25% of lignin), but less than rami fiber (68-76% of cellulose) or cotton (90-95% of cellulose). The high cellulose content is important for nano fibril cellulose obtention. Cellulose and hemicellulose are structural components, although with greater affinity for water due to hydrophilic hydroxyl (-OH) groups, they can improve mechanical properties such as stiffness and strength of composites (Platnieks et al., 2020).

Despite its abundance and promising composition, there is a lack of research on the application of canabrava fiber (*Gynerium sagittatum*) in more advanced or technological materials. Most of the existing literature focuses on its traditional uses, particularly in artisanal or low-tech applications. For instance, Osorio et al., 2018, (Osorio et al., 2018) investigated the use of canabrava fiber in the production of plywood panels, demonstrating its potential as a renewable raw material for structural purposes. However, no studies to date have explored its incorporation into hybrid bio-composites, especially in formulations that combine biopolymers with functional additives such as lignin, clay, and bio-based compatibilizer/plasticizer. This represents a significant knowledge gap and an opportunity to evaluate the technological viability of canabrava fiber in sustainable composite systems.

Another important natural component that can be incorporated into PBS composites is lignin (LIG) (Shah et al., 2023), a natural aromatic polymer found in plant cell walls. LIG is produced in large quantities as a low-value byproduct of pulp and paper industries and is typically burned for energy generation. LIG can bring beneficial properties including biodegradability, thermal stability, low density and some mechanical properties (flexural modulus), making a viable option to produce composites with biopolymers such as polybutylene succinate (PBS) (Ewurum and McDonald, 2025). LIG can be used in

applications in the packaging and healthcare industries, due to its antioxidant and antimicrobial properties (Domínguez-Robles et al., 2020; Basbasan et al., 2023).

To modulate some mechanical and physical properties of composites, nano clay fillers can be used, because they are natural minerals that can achieve a high dispersed state in the matrix, enhancing interesting properties. Many natural or synthetic fillers have been studied, unlike sepiolite (SEP), which has few studies, even though it is a natural fibrous mineral clay similar to talc (Chikh et al., 2016). SEP is a needle form nanofiller with open channels along fiber direction with hydrated magnesium silicate, having unit cell formula of $\text{Mg}_4\text{Si}_6\text{O}_{15}(\text{OH})_2 \cdot 6\text{H}_2\text{O}$ (Farshchi and Ostad, 2020; García-Villén et al., 2020). Some properties of hydrophilicity, fibrillary needle shape, high porosity, low cost, easily dispersible in polymer matrix by shearing (Chikh et al., 2016), improved tensile, flexural, and thermal properties (Farshchi and Ostad, 2020), elongation to break (Huo et al., 2017).

The use of high content of natural fiber (such as CANA) can minimize the cost of PBS compared to polyolefins, but it can lead to difficult processability due to reduced melt fluidity and may bring some loss of properties such as impact strength and ductility, especially due to poor interfacial adhesion of fiber-polymer (Platnieks et al., 2020). In principle, increasing the processing temperature can lead to an increase in the fluidity of the melt, but on the other hand, great care must be taken to avoid thermal degradation of PBS, which is very sensitive to temperature increases and can result in chain scission, decreasing its molecular weight, and decreasing its mechanical properties (Abderrahim et al., 2015). In addition, higher processing temperature can lead to hydro degradation in polymers obtained by polycondensation (Muthuraj et al., 2015), such as PBS, due to the residual moisture present in natural fibers such as CANA and enhanced by high temperatures (such as processing temperatures), shifting the reaction equilibrium in the opposite direction to that of polymerization, that is, in the direction of the reactants. An

interesting option instead of increasing processing temperature is the use of LIG (a low-cost byproduct from cellulose industry) that can improve melt flow rate of composite because it has lubricant effect (Possari et al., 2021), SEP (a natural mineral clay) can modulate flexural and thermal properties. The high CANA content also reduced ductility and impact strength, so natural plasticizer can be used to improve these issues. Plasticizer such as castor oil (De Oliveira Santos et al., 2014), linseed oil (epoxidized) (Liminana et al., 2018), soybean oil (epoxidized) (Zhao et al., 2012; De Oliveira Santos et al., 2014; Liminana et al., 2018; Rafiqah et al., 2021), which are obtained from renewable source and they are known as plasticizers properties, but some authors found good results with these additives acting as compatibilizer, improving interfacial adhesion fiber-polymer for impact strength and enhancing elongation at break for composites (Sahoo et al., 2013; Liminana et al., 2018; Turco et al., 2024).

This study aims to develop and characterize hybrid eco-friendly composites based on PBS, reinforced with CANA, LIG, and SEP, with ESB serving as a compatibilizer and plasticizer. The effects of these components on the mechanical, thermal, and biodegradation properties of the PBS composites will be systematically evaluated. The ultimate goal is to assess the potential of these materials for sustainable applications, particularly in agricultural packaging, as an environmentally friendly alternative to fossil-based plastics. The effects of these components on the mechanical, thermal, and biodegradation properties of PBS composites will be comprehensively evaluated.

This system represents an advanced biodegradable material, developed by combining bio-based PBS with underexploited Canabrava fibers (a low-cost waste fiber), bio-based ESB compatibilizer/plasticizer, lignin (a byproduct of the pulp and paper industry) and sepiolite (a natural mineral clay), all sourced from natural or renewable material. This innovative biocomposite differs from conventional alternative materials due to its

multifunctional formulation, integrating natural fibers, a bio-based compatibilizer/plasticizer and an inorganic reinforcement, resulting in an eco-friendly biocomposite with enhanced processability, mechanical and thermal performance, sustainability and a more cost-effective profile.

4.2 MATERIALS AND METHODS

4.2.1 Materials

The bio-PBS was provided by PTT-MCC Biochem, melt flow rate (MFR) of 22 g/10min (190°C, 2.16 kg), glass transition temperature of -36°C, melting temperature of 115°C, and specific mass of 1.26 g/cm³ (PTT MCC Biochem, 2023). The lignin (kraft type) was provided by a Brazilian paper and cellulose industry. The canabrava fiber was collected from a Brazilian local community in Salvador, Bahia called Ilha de Maré, as a residue of the handcraft production. This canabrava residue was in a long strips form varying from 1 m to 2 m in length. To be used in the composite, the CANA fiber was initially crushed in a TRE40MA crusher (Tramontina S.A., Carlos Barbosa, Brazil) with the aim of reducing the size of the fibers to a few centimeters in length. After that it was grinded in a LQL8BIVMF60N5 blender (BIMG Ltda, Brusque, Brazil), and the material was sieved to obtain CANA fibers with mean length of 3.18 ± 1.90 mm and a width of 0.45 ± 0.23 mm. These values were calculated using image analyzer software ImageJ by measuring more than one thousand fibers of CANA from images obtained in an optical microscopy. The sepiolite clay type PS9 (Pangel S9, Tolsa S.A., Madrid, Spain) with specific surface area (BET, N₂) of 344 m²/g, total pore volume of 0.4476 cm³, with high purity, and used with no modification. The epoxidized soybean oil (ESB) was obtained from Dipa Química (Curitiba, Brazil), with epoxy index of 6.60 g O/100g, molecular weight 975.4 g/mol (DIPA Química, 2022).

4.2.2 Design of experiments (DOE)

To optimize the quantity of tests, a DOE was elaborated using PBS and CANA with a fixed quantity (70 wt.% and 30 wt.% respectively), and varying the percentage of LIG, SEP and ESB. So, a two-level full factorial DOE with 3 variables (2^3), with 3 repetitions of the center point (to estimate variability) and randomized run order (to balance the effect of extraneous or uncontrollable conditions) were performed. The upper and lower limits of each variable were defined as, LIG 2.5 to 7.5 part per hundred of resin (phr), SEP 2.5 to 7.5 phr and ESB 5 to 15 phr. The LIG and SEP level were defined according to the results of previous study, and the ESB level, was adopted after search in the literature (De Oliveira Santos et al., 2014; Liminana et al., 2018; Ayu et al., 2020; Rafiqah et al., 2021). The DOE experiments were presented in **Table 9**, and the results were analyzed as the effect of the variable on each property characterized. In addition to these DOE samples, tests were performed with neat PBS and PBS/CANA (30 wt.%) for comparison.

Table 9: DOE formulation of PBS bio-composites.

Sample Id	run order	DOE range			Part per hundred of resin (phr)		
		LIG	SEP	ESB	LIG	SEP	ESB
2PBS-01	11	-1	-1	-1	2.5	2.5	5.0
2PBS-02	8	+1	-1	-1	7.5	2.5	5.0
2PBS-03	6	-1	+1	-1	2.5	7.5	5.0
2PBS-04	3	+1	+1	-1	7.5	7.5	5.0
2PBS-05	10	-1	-1	+1	2.5	2.5	15.0
2PBS-06	1	+1	-1	+1	7.5	2.5	15.0
2PBS-07	7	-1	+1	+1	2.5	7.5	15.0
2PBS-08	5	+1	+1	+1	7.5	7.5	15.0
2PBS-09	4	0	0	0	5.0	5.0	10.0
2PBS-10	9	0	0	0	5.0	5.0	10.0
2PBS-11	2	0	0	0	5.0	5.0	10.0

4.2.3 Preparation of hybrid bio-composites

Firstly, all materials were dried at 80°C for 5 hours in a drying oven to remove moisture and prevent PBS hydro-degradation which occurs due to the high processing temperature, high shear mixing in the polymer melt promoted to the extruder screw and the presence of water molecules, causing degradation of the PBS (Abderrahim et al., 2015; Muthuraj et al., 2015). The optimal drying conditions were found considering the producer's technical sheet (PTT MCC Biochem, 2023) and some preliminary tests carried out. The formulations were previously prepared by mixing CANA+ESB in the blender for 5 minutes. After that, LIG+SEP were added and mixed for 3 minutes in the blender. Then PBS was added and mixed for another 2 minutes. These formulations were extruded in a twin-screw and co-rotating extruder, model DR.16.AX (AX Plásticos Máquinas Técnicas Ltda, Diadema, Brasil), 16 mm screw diameter (D) and relation length/diameter (L/D) of 40, using a temperature profile of 100/110/115/120/125/130/135/140°C and screw speed of 120 rpm. The literature refers to the temperature of PBS processing around 150°C (Wang et al., 2019; Possari et al., 2021). The extruded filament was cooled by air ventilation instead of water bath to avoid water absorption by the composite, especially by CANA fiber. The filament produced by extrusion was granulated using rotating blades coupled to the extruder (AX Plásticos Máquinas Técnicas Ltda, Diadema, Brazil), and they were dried for 8 hours at 80°C to remove moisture.

The granulated samples were injection molded in ISO 527-1:2012 test specimen format, in an injection molding machine, with temperature profile 150/160/170/180°C, injection pressure of 800 bar and flow rate of 40 cm³/s, holding pressure of 700 bar for 12 seconds. The injected test specimens were used for mechanical characterization. For thermal tests, melt flow tests and FTIR analysis, the granulated samples were used. For others analysis, as well as XRD, the samples preparation is described in each topic below.

4.2.4 Characterization

4.2.4.1 *Melting Flow Rate (MFR)*

The behavior of fluidity of composites in the molten state was evaluated by melting flow rate (MFR) analysis using a plastometer (Maqtest Ltda, Franca, Brazil), according to ISO 1133-1:2011, at 190°C and 2.16 kg weight. Each composite sample was measured at least 8 times to obtain MFR mean value.

4.2.4.2 *Soil biodegradation test*

The soil biodegradation test was carried out through ISO 16929, which is referenced by ASTM D6400. The test determines the degree of disintegration of plastics materials under defined composting conditions.

The first step is soil preparation. The organic soil was obtained by biodegradation of a mixture of vegetables residues, occasionally with other organic material, and having a limited mineral content. The soil moisture is determined by initially weighing the soil, drying it in an oven at 100°C for 24 hours and finally weighing it to determine the water content in its natural state and its maximum water absorption capacity. Then, soil moisture was adjusted to maintain between 30% and 35% of its maximum water retention capacity, with weekly checks and adjustments throughout the test period, by weighing soil samples.

The biodegradation test was performed on only two formulations, neat PBS (reference sample) and 2PBS09, which corresponds to the center point formulation (0 0 0) of the DOE due to the limitation of container test. The films were prepared from 6 g of extruded pellets of sample, which were heated and compressed manually using two flat stainless-steel plates (one upper and other lower side) and IKA C-MAG HS7 heating plates. The temperature used was 180°C, heated and pressed for 1 minute and cooled for 3 minutes under compression, and 4 minutes without compression until the film solidifies (around

50°C), so that it can be detached from the plates. The target film thickness was 0.20 ± 0.05 mm, and size of 3 x 3 cm (cut using scissors). For the biodegradation test, five replicates' samples for each condition/formulation were initially weighed (M_o) to determine weight loss (**Equation 2**). The samples were buried and arranged horizontally in containers filled with the prepared soil. The containers with the samples were placed inside an OBD incubator, model SL-225/364 from SOLAB, the temperature was adjusted to 30°C ($\pm 2^\circ\text{C}$) and relative humidity of 75% to 95%.

The degradation of the films was evaluated by their weight loss. To determine the weight loss ($WL\%$), an analytical balance (4 decimal digits) was used and calculated using **Equation 2**.

$$WL\% = \frac{M_o - M_f}{M_o} \times 100 \quad (\text{Equation 2})$$

Where M_o is the initial mass of the films on day 0 (start of the test) and M_f is the final mass obtained after biodegradation, after 30 days and 90 days of test exposure. For the measurements, the films were washed with water to remove soil residues, air-dried at room temperature for 24 hours to eliminate moisture, and subsequently weighed to calculate the weight loss.

4.2.4.3 Mechanical Properties

The Young's modulus, yield stress, yield elongation, tensile strength and elongation at break were obtained to study tensile properties. The tensile test was performed in a universal testing machine EMIC DL-2000 (Instron Brasil Scientific Equipment Ltd., São Paulo, Brazil), according to the ISO 527-1:2012 standard with atmosphere of $23 \pm 2^\circ\text{C}$ and $50 \pm 10\%$ relative humidity. Specimen size 1A, 110 mm gauge length, 5 mm/min speed test, with 9 kN load cell, and 5 specimens tested for each sample (replicates, n=5).

The flexural test parameters were also analyzed (flexural modulus and flexural strength). The test was carried out in a universal testing machine EMIC DL-2000, with 9 kN load cell (Instron Brasil Scientific Equipment Ltd., São Paulo, Brazil), length of span between supports 64 mm, speed 2 mm/min, maximum displacement of 20 mm, according to the ISO 178:2019 standards.

The impact resistance was analyzed according to ISO 180:2019 standard for Izod type test, at 23°C, in an EMIC impact instrument, sample V-notched (2 mm deep) in a notch sample making machine, model X1S-V (Philpolymer Engineering Thermoplastics Inc, São Roque, Brazil). The hardness SHORE D were measured using Bareiss HPE II Shore D (Bareiss Prüfgerätebau GmbH, Oberdischingen, Germany). The mechanical properties of the composites were also compared to EP-440L polypropylene resin (PP) used to produce tray and tubes for seeding for agriculture.

4.2.4.4 Fourier Transform Infrared Spectroscopy (FT-IR)

To evaluate changes in the chemical structure of the composite constituents, the FT-IR spectra of the samples were obtained using a FT-IR spectrometer, model Nicolet iS10 (Thermo Scientific, Massachusetts, EUA), diamond crystal, flat tip, room temperature (23°C), in ATR mode, wavenumber range 4000-400 cm^{-1} , and sample in pellet form (for composites), liquid (for ESB), and powder form (SEP, LIG and CANA) was used.

4.2.4.5 Thermal Analysis

The crystallization and melt behavior of PBS and composites were evaluated by differential scanning calorimetry (DSC), model Q10 (TA Instruments, New Castle, USA), about 5 mg of sample, sealed aluminum pan, under N_2 flow (50.0 ml/min). First heat from 30 °C to 180 °C (heating rate 10°C/min) and held for 3 min to remove previous thermal

history, then cooled to 30 °C (cooling rate -10°C/min) and reheated to 180°C (heating rate 10°C/min) and cooled to 30°C (cooling rate -10°C/min). Only the second scan was recorded for data analysis. The degree of crystallinity (X_c) of PBS (neat PBS and PBS inside the composites) was calculated using the following **Equation 3**.

$$X_c (\%) = \frac{\Delta H_m}{\Delta H_m^o \times W_{PBS}} \times 100 \quad \text{(Equation 3)}$$

where X_c is the degree of crystallinity of PBS, ΔH_m is the melting enthalpy of the PBS composites obtained by integral of melting peak of PBS on DSC curve, ΔH_m^o is the enthalpy of fusion of 100% crystalline PBS (200 J.g⁻¹) (Lule et al., 2020), and W_{PBS} is the weight fraction of PBS in the composites.

The thermal stability of the PBS composites was evaluated by thermo-gravimetry analysis (TGA) in a model Thermal Analysis System TGA/DSC 3+ (Mettler Toledo, Columbus, USA). The samples were heated from 30°C to 600°C, heating rate of 10°C/min, air flow of 50 mL/min.

4.2.4.6 X-Ray Diffraction (XRD)

The structure of crystalline part of PBS and composite components were investigated using XRD analysis. The main aspect is the increase in the d -value of the crystalline planes of the sepiolite clay lamellae. For XRD analysis, the samples were ground in a grain grinder and sieved through a 100-mesh sieve to obtain a fine powder. The analysis was performed in XRD-6000 diffractometer (Shimadzu, Kyoto-Japan), source Cu tube, radiation wavelength (λ) of 0.154056 nm, scan range from 2° to 45° and 2.0°/min (scanning rate).

4.2.4.7 Density analysis

The density of samples was analyzed by density meter DSL-910 (Gehaka, São Paulo – Brazil), using anhydrous ethyl alcohol as the fluid, measuring the weight of sample in the air (m_a) and immersed in the alcohol (m_f). The density can be calculated by using **Equation 4**, where ρ_s is the density of sample, m_a is the sample weight in air, m_f is the sample weight under fluidity (alcohol), ρ_f is the density of the fluid (anhydrous ethyl alcohol, density of 0.81659 g/cm³).

$$\rho_s = \frac{m_a}{m_a - m_f} \times \rho_f \quad (\text{Equation 4})$$

4.2.4.8 Scanning Electron Microscopy (SEM–EDS)

The morphology of the fractured samples from impact test of the PBS composite were analyzed through scanning electron microscopy (SEM), Jeol JSM-5800 LV (JEOL Ltd, Tokio, Japan), with accelerating voltage of 3 to 20 kV, to analyze the morphology and adhesion of the polymer matrix to the fibers. The energy dispersive X-ray microanalysis system (EDS) (JEOL Ltd, Tokio, Japan) coupled to SEM was used to study elemental and the distribution of the components (mapping composition) inside the composite.

4.2.4.9 Statistical Analysis

All tests performed on replicates were subjected to the Tukey test (using Statistica 7.1 software) to verify if there are significant differences between the mean values. The Tukey test results are presented using letter (in superscript). Same letters in the same column, the mean value does not differ at the 5% significance level (Tukey, $p < 0.05$). The order of the letters is in decreasing order of mean values.

4.3 RESULTS

The results of all PBS composites can be compared to the properties of Braskem's EP440L polypropylene resin, that is a typical resin used in the fabrication of tubes and trays for seedling in agriculture. EP440L is a heterophasic polypropylene copolymer of intermediate melt flow rate value and suitable for the injection molding process. According to the manufacturer datasheet, EP440L has melt flow rate of 6.0 g/10min (at 230°C / 2.16 kg), flexural resistance of 24 MPa, flexural modulus of 1050 MPa, flexural elongation of 6%, hardness Rockwell R-scale of 60, no breakage in Izod impact test at 23°C (impact resistance of 75 J/m at -20°C), heat deflection temperature of 85°C (at 0.455 MPa) (Braskem S.A., 2018).

For illustrative purposes, **Figure 15** presents images of PBS composite samples, produced through extrusion and subsequently granulated.



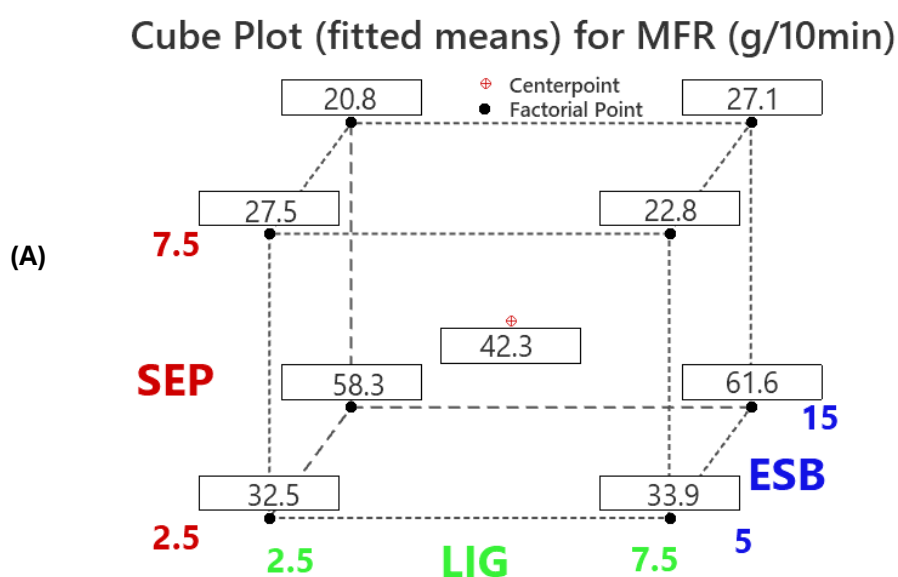
Figure 15: Granulated samples of composite formulations. *2PBS-00 = Neat PBS.
**2PBS-12 = PBS/CANA (30 wt.%).

4.3.1 Melt Flow Rate (MFR)

Adequate melt flow rate is important to ensure good composite processing condition, especially for injection molding processes that require higher melt fluidity (Possari et al., 2021). The MFR results are shown in **Figure 16A** as a cube plot of fitted means and **Figure 16B** as main effects plot of MFR based on previously presented DOE. As can be seen in **Figure 16A**, LIG promotes an increase in the melted fluidity of the PBS, as reported in other studies it has a lubricating effect, without having a plasticizing effect that could decrease the rigidity and increases the elongation of the composite (Possari et al., 2021). Furthermore, it can be noted that at first, with the increase from 2 to 5 phr of LIG, there seems to be an increasing effect on the MFR value as expected, however with a greater addition of LIG (7.5 phr) there was a decrease in the MFR, and there seems to be a limit on the amount of LIG that can increase the MFR value. In fact, Ewurum and McDonald, 2025 showed that lignin initially (low content) acts as filler that disrupts the polymer matrix, reducing chain entanglements and improving flow under shear stress, but high lignin level can rise viscosity because it acts making interconnected network reflect in the crosslink density increase (Ewurum and McDonald, 2025). The crosslink behavior of high lignin content can also explain the decrease in some mechanical properties, such as flexural modulus (**Figure 20A**) and impact strength (**Figure 21A**). SEP showed a tendency to reduce the MFR value, which can be observed in **Figures 16A** and **16B**, as it acts as an inorganic reinforcement, which restricts the movement of the polymer melt matrix molecules (Farshchi and Ostad, 2020). ESB has an increasing effect on the MFR, as expected, since it is a plasticizer (Jia et al., 2018).

The MFR of pure PBS is 22 g/10min (190°C, 2.16 kg). The addition of CANA (30 wt.%) to PBS strongly reduces the MFR (MFR=0). This decrease in melt fluidity directly impacts the injection molding process, which requires higher MFR values (above 20 g/10

min) compared to the extrusion process, for example ($\text{MFR} < 5 \text{ g/10min}$) (Possari et al., 2021). However, in the present study, it was observed that higher ESB contents (15 phr) resulted in high MFR values (around 50-60 g/10min) but caused difficulties in injection, since the ESB began to act as an external lubricant, causing the molten polymer to slide inside the barrel and thread, making it difficult to pressurize the molten composite to be injected into the mold cavities. Therefore, high ESB loadings (above 15 phr) are not desirable. Although they lead to an increase in MFR, the results suggest that a solubility limit has been reached, leading to the migration of some ESB to the composite surface. In fact, Zhao et al., 2012 reported that ESB is only partially miscible with the PBS matrix during mixing (Zhao et al., 2012). They found that elongation at break peaked at 5 wt.% ESB (reaching 346%, up to 15 times higher than that of pure PBS), although values higher than those of pure PBS were still observed with ESB contents up to 17.5 wt.% (the maximum tested). SEM morphological analysis further confirmed the partial compatibility between ESB and PBS, as evidenced by phase separation, micro void formation, and signs of phase segregation.



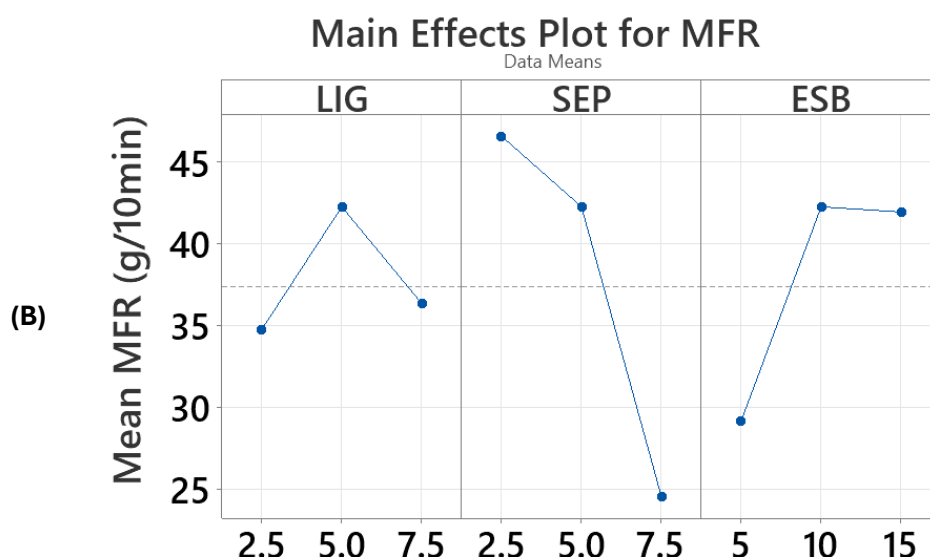
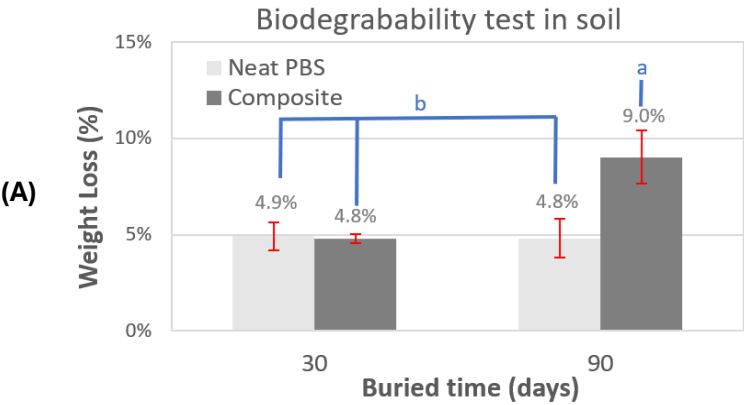


Figure 16: (A) Cube plot and (B) Main effects plot of MFR (190°C, 2.16 kg).

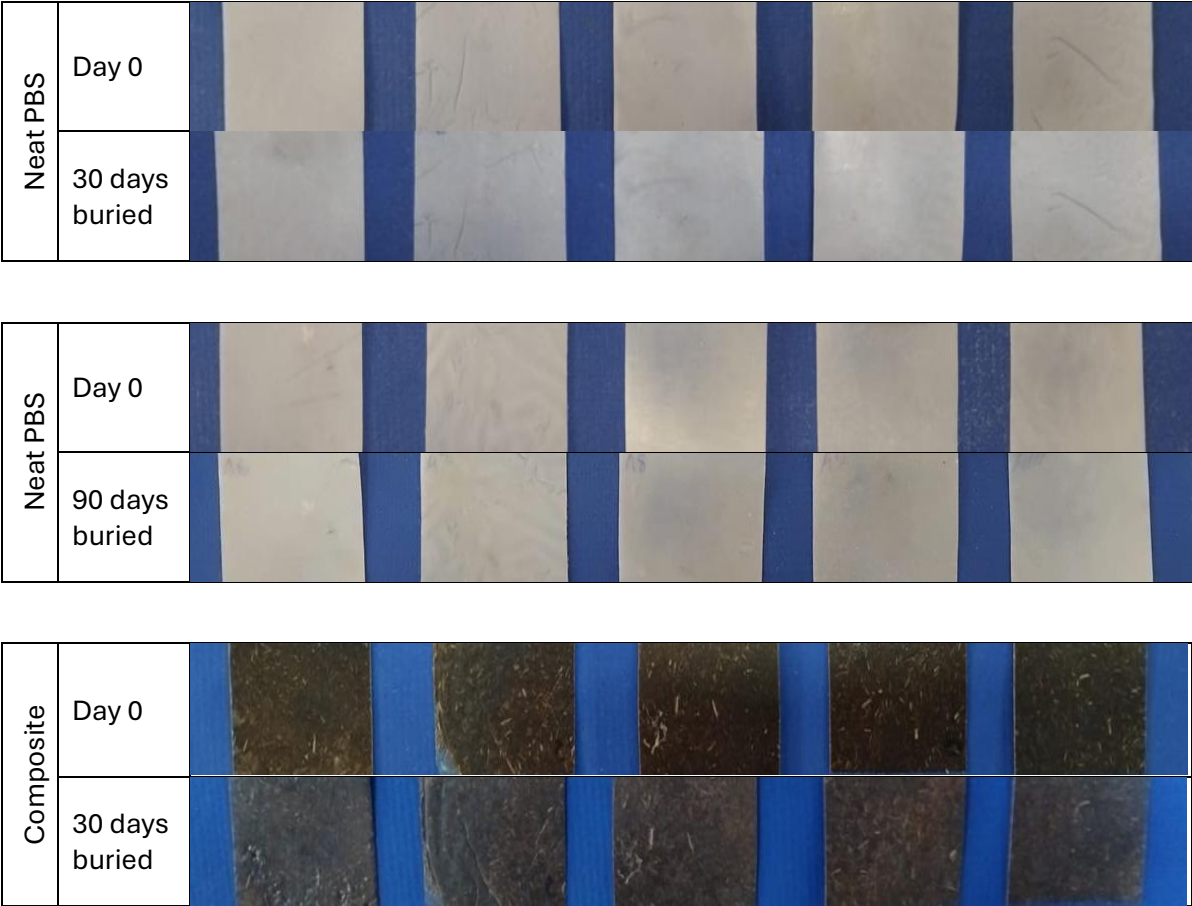
4.3.2 Soil Biodegradation test

The biodegradation test results (**Figure 17A**) indicate that pure PBS has a rapid initial biodegradation rate and that it reached a steady-state weight loss at 60 and 90 days (Phua et al., 2012).] Phua et al., 2012 attributed the high initial biodegradation rate to degradation of low molecular weight fragments and exposed end groups of PBS (Phua et al., 2012). According to Huang et al., 2018 the biodegradation of PBS occurs in the amorphous area of the surface of PBS with the contact of microorganisms, that secrete enzymes which can break down PBS into lower molecular weight segments by hydrolysis and oxidation (Huang et al., 2018). The gradual erosion caused by microorganisms and enzymes led to the disintegration of PBS. The composite (2PBS-09, center point of DOE = 000) initially biodegrades at a rate similar to pure PBS (0 to 30 days), but the degradation continues in the composite (from 30 to 90 days), unlike neat PBS which reaches a plateau and does not progress. The higher biodegradation rate of composites can be attributed to the natural fiber content (as for CANA fiber, in this case), which has hydrophilic groups that can easily absorb water and microorganisms from soil and increase the contact area with PBS, enhancing degradation (Huang et al., 2018).

Unmodified sepiolite has high water uptake capacity between the pores, and lesser amount of water will be available for PBS hydrolysis (inhibiting biodegradation at an early stage), but some water segregation may occur in case of excess of moisture which may affect the degradation rate, increasing biodegradation (Dilsad et al., 2024).



(B)



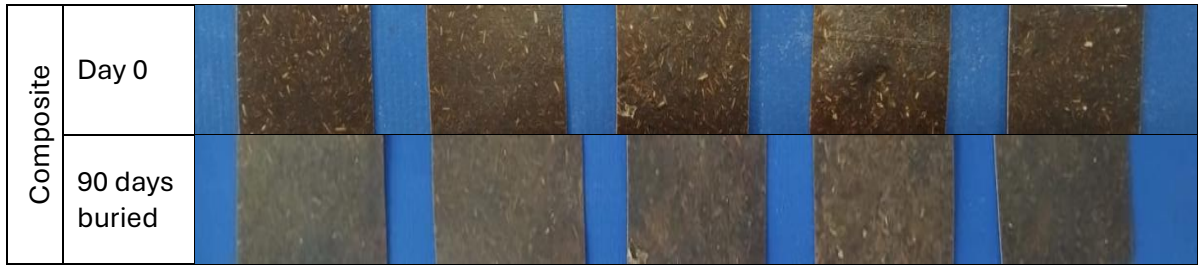


Figure 17: Biodegradation test in soil after 30 and 90 days, for Neat PBS and for composite (2PBS-09 = DOE 0 0 0). (A) Weight loss graphics. (B) Surface image of samples before and after biodegradation test.

Note: Tukey statistical test, mean value with same superscript letters do not differ at the 5% significance level (Tukey, $p < 0.05$). The letters are in descending order of mean values. Mean values \pm s.d. (n = 5).

Figure 17B shows the image of the surface of film of neat PBS and for composite (2PBS-09) subjected to the biodegradation test in soil in day 0, after 30 days and after 90 days, Biodegradation causes a slight darkening in the color of Neat PBS and, in the composite sample, the CANA fibers became more exposed and evident, due to the degradation of PBS. The literature indicates that PBS has a low biodegradation after 30 days (Kim et al., 2006; Liu et al., 2009; Phua et al., 2012; Muniyasamy et al., 2013; Huang et al., 2018). In fact, the biodegradation of PBS depends on composite components and its interaction with PBS. Liu et al. (2009) reported that PBS/Jute composites underwent biodegradation, exhibiting a weight loss of 8% after 60 days, 15% in 90 days, reaching 62.5% in 180 days, at 30°C and controlled humidity (Liu et al., 2009). Phua et al. (2012) found a weight loss of PBS/MMT of 8.5% at 90 days buried in soil at 25°C (Phua et al., 2012). The Mitsubishi Chemical Co. presents a bio-PBS folder in which 90% biodegradation (measured by CO₂ generation analysis, comparing to natural cellulose biodegradation), in 6 months at 60°C or 12 months at 30°C, or 2 years at 20-25°C (Mcc Biochem Company Limited, 2025).

4.3.3 Fourier Transform Infrared spectroscopy (FT-IR)

The FT-IR was performed to analyze if there are interactions between PBS polymer and the other components added into the composites, this can be done by observing change in the band position of spectrum obtained from each raw material and in the composite. **Figure 18A** shows FTIR spectra of raw materials, in which PBS has bands in 2944 cm^{-1} and 1328 cm^{-1} that were assigned to the asymmetric and symmetric deformational vibrations of $-\text{CH}_2-$ groups, and there are other bands in 1712 cm^{-1} related to the $\text{C}=\text{O}$ stretching vibration of ester group (Zhang and Zhang, 2016; Zhu et al., 2017), and in 1149 cm^{-1} a band due to the $-\text{C}-\text{O}-\text{C}-$ stretching in the ester linkages [47]. CANA has a peak in wavelength $3400\text{--}3200\text{ cm}^{-1}$ attributed to free water (moisture) presence or due to hydrogen bonded $-\text{OH}$ stretching vibration (Liu et al., 2009; Zhang and Zhang, 2016). Sepiolite has a stretching vibrations band of $\text{Mg}_3\text{O}-\text{H}$ in wavelength of 3616 cm^{-1} corresponding to the OH , another band in 1656 cm^{-1} due vibrational distortion of water inside the clay structure, and finally 3 other bands in 980 , 1010 and 1206 cm^{-1} due $\text{Si}-\text{O}$ bonds within silica tetrahedra (Chikh et al., 2016).

Figure 18B shows the FTIR spectra of neat PBS, SEP, and 3 composite formulations (representing the central point $0\ 0\ 0$, minimum point $-1\ -1\ -1$, and maximum point $+1\ +1\ +1$ of the DOE), with the purpose of evaluating the interaction of the components within the composite. The band of 1712 cm^{-1} that featured on neat PBS did not change position in the composite samples, but a small shoulder appeared at $1612\text{--}1608\text{ cm}^{-1}$ with addition of SEP clay, this band corresponding to the hydrogen-bonded carbonyl groups (Chikh et al., 2016), indicating good interactions between SEP clay and PBS. Good interaction represents good dispersion of clay in PBS polymer matrix, that is essential to obtain nanocomposite, which clay nanoparticles can act as reinforcement rather than filler.

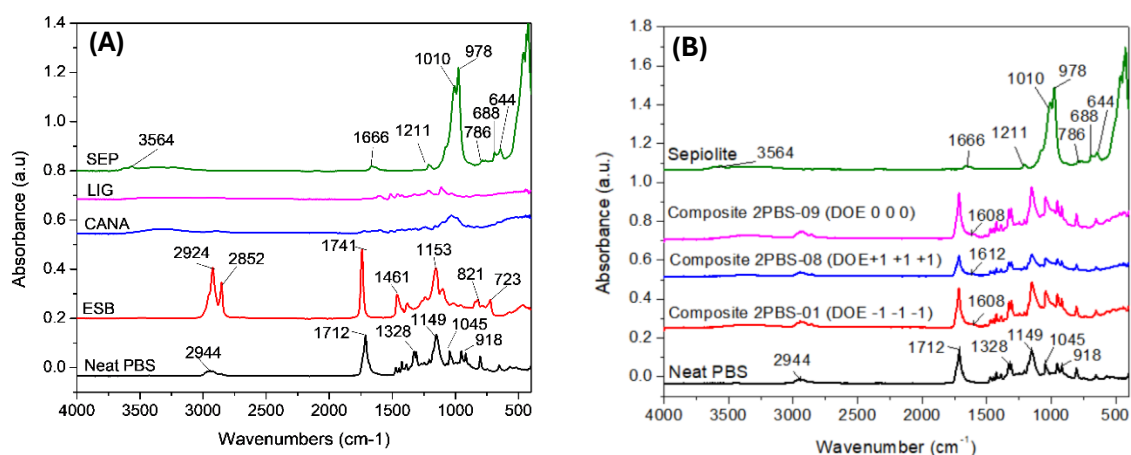


Figure 18: FT-IR spectrum of (A) PBS and raw materials; (B) PBS, SEP and composites. Composites spectra show a shoulder at 1602-1608 cm^{-1} denoting good interaction SEP-PBS.

4.3.4 Mechanical characterization

The main tensile test results are summarized in **Table 10**, **Figures 19 A to D**. As can be observed, the Young's modulus of all composites increased as expected in relation to neat PBS, reaching an increase of up to 309% (569 MPa to 2326 MPa). It is worth highlighting the relevant hybrid effect of SEP on this result, without forgetting that the composites presented a high content of CANA fiber (30 wt.%), which also strongly contributed to this increase in stiffness related to neat PBS. Another interesting point was the increase in yield stress, mainly in the formulations with higher SEP content, representing a 61% increase in yield strength in relation to neat PBS (from 9.3 MPa for neat PBS, it increased to 15 MPa for formulation 2PBS-04 and 14.6 MPa for formulation 2PBS-03). SEP clay has a fibrous structure morphology with micropores and needle-like arrangement with silanol groups (Si-OH) on its surface that allows a certain compatibility with PBS molecules to improve properties, such as Young's modulus, tensile strength and yield strength (Huo et al., 2017). The tensile strength of composite (23.3 MPa for 2PBS-04) almost reaches the value for neat PBS (27.0 MPa), mainly due to SEP high content

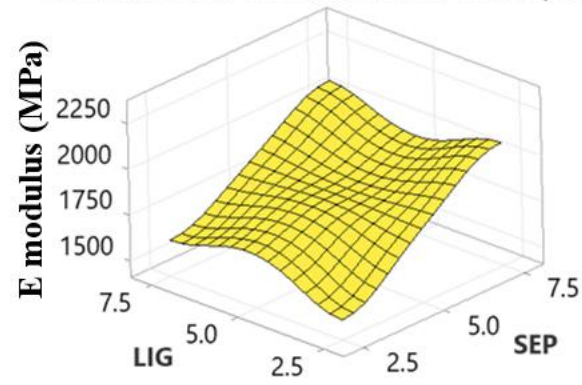
and ESB minimum content formulation. Liang et al., 2009 (Liang et al., 2009) investigated PBS composites reinforced with natural kenaf fiber and observed a decrease in tensile strength from 33.5 MPa for neat PBS to 18.6 MPa for composites containing 30 wt.% fiber, along with a reduced elongation at break of just 5%. This decline in tensile performance was attributed to poor interfacial adhesion, which led to matrix–fiber debonding and void formation, facilitating crack propagation in these weakened regions. Additionally, the high fiber content reduced the amount of polymer available to accommodate deformation. The excessive fiber loading also promoted fiber agglomeration, creating stress concentration zones that require less energy for crack initiation and propagation, ultimately causing failure before yielding. The composites formulations still have limited values of elongation (elongation at break and yield elongation) compared to those of neat PBS, indicating that the ESB plasticizer did not act to effectively increase elongation.

Table 10: Tensile test results.

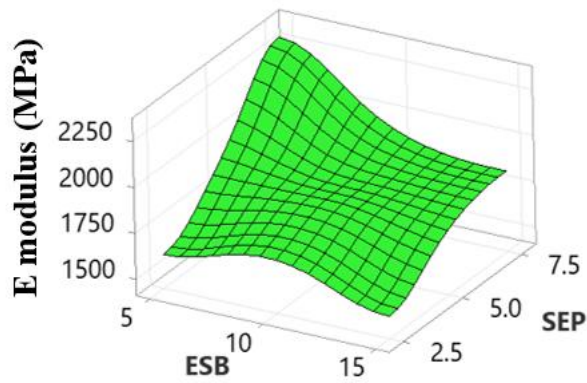
Sample ID	Young Modulus (MPa)	Yield Strength (MPa)	Yield elongation (%)	Tensile strength (MPa)	Elongation at break (%)
2PBS-01	1461 ± 111 ^d	6.9 ± 0.8 ^e	0.69 ± 0.08 ^d	13.2 ± 1.9 ^e	3.1 ± 0.1 ^{b c}
2PBS-02	1727 ± 94 ^{b c}	9.3 ± 2.1 ^{c d}	0.74 ± 0.13 ^{c d}	16.0 ± 4.2 ^{d e}	2.5 ± 0.1 ^{c d}
2PBS-03	2326 ± 87 ^a	14.6 ± 0.5 ^a	0.83 ± 0.03 ^{b c}	22.8 ± 0.9 ^b	2.4 ± 0.0 ^d
2PBS-04	2280 ± 64 ^a	15.0 ± 1.1 ^a	0.86 ± 0.03 ^b	23.3 ± 1.3 ^{a b}	2.3 ± 2.4 ^d
2PBS-05	1577 ± 11 ^{c d}	8.9 ± 0.1 ^{d e}	0.77 ± 0.01 ^{b c d}	15.1 ± 0.4 ^{d e}	2.6 ± 0.2 ^{c d}
2PBS-06	1486 ± 17 ^d	9.2 ± 0.1 ^{c d}	0.83 ± 0.01 ^{b c}	16.2 ± 0.4 ^{d e}	2.9 ± 0.1 ^{b c d}
2PBS-07	1833 ± 85 ^b	10.1 ± 0.4 ^{b c d}	0.76 ± 0.01 ^{b c d}	17.2 ± 0.7 ^d	2.7 ± 0.3 ^{b c d}
2PBS-08	1860 ± 72 ^b	11.1 ± 0.1 ^{b c}	0.80 ± 0.02 ^{b c d}	18.7 ± 0.4 ^{c d}	2.7 ± 0.2 ^{c d}
2PBS-09	1878 ± 100 ^b	11.6 ± 0.4 ^b	0.82 ± 0.01 ^{b c}	18.9 ± 1.1 ^{c d}	2.5 ± 0.1 ^{c d}
2PBS-10	1794 ± 55 ^b	10.9 ± 0.3 ^{b c d}	0.82 ± 0.01 ^{b c}	18.1 ± 0.7 ^{c d}	2.6 ± 0.1 ^{c d}
2PBS-11	1812 ± 41 ^b	11.1 ± 0.5 ^{b c d}	0.82 ± 0.02 ^{b c}	18.3 ± 0.9 ^{c d}	2.5 ± 0.1 ^d
Neat PBS	569 ± 39 ^e	9.3 ± 0.7 ^{c d}	1.83 ± 0.09 ^a	27.0 ± 1.8 ^a	11.3 ± 0.1 ^a
PBS/CANA	1740 ± 28 ^{b c}	11.8 ± 0.2 ^b	0.88 ± 0.01 ^b	21.2 ± 0.4 ^{b c}	3.2 ± 0.1 ^b

Note: Tukey statistical test, mean value with same superscript letters do not differ at the 5% significance level. The letters are in descending order of mean values. Number of replicates, n=5.

Surface Plot of E modulus vs LIG; SEP

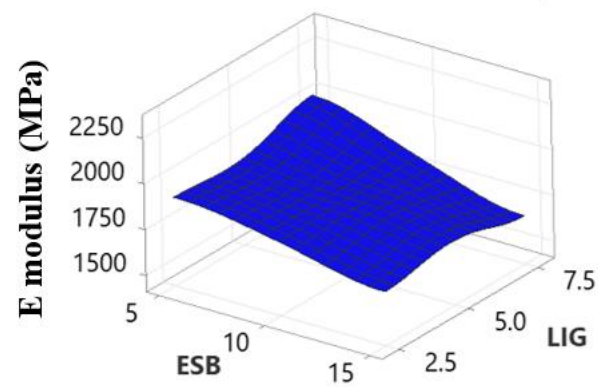


Surface Plot of E modulus vs SEP; ESB



(A)

Surface Plot of E modulus vs LIG; ESB



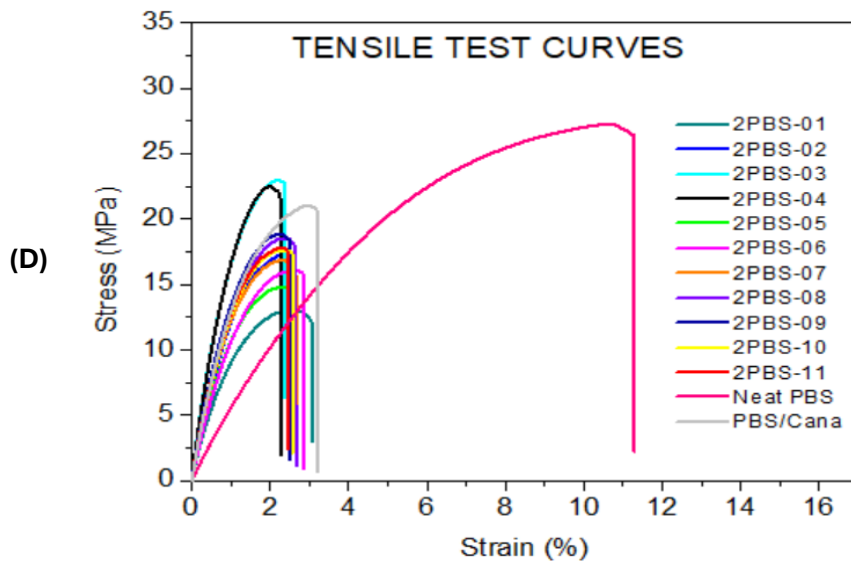
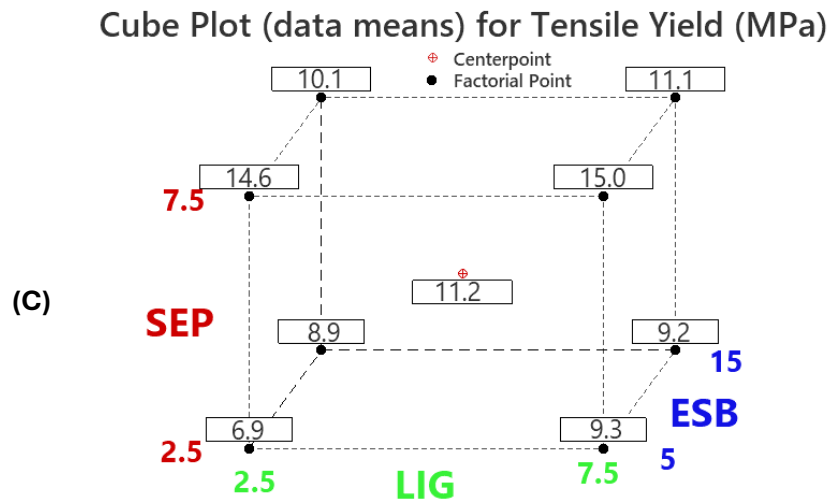
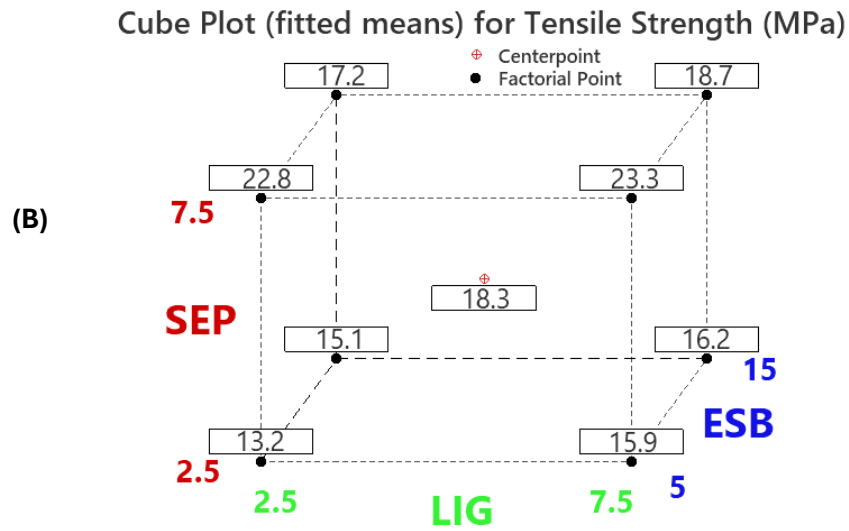


Figure 19: Tensile test results. (A) Surface plot of Young's modulus. (B) Cube plot of tensile strength. (C) Cube plot of tensile yield. (D) Tensile test curve of Neat PBS and composites.

In fact, natural fiber in high content as such used here, generally negatively affects the ductility, impact resistance, and in some cases the tensile strength, because these types of composites are strongly dependent on fiber content and its characteristics, compatibility, interfacial adhesion. Platnikers et al., 2020 explain that this can be caused by voids in the composite structure, aggregates formation, and weak bonding between filler and polymer (Platnieks et al., 2020), and suggest chemical modification of cellulose to improve the compatibility of the interface with the polymer, using compatibilizers such as maleic acid anhydride (MAH), polymeric diphenylmethane diisocyanate (PMDI), carbodiimide (CDI), 3-aminopropyl trimethoxysilane (APTMS) during melt processing.

Table 11: Flexural test, impact resistance and hardness Shore D results.

Sample ID	Flexural Strength (MPa)	Flexural Modulus (MPa)	Flexural Strain (%)	Impact Resistance (kJ/m ²)	Hardness Shore D
2PBS-01	43.3 ± 0.4 ^c	1770 ± 41 ^c	6.23 ± 0.39 ^{bc}	8.8 ± 0.7 NR ^{bcde}	65.3 ± 1.1 ^{bcd}
2PBS-02	42.4 ± 0.9 ^{cd}	1798 ± 28 ^c	5.05 ± 0.20 ^{defg}	7.9 ± 0.6 NR ^{cde}	68.0 ± 1.0 ^{ab}
2PBS-03	51.3 ± 0.7 ^a	2550 ± 19 ^a	4.53 ± 0.17 ^{fgh}	7.0 ± 2.0 NR ^e	68.9 ± 1.0 ^a
2PBS-04	49.4 ± 0.5 ^{ab}	2462 ± 53 ^a	3.85 ± 0.15 ^h	8.1 ± 0.4 NR ^{cde}	67.7 ± 0.6 ^{ab}
2PBS-05	36.2 ± 0.4 ^f	1499 ± 23 ^d	5.82 ± 0.01 ^{bcd}	9.5 ± 0.3 NR ^{bc}	61.2 ± 3.5 ^f
2PBS-06	35.9 ± 0.6 ^f	1456 ± 48 ^d	5.50 ± 0.24 ^{cde}	9.7 ± 0.5 NR ^{bc}	62.0 ± 1.4 ^{ef}
2PBS-07	39.7 ± 2.5 ^e	1776 ± 173 ^c	5.30 ± 0.01 ^{def}	7.3 ± 0.3 NR ^{de}	63.8 ± 1.2 ^{def}
2PBS-08	41.7 ± 0.8 ^{cde}	2037 ± 120 ^b	4.40 ± 0.20 ^{gh}	7.9 ± 0.6 NR ^{cde}	63.9 ± 0.6 ^{def}
2PBS-09	40.5 ± 1.0 ^{de}	1897 ± 24 ^{bc}	4.79 ± 0.38 ^{efg}	8.7 ± 0.5 NR ^{bcde}	65.3 ± 1.0 ^{bcd}
2PBS-10	41.0 ± 1.0 ^{de}	1863 ± 38 ^c	4.90 ± 0.01 ^{efg}	8.7 ± 0.6 NR ^{bcde}	64.6 ± 1.5 ^{cde}
2PBS-11	41.6 ± 0.4 ^{cde}	1889 ± 21 ^c	5.08 ± 0.15 ^{defg}	8.9 ± 0.7 NR ^{bcd}	65.3 ± 0.3 ^{bcd}
Neat PBS	35.2 ± 1.4 ^f	626 ± 7 ^e	12.67 ± 0.01 ^a	12.1 ± 0.7 ^a	66.7 ± 0.5 ^{abc}
PBS/CANA	47.9 ± 0.4 ^b	1899 ± 9 ^{bc}	6.71 ± 0.26 ^b	10.3 ± 0.7 NR ^b	68.8 ± 1.0 ^a

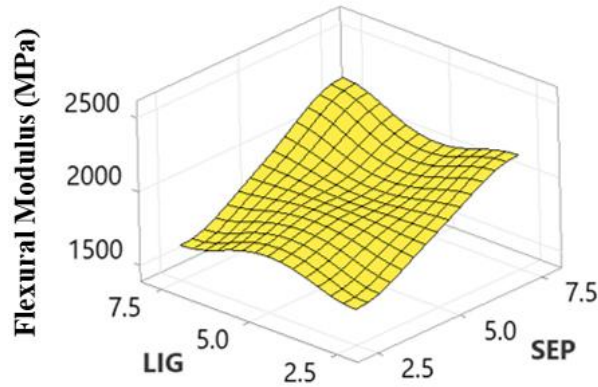
NR: the specimen did not present a total rupture.

Note 1: Tukey statistical test, mean value with same superscript letters do not differ at the 5% significance level. The letters are in descending order of mean values. Number of replicates n=5 for flexural and Izod impact test, and n=6 for Shore D.

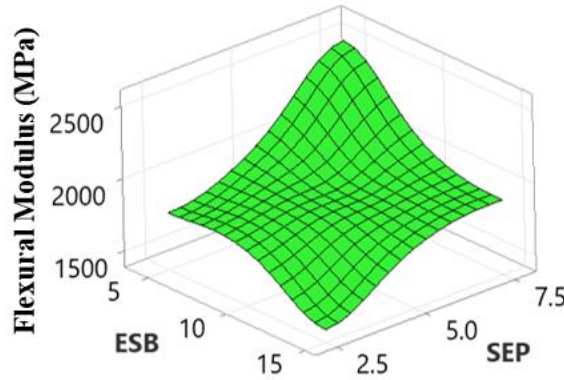
Flexural tests results are presented in **Table 11**, and the average curves of each sample are shown in **Figure 20C**. The flexural properties are important for this

application (seed tray for agriculture). The flexural modulus and flexural strength increase across all composite formulations when compared to neat PBS, reaching an increase of 308% in modulus and 46% in flexural strength. However, the elongation of the composites had limited values, compared to neat PBS. Analyzing the effect of additives on composites (**Figure 20A** and **20B**), SEP has a strong tendency to increase flexural modulus and flexural strength, while ESB has a tendency to decrease it and LIG has a more limited effect. The flexural modulus of EP440L resin is 1050 MPa, while the hybrid bio-composites exhibit flexural modulus values ranging from 1456 MPa (2PBS-06, formulation with high content of ESB and low SEP) to 2550 MPa (2PBS-03, formulation with higher content of SEP and low ESB), surpassing the EP440L.

Surface Plot of Flex Mod [MPa] vs LIG; SEP

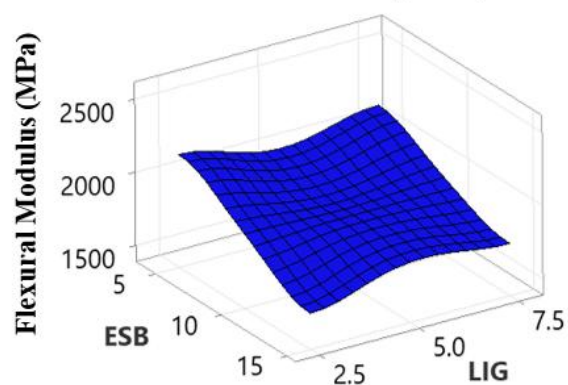


Surface Plot of Flex Mod [MPa] vs SEP; ESB

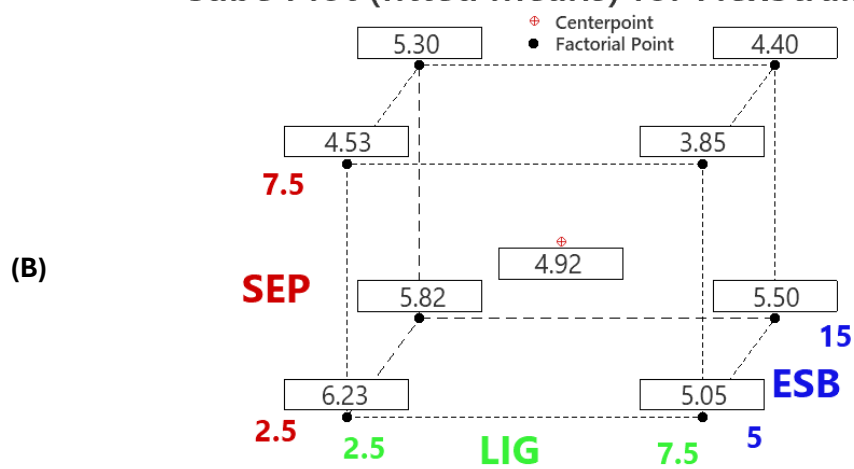


(A)

Surface Plot of Flex Mod [MPa] vs LIG; ESB



Cube Plot (fitted means) for FlexStrain%



(C)

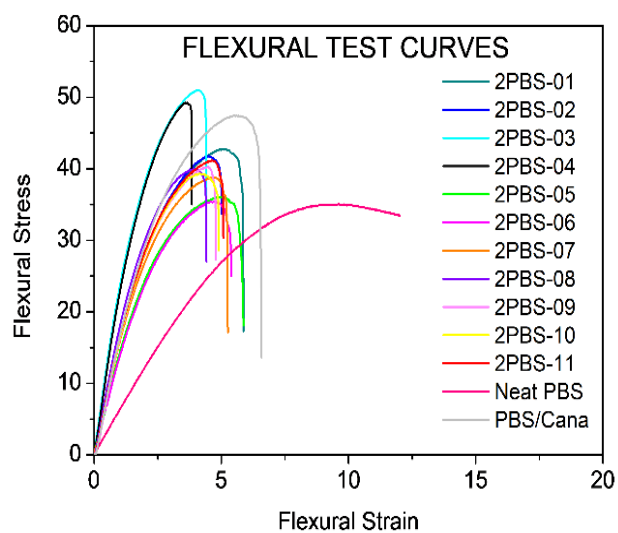


Figure 20: (A) Surface plot of Flexural modulus, (B) Cube plot of flexural strain, and (C) Flexural test curves.

The impact resistance of the composites decreases compared to neat PBS (10.3 kJ/m²) (**Figure 21A** and **Table 11**). SEP has a pronounced effect of reducing the impact strength of the composites. LIG initially increased impact strength as the concentration increased from 2.5 phr to 5 phr, but at a higher level (7.5 phr) a decrease in impact strength occurred, indicating that LIG has no toughness-enhancing or plasticizing effect. With the increase in the ESB content (from 5 phr to 10 phr) in the composite, an increase in impact resistance was observed, as expected, however, the additional increase in the ESB content (from 10 to 15 phr) did not promote an increase in impact resistance, indicating that in these compositions maybe the ESB reached a limit in its ability to act on tenacity improvement, or ESB incorporation was not done well. ESB was initially intended to improve fiber–polymer interfacial adhesion by acting as a compatibilizer between CANA and PBS. In the present study, it was also evaluated for its potential to enhance the composite’s tenacity and ductility. However, based on the impact and tensile/flexural test results, such enhancements were not observed. Zhao et al., 2012 found that in PBS/ESB systems, phase separation and micro void formation occurred when ESB content exceeded 5.0 wt.%, leading to a decrease in elongation at break (Zhao et al., 2012). This phenomenon may have also occurred in the composites studied here, contributing to the observed reductions in tensile and impact strengths. Liminana et al., 2018 used 4.5wt.% of some vegetable oil as epoxidized linseed oil (ELO), epoxidized soybean oil (ESBO), maleinized linseed oil (MLO) to act as compatibilizers of ASF (almond shell flour) to be incorporated into PBS, achieving remarkable increase in ductile properties (Liminana et al., 2018). There are some negative effects of LIG and SEP, because increasing the amount of LIG (from 2.5 to 7.5 phr) the drop in impact resistance seems to be smaller with the smaller amount of SEP (2.5 phr) compared to the larger amount of SEP (7.5 phr). Relative to EP440L polypropylene resin, it has a ductile behavior because no ruptures

shown in the impact test at 23°C, indicating the need to improve this aspect of PBS hybrid composite. Generally, composites with natural fiber show brittle impact behavior with a fragile fracture and low impact energy (low toughness), because composites have two phases, inherently presenting some discontinuities, which can lead to the initiation of crack propagation, while pure thermoplastic represents continuous material (Frollini et al., 2013).

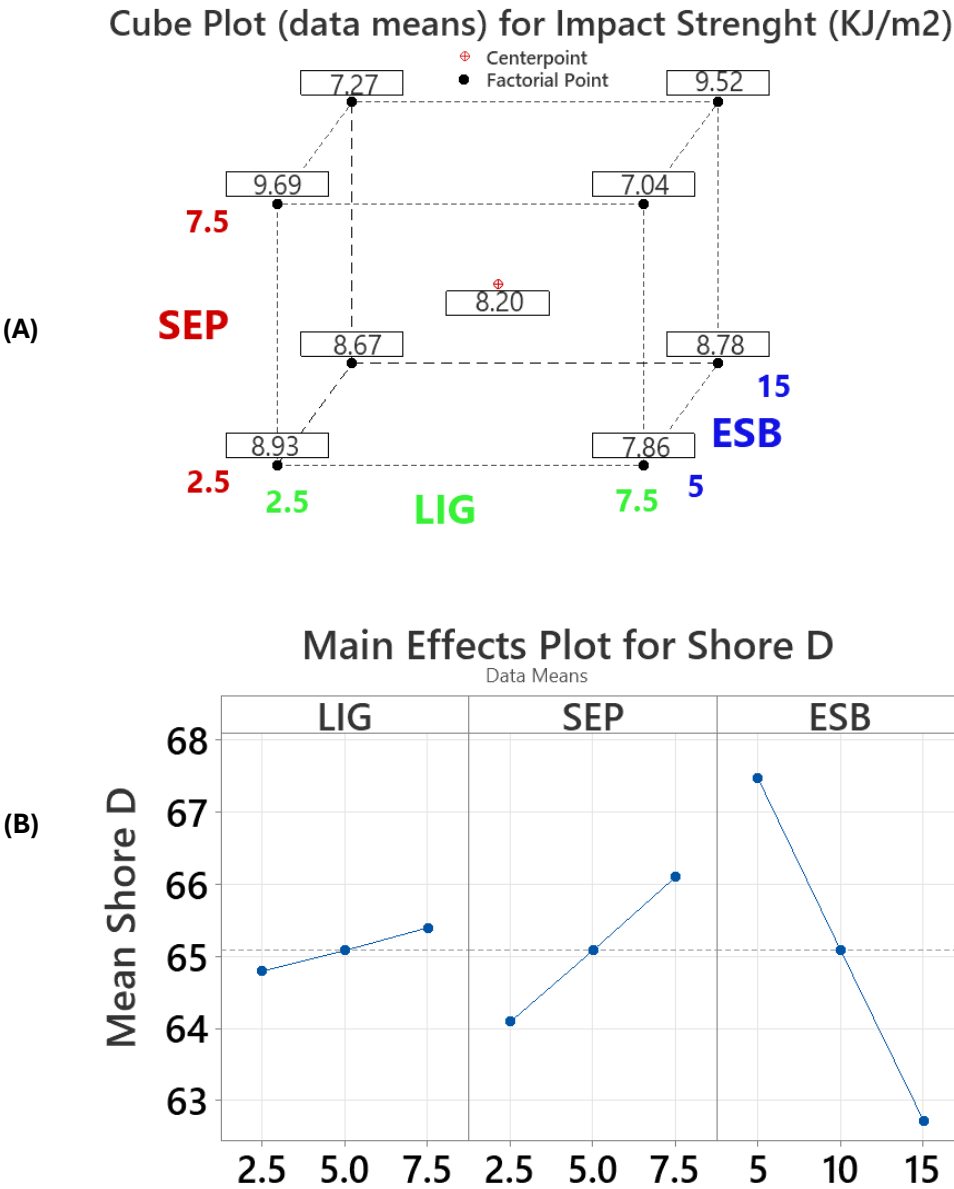
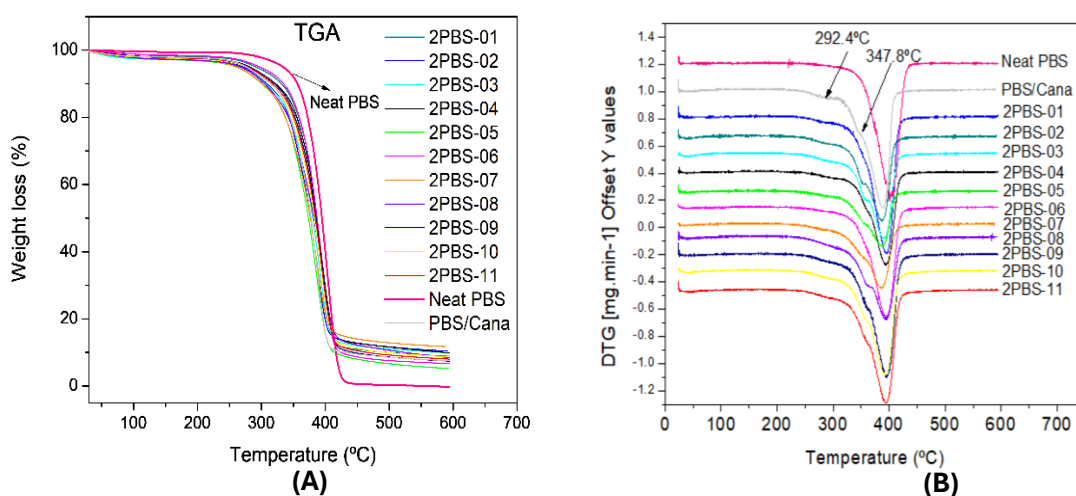


Figure 21: Main effects plot of LIG-SEP-ESB for (A) impact strength and (B) Shore D.

The hardness of the PBS hybrid biocomposites decreased considerably with the use of ESB, evidence of its plasticizing effect (**Figure 21B**). It increased with the use of SEP and had a small increase in effect with LIG. Comparing the hardness of pure PBS (Shore D of 66.7) (**Table 11**), the addition of 30 wt.% of CANA increased the hardness significantly (to Shore D of 68.8). The use of additives (LIG, SEP and ESB) at the minimum DOE dosage (2PBS-01) caused the hardness to drop (to 65.3), managing to recover the hardness with the highest dosage of SEP (2PBS-03 and 2PBS-04). With these results, it is possible to hypothesize that the main responsible for hardness increase are CANA and SEP, and the main responsible for decrease for hardness is ESB. LIG has little or no effect on hardness (**Table 11**).

4.3.5 Thermal analysis

Thermal gravimetry analysis is an effective method for evaluating flame retardancy and thermal degradation properties. The TGA thermograms are shown in **Figure 22A** and **22B** and the values of temperature of weight loss of 5 wt.% ($T_{WL5\%}$), 50 wt.% ($T_{WL50\%}$), 90 wt.% ($T_{WL90\%}$), temperature at the maximum rate of weight loss (T_{max}) of PBS and composites are presented in **Table 12**.



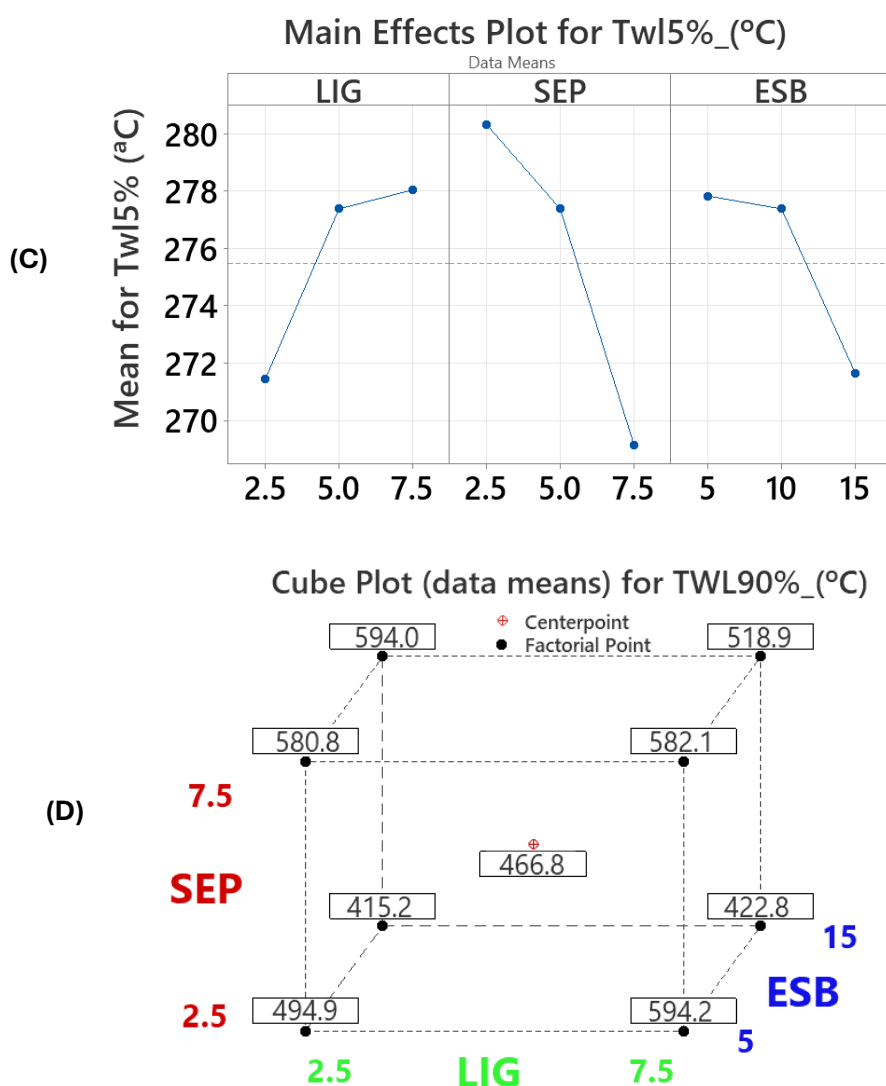


Figure 22: (A) Thermogravimetric Analysis (TGA), (B) Differential Thermogravimetric (DTG), (C) Main effects plot on $T_{WL5\%}$, (D) Cube plot of $T_{WL90\%}$ for PBS composites.

The thermogram in **Figure 22A** shows that weight loss of all composites starts earlier than neat PBS due to dehydration of water and other volatiles of organic components of composite (CANA and LIG). According to literature, (Frollini et al., 2013; Liminana et al., 2018) the weight loss up to 180.0 °C is due to dehydration of chemically bonded water and hydroxyl groups in LIG. In **Figure 22B**, there is a shoulder at about 297.1°C that can be attributed to the partial decomposition of carboxylic and anhydride groups and residual hemicellulose in kraft lignin, with weight loss of 6.7% (Frollini et al.,

2013). The maximum LIG weight loss occurs between 290°C and 600°C which corresponds to the pyrolysis of LIG (Yan et al., 2021). The degradation of PBS occurs as chain scission and exhibits a single stage degradation (single DTG peak) that starts at approximately 280-300°C, with a peak at 410°C, and the decomposition is almost complete at 430-440°C (weight loss >90 wt.%) (Frollini et al., 2013).

Table 12: Degradation results of TGA analysis.

Sample ID	$T_{WL5\%}$ (°C)	$T_{WL50\%}$ (°C)	$T_{WL90\%}$ (°C)	T_{max} (°C)	Residual Mass (%)
2PBS-01	290.7	386.9	494.9	394.8	8.9%
2PBS-02	273.8	379.3	594.2	389.1	10.4%
2PBS-03	267.7	381.2	580.8	391.4	9.9%
2PBS-04	279.1	385.4	582.1	392.1	9.9%
2PBS-05	260.5	374.6	415.2	389.1	5.2%
2PBS-06	296.3	386.6	422.8	393.8	6.7%
2PBS-07	266.8	382.5	594.0	393.5	11.7%
2PBS-08	263.0	378.7	518.9	390.3	8.4%
2PBS-09	280.4	385.0	441.7	393.7	7.4%
2PBS-10	274.4	382.5	491.9	392.3	8.7%
2PBS-11	277.4	383.8	466.8	393.0	8.0%
Neat PBS	330.7	391.8	413.3	398.0	1.4%
PBS/CANA	280.6	382.2	434.5	394.5	7.6%

As can be seen in **Table 12**, $T_{WL5\%}$ and $T_{WL50\%}$ of Neat PBS and PBS/CANA samples are higher than those of the composites (as explained before), and since CANA and LIG are organic compounds that usually degrade at lower temperatures favored by the presence of clay particles that can “disperse” organic molecules in the composite structure, making them more susceptible to thermal degradation. The addition of SEP which are inorganic minerals whose thermal events are mainly due to water loss (free water, bound water) from 30-500°C and dehydroxylation from 500°C (SEP) and 600°C (MMT) (García-Villén et al., 2019, 2020). The evaporation of water bounded to clay

structures can explain the decrease in $T_{WL5\%}$ (**Figure 22C**) and $T_{WL50\%}$. In all cases, the weight loss experienced by clays during these events is small (2-7%, depending on the environmental conditions in which they were preserved until use).

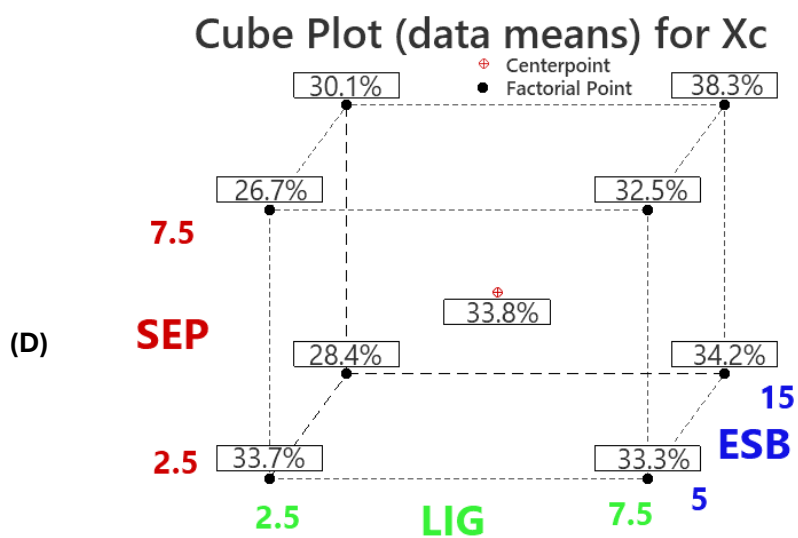
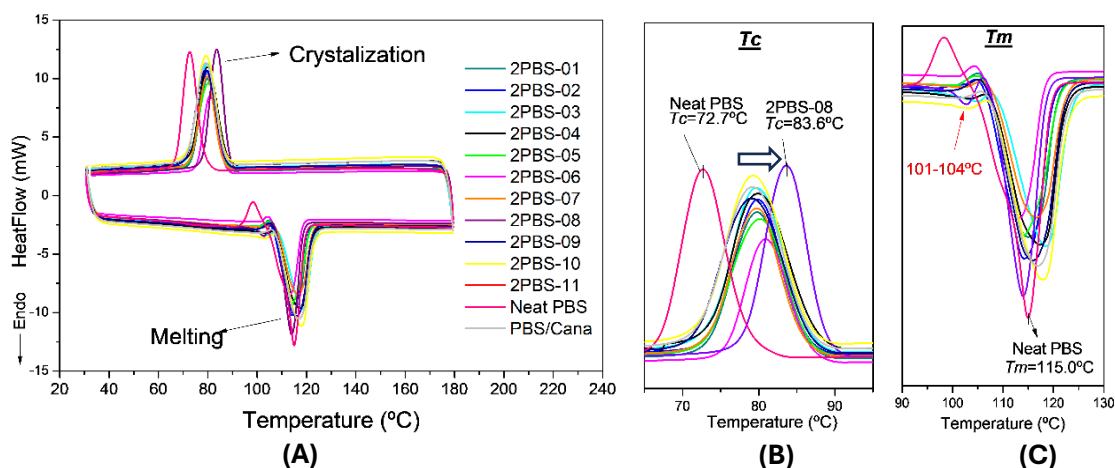
As can be observed in **Figure 22D**, the $T_{WL90\%}$ increase with SEP and LIG increase, but reduced with ESB, as usual plasticizers (including ESB) induce more macromolecular mobility, promoting the degradation of the polymer (Turco et al., 2024). In fact, no significant variations were observed in $T_{WL5\%}$, $T_{WL50\%}$, $T_{WL90\%}$ and T_{max} , indicating that the thermal stability of the composites remains consistent. Thermal stability is commonly associated with TGA analysis by determining the temperature (or range of temperature) at which mass loss occurs, being a relatively good measure. However, it is important to highlight that the composites contain a considerable proportion of natural components, sum of the content of CANA fiber, LIG and clay (from 28.6% to 37.5% by weight in the composite formulations), which inherently have structurally bound water molecules (bound water in fibers and interlayer water for clays), which do not evaporate with a simple drying of the material, requiring higher temperatures, 150-200°C for fibers and 400°C or more in the case of clays (García-Villén et al., 2019, 2020). These molecules are gradually released at the high temperatures applied during the TGA tests, and which end up adding to the mass loss due to the effective thermal decomposition reaction of the material.

Analyzing the residual mass result in TGA, it is important to know that the temperature range was limited from 30 to 600°C (due equipment restrictions), in this condition the results seem to be consistent with the materials composition, in which neat PBS presented a lower residual (1.4 wt.%). The addition of CANA fiber (30 wt.%) resulted in a residual mass of 7.6%, indicating some ash content in this natural fiber. The

residual mass results for the other composites appear to be in line with expectations, with higher residual mass for the samples with higher SEP and LIG contents.

The DSC curves (**Figure 23A**) show two main thermal events, one endothermic event at 114.5°C (for neat PBS) that can be attributed to a crystalline melting transformation (T_m) and other exothermic event at 77.1 °C (for neat PBS), corresponding to crystallization of PBS. The T_c values in the composites increased slightly compared to neat PBS (**Figure 23B**). The T_m values of PBS in the composites changed from 113.4 to 118.6 °C, with the addition of CANA, LIG, SEP and ESB (**Figure 23C** and **Table 13**). SEP seems to cause an increase in the T_m value, as can be observed in **Figure 23E**, in which the highest T_m value is for SEP high quantity (and ESB and LIG lower level). In some composite samples, in a more pronounced way for 2PBS-08, there is a minor endothermic shoulder at 101-104 °C, while for neat PBS it does not appear. Several author (Liang et al., 2009; Liminana et al., 2018; Arabeche et al., 2022) explained that PBS can present three peaks (T_{m1} , T_{m2} and T_{m3}), the main and higher temperature T_m peak (T_{m1}) is not related to the crystallization of previous cooling process and attributed to the recrystallization of the partially melted crystals during heating process (melting–recrystallization–remelting process). The others small T_m peaks (T_{m2} and T_{m3}) can be attributed to the melting of original crystals with different crystalline lamella distribution with different thermal stabilities. The presence of the T_{m3} peak when SEP is added to PBS is a strong indication of good SEP-PBS interaction, since T_{m3} peak is attribute the formation of original crystals in the interfacial area between the clay and the polymer (Arabeche et al., 2022), while the melting temperature T_{m1} remains unchanged. In the present study, some composites, especially 2PBS-08 (higher SEP content) have this T_{m3} peak, so this is strong evidence that there is a good dispersion of SEP and its ability to crystallize PBS at its interface.

Neat PBS has a low crystallization temperature (77.1°C) (**Figure 23B** and **Table 13**) but the peak shifted to a higher temperature value with the addition of CANA, LIG, ESB and SEP (around 79-80 °C). A particular sample, 2PBS-08 (DOE +1+1+1) presented a higher T_c (83.6 °C), indicating that the crystallization of PBS was enhanced with the addition of these.



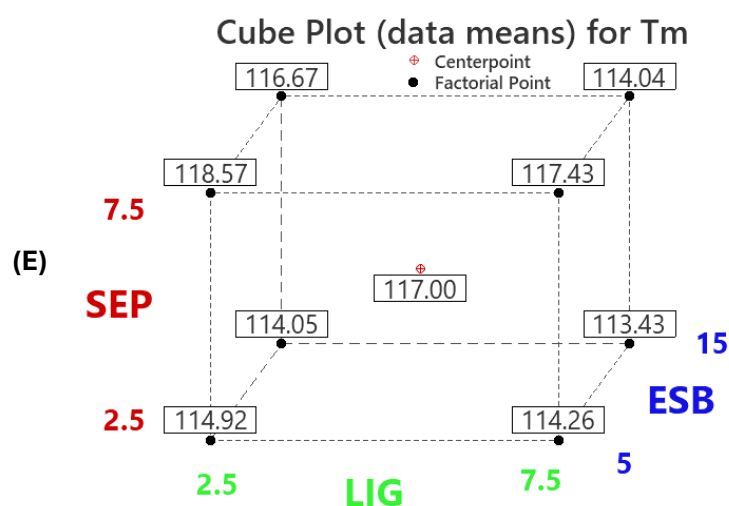


Figure 23: DSC analysis results of PBS composites: (A) Full thermal profiles; (B) Detailed view of crystallization region; (C) Detailed view of the melting temperature region; (D) Cube plot for degree of crystallinity (X_c); (E) Cube plot for melting temperature.

Table 13: parameters result of DSC analysis.

Sample ID	T_c (°C)	T_m (°C)	ΔH_m (J/g)	X_c (%)
2PBS-01	79.79	114.92	48.20	33.7%
2PBS-02	79.91	114.26	45.95	33.3%
2PBS-03	79.70	118.57	36.76	26.7%
2PBS-04	79.89	117.43	43.37	32.5%
2PBS-05	80.16	114.05	37.84	28.4%
2PBS-06	80.90	113.43	44.10	34.2%
2PBS-07	79.74	116.67	38.84	30.1%
2PBS-08	83.64	114.04	47.90	38.3%
2PBS-09	79.08	115.92	48.34	36.3%
2PBS-10	79.28	118.08	41.69	31.3%
2PBS-11	79.18	117.00	45.02	33.8%
NeatPBS	72.72	114.98	67.17	33.6%
PBS/CANA	77.34	115.21	54.48	38.9%

Table 13 shows that melting enthalpy (ΔH_m) and degree of crystallinity (X_c) decreased with the addition of CANA, LIG, SEP and ESB. The degree of crystallinity (X_c) was possibly impacted by the addition of plasticizer (ESB), neutralizing the nucleation effect of the other components (CANA, SEP and Lig), with no relevant increase in X_c being observed (**Figure 23D**), as could be expected from the increase in PBS crystallization

attributed to the effect of fillers such as natural fibers and clay in the nucleation of crystallization (Liang et al., 2009).

4.3.6 X-Ray Diffraction (XRD)

The SEP and composites were analyzed by XRD to evaluate the interlayer space (*d-value*) variation of SEP characteristics reflections planes (**Figure 24A**). The approximate width of the extended molecular chain of PBS is about 0.4–0.6 nm (Someya et al., 2003). If the interlayer space variation (Δd) of SEP before (in neat SEP) and after (in the composite) is greater than the width of the PBS molecular chain, then this is a good indication (but not only one) of exfoliation of SEP interlayers, as the PBS molecules were able to penetrate the clay interlayer space. Sepiolite is characterized by presenting reflections in the planes (1 1 0), (0 4 0) and (4 0 0), and using the Bragg condition, $n\lambda = 2d \cdot \sin(\theta)$, it is possible to calculate the respective reflection angles $2\theta = 7.2^\circ$, 19.6° , 26.5° of these planes (Nikolic et al., 2017). Thus, for each composite formulation, the interplanar distance and the variation (Δd) in relation to the interplanar distance of pure sepiolite were calculated, as shown in **Table 14**. As can be observed in the (0 4 0) and (4 0 0) planes, there was practically no change in the interplanar distance. However, in the (1 1 0) plane, there are some separations of the planes (up to 0.041 nm), although much smaller than the possibility of the PBS molecules having intercalated in the SEP layers. Fukushima et al., 2012 explains that the needle-shaped SEP has a non-periodic stacking structure which the dispersion is difficulted to be examined through X-ray diffraction (Fukushima et al., 2012). So, the small interlayer space variation for SEP does not mean that exfoliation was not effective.

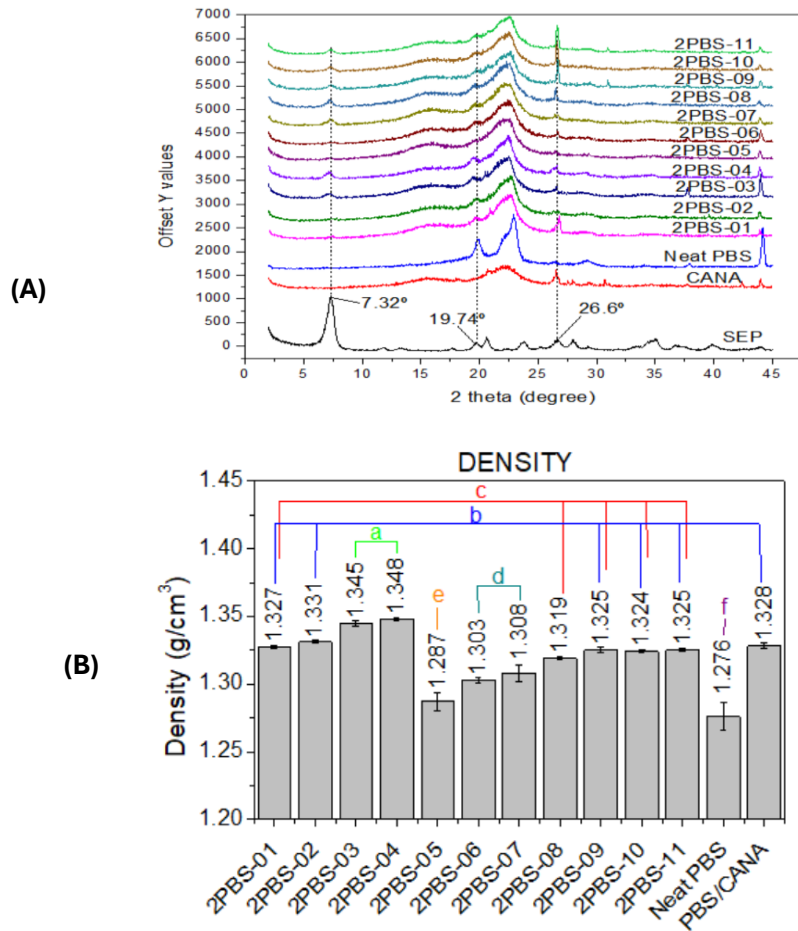


Figure 24: (A) XRD diagrams and (B) Density of SEP and PBS composites. Note: Tukey statistical test, mean value with same letters do not differ at the 5% significance level. The letters are in descending order of mean values. Number of replicates, $n=5$.

Table 14: interlayer space (d -value) and interlayer space variation (Δd) for SEP reflections planes, in SEP and composites.

Plan	(1 1 0)			(0 4 0)			(4 0 0)		
Sample	2θ	d (nm)	Δd (nm)	2θ	d (nm)	Δd (nm)	2θ	d (nm)	Δd (nm)
Neat SEP	7.30	1.210	-	19.74	0.449	-	26.60	0.335	-
2PBS-01	7.24	1.220	0.010	19.56	0.453	0.004	26.46	0.337	0.002
2PBS-02	7.42	1.190	-0.020	19.50	0.455	0.005	26.34	0.338	0.003
2PBS-03	7.06	1.251	0.041	19.26	0.460	0.011	26.25	0.339	0.004
2PBS-04	7.08	1.248	0.038	19.46	0.456	0.006	26.60	0.335	0.000
2PBS-05	7.08	1.248	0.038	19.72	0.450	0.000	26.46	0.337	0.002
2PBS-06	7.32	1.207	-0.003	19.48	0.455	0.006	26.70	0.334	-0.001
2PBS-07	7.26	1.217	0.007	19.52	0.454	0.005	26.44	0.337	0.002
2PBS-08	7.14	1.237	0.027	19.48	0.455	0.006	26.46	0.337	0.002
2PBS-09	7.40	1.194	-0.016	19.66	0.451	0.002	26.64	0.334	0.000
2PBS-10	7.24	1.220	0.010	19.60	0.453	0.003	26.56	0.335	0.000
2PBS-11	7.24	1.220	0.010	18.20	0.487	0.008	26.62	0.335	0.000

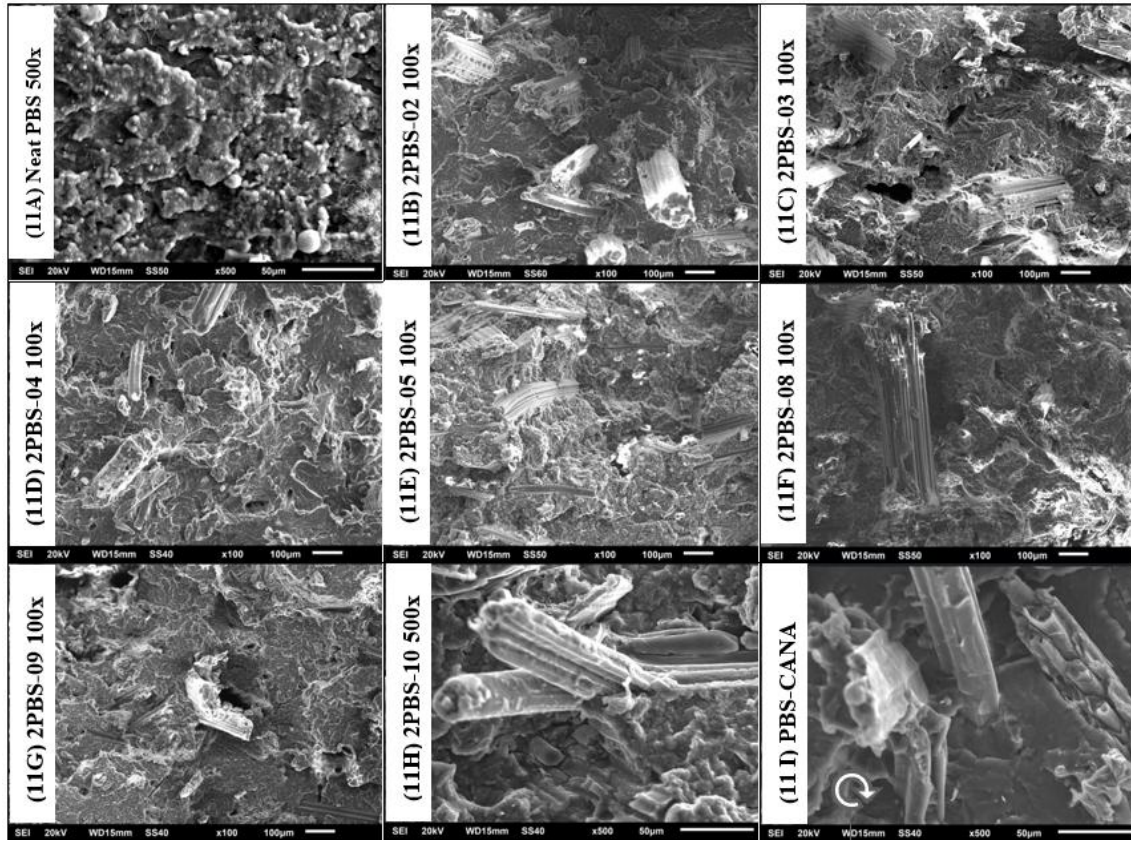
4.3.7 Density

The density (**Figure 24B**) of PBS composites was influenced by the addition of lignin (LIG), sepiolite (SEP), and epoxidized soybean oil (ESB). LIG is a relatively low-density organic filler, initially had a minimal impact on density. However, at higher concentrations, LIG may promote crosslinking reactions (Ewurum and McDonald, 2025), leading to a more compact polymer network and a potential increase in density due to reduced free volume. SEP, as an inorganic nanofiller, slightly increased density due to its higher mass and strong interaction with the PBS matrix. Conversely, ESB acted as a plasticizer, increasing polymer chain mobility and free volume, thereby reducing density. The combined effects of these components indicate that while SEP reinforces the structure and LIG may induce densification, ESB counterbalances this effect by enhancing molecular flexibility, influencing both mechanical performance and processability.

4.3.8 Morphology Analysis

The morphology of the fractured samples from Izod impact test were studied by SEM. Neat PBS (**Figure 25A**) presents a fracture surface morphology with rounded regions, appearing to be a more ductile fracture, consistent with impact/tensile/flexural results, which presented higher impact energy and elongation at break, in comparison to the composites. The composite samples are shown in **Figures 25B to 25H**, in which the polymer matrix presents an irregular, brittle-type appearance, with exposed CANA fiber due to fracture, without evident detachment of the fiber from the matrix, indicating a certain good interfacial adhesion. **Figure 25 I** shows the PBS/CANA composite fractured surface and can be observed that polymer matrix has a different fracture surface (flatter) when compared to the other composites, but due to the high percentage of CANA fiber

(up to 30% by weight), it led to a reduction in impact resistance compared to neat PBS. The EDS analysis can prove the presence of clay mineral particles by the detection of Si and Mg, and LIG can be associated with the presence of sulfur. The distribution of these elements (Si, Mg, S) in the composite 2PBS-03 (**Figure 25 J**) show a good dispersion of the clay and LIG in the PBS matrix, mainly due the high shear mixing promoted by the twin screw extruder processing. The SEM images are consistent with the impact strength results, since no statistically significant differences were found between almost composite samples (excluding Neat PBS).



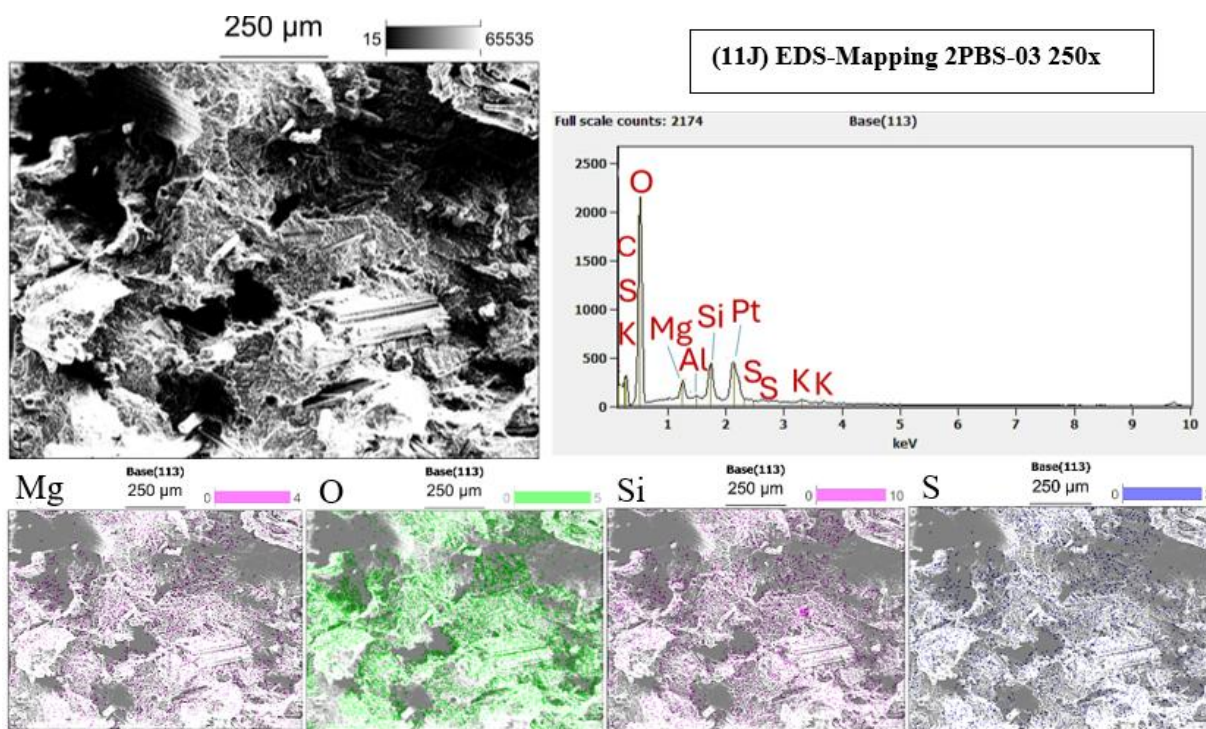


Figure 25: SEM images and EDS analysis of PBS composites.

The low Izod impact strength indicates that the matrix did not have its ductility increased by the addition of ESB, as expected. ESB is a functionalized vegetable oil, with flexible molecules that can either react with hydroxyl groups of PBS and hydroxyl groups in the lignocellulosic filler (and provide different effects on polyester type polymer such as PBS, related to plasticizing phenomena, chain extension, compatibilization, crosslinking, due to the high reactivity of epoxy groups. (Liminana et al., 2018) ESB was used here as compatibilizer agents (see mechanism in **Figure 26**), plasticizers and to increase ductility (Platnieks et al., 2020), but the results did not show these, maybe due to the incorporation of LIG which is present in all composites except PBS-CANA, and LIG can promote crosslink network that limits the ductility of the samples (Ewurum and McDonald, 2025). As previously explained in the MFR section, it seems that the ESB did not act effectively as a plasticizer, probably due to the solubility limit in PBS, leading to migration to the composite surface.

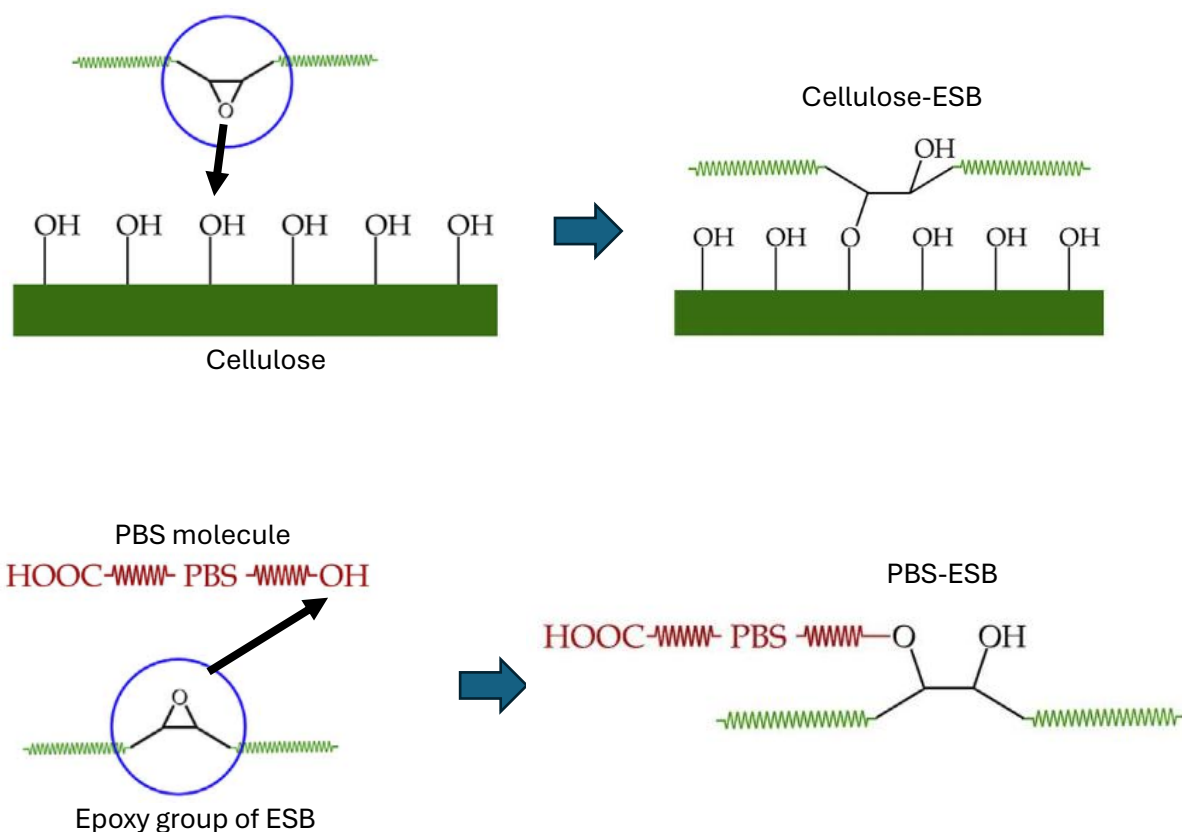


Figure 26: Schematic of the reactions of epoxy group of ESB and hydroxyl groups of PBS and cellulose (applicable for CANA fiber). Adapted from Liminana, et al., 2018*.

* Permission to use the figure was granted through Rightslink by Elsevier and Copyright Clearance Center. License #6027321050107.

4.4 CONCLUSION

This study successfully developed and characterized biodegradable polybutylene succinate (PBS) composites reinforced with canabrava fiber (CANA), lignin (LIG), and sepiolite (SEP), with epoxidized soybean oil (ESB) as a plasticizer and potential compatibilizer. The experimental results demonstrated significant improvements in mechanical, thermal, and biodegradability properties, confirming the viability of these hybrid bio-composites for sustainable applications, particularly in agricultural packaging. From the mechanical characterization, the addition of CANA at 30 wt.% significantly increased stiffness, as reflected in the Young's modulus, which improved by up to 309%

(from 569 MPa for neat PBS to 2326 MPa for 2PBS-03). Similarly, the flexural modulus increased by up to 307%, and the flexural strength by 46%, compared to neat PBS. The highest flexural modulus (2550 MPa) was obtained for composites with high SEP content (2PBS-03). However, the incorporation of CANA and SEP reduced impact resistance, making the composites more brittle. ESB was expected to improve ductility, but at higher concentrations (15 phr), it acted as an external lubricant, leading to processing difficulties and limited plasticizing effects. Future works should focus on improving the toughness of these composites, such as by testing different compatibilizers, surface treatments for natural fibers, or hybrid plasticizer systems that better balance ductility and stiffness, without compromising processability.

The melt flow rate (MFR) analysis showed that LIG initially improved processability by increasing fluidity, but excessive LIG content led to a rise in viscosity due to crosslinking effects. SEP restricted polymer chain mobility, reducing MFR, whereas ESB significantly increased fluidity, though excessive amounts negatively affected injection molding.

Thermal analysis indicated that PBS degradation occurred at temperatures above 280°C, with composites showing earlier degradation onset due to the presence of organic fillers. DSC results revealed that SEP played a key role in increasing the crystallization temperature (T_c), reaching 83.6°C for 2PBS-08, compared to 77.1°C for neat PBS. Additionally, SEP improved the degree of crystallinity (X_c), indicating strong filler-matrix interactions. XRD analysis confirmed some intercalation of PBS into SEP, supporting its role as a reinforcement.

The soil biodegradation test revealed that PBS composites degraded at a faster rate than neat PBS, with the composite (2PBS-09) losing 9.0% of its mass after 90 days compared to 4.8% for pure PBS. This accelerated degradation was attributed to the

hydrophilic nature of CANA and the porous structure of SEP, which facilitated microbial activity. Long-term evaluations, including accelerated aging and water resistance tests—given the material's exposure to moisture and UV-radiation, which may necessitate the use of photo-stabilizing additives—together with biodegradation studies under real field or composting conditions, are essential to further validate the environmental performance and practical applicability of these materials.

Morphological analysis via SEM confirmed good fiber-matrix adhesion, with limited fiber pullout, suggesting some degree of compatibilization. However, voids and brittle fracture surfaces indicated that further optimization is required to enhance impact resistance. EDS mapping demonstrated uniform dispersion of SEP and LIG within the polymer matrix.

In conclusion, PBS-based bio-composites reinforced with natural fibers, lignin, and sepiolite demonstrate enhanced mechanical properties, biodegradability, and sustainability. This is an efficient and very convenient way to obtain biodegradable composites with PBS, for example, considering the possibility to finely tune the functional properties by playing with the respective proportions of each component. By optimizing filler content and processing conditions, these composites can serve as a viable material for biodegradable applications, particularly in agricultural products such as seed trays, contributing to a more circular plastic economy. Furthermore, these materials present a favorable cost–performance ratio, as up to 37.5 wt.% of the composite consists of low-cost, renewable materials such as canabrava residue and lignin, both of which are typically considered waste and would otherwise incur disposal costs. This partial replacement of PBS, a relatively expensive polymer, can significantly reduce overall material expenses. However, a more detailed economic assessment is needed to accurately quantify the effective cost reduction achieved by using these bio-fillers.

5.0 FINAL CONSIDERATION

5.1 CONCLUSIONS

This work aimed to develop and characterize hybrid eco-composites based on poly(butylene succinate) (PBS), reinforced with natural Canabrava fiber (CANA), kraft lignin (LIG), and sepiolite clay (SEP), targeting sustainable agricultural applications such as seedling trays and tubes. The research was conducted through two experimental stages, ranging from initial formulations with natural additives to a design of experiments (DOE) focused on optimizing performance and processability.

The main results demonstrated that adding 30 wt% of Canabrava fiber to PBS significantly increased the Young's modulus (from 666 MPa to 2350 MPa) and flexural modulus (from 664 MPa to over 2400 MPa), evidences that its acted as a structural reinforcement. However, this addition drastically reduced the melt flow rate (MFR), compromising injectability. The incorporation of 5% lignin mitigated this effect, partially restoring fluidity and allowing injection processing.

The use of sepiolite (up to 1.7 wt%) contributed to additional gains in thermal stability, crystallinity (up to 40.9%), and mechanical strength, outperforming montmorillonite in overall performance. Sepiolite-containing composites showed an increase in crystallization temperature (from 72.7 °C to over 86 °C) and an elevation in the thermal decomposition temperature, $T_{WL90\%}$ (from 413 °C to 594 °C), desirable attributes for applications under adverse environmental conditions.

On the other hand, the high presence of fiber reduced the ductility and impact strength of the composites, even with the use of lignin and clays. Elongation at break decreased from 16.8% (pure PBS) to about 2.5%, and impact strength was reduced from 19.4 to 14.6 kJ/m². The addition of epoxidized soybean oil (ESB) as a plasticizer and compatibilizer had a limited effect, indicating the need for improved strategies to enhance the interfacial adhesion of CANA fibers to PBS. Such strategies may involve assessing the influence of fiber size, moisture sensitivity, or applying mild chemical surface treatments (e.g., NaOH). Furthermore, alternative bio-based compatibilizers or

plasticizers—including epoxidized linseed oil (ELO), maleinized linseed oil (MLO) (Liminana, 2018), castor oil (CO), and canola oil (CA) (Castro, 2014)—should be further explored.

The soil biodegradation test revealed that the composites degraded more rapidly than pure PBS, with a mass loss of up to 9.0% in 90 days, attributed to the hydrophilic nature of CANA and the porous structure of SEP. EDS mapping confirmed good dispersion of the natural additives in the polymer matrix, with satisfactory interfacial adhesion observed via SEM. And for the intended application in agricultural packaging, given the demanding service conditions, complementary studies such as accelerated aging, water resistance testing, and biodegradation assessments under real field or composting environments may be necessary to validate both the environmental performance and the practical applicability of the biocomposites.

In summary, the partial replacement of PBS with low-cost natural materials not only enhanced key properties but also resulted in a significant reduction in material costs—approximately 32% (see Appendix D)—demonstrating competitive potential compared to other commercial biopolymers and, to a more limited extent, polyolefin resins. By replacing up to 37.5 wt.% of the relatively expensive PBS polymer with low-cost, renewable materials like canabrava residue and lignin—both typically considered waste products—the overall material expenses can be substantially reduced. This strategic use of abundant, low-value biomass residues and natural minerals not only contributes to the circular economy and sustainable materials engineering but also validates the technical and environmental feasibility of the developed composites, highlighting their potential for agricultural applications and their role as a competitive and scalable solution for reducing plastic waste.

5.2 RECOMMENDATIONS FOR FUTURE WORKS

Despite the positive outcomes achieved in this study, several opportunities for further research remain, as outlined below:

- Improvement of interfacial adhesion: Future studies should explore the influence of fiber size, moisture sensitivity, or applying mild chemical surface treatments (e.g., NaOH) or functionalization strategies (e.g., coupling agents) or alternative bio-based compatibilizers or plasticizers, such as epoxidized linseed oil (ELO),

maleinized linseed oil (MLO) (Liminana, 2018), castor oil (CO), and canola oil (CA) (Castro, 2014), to enhance fiber-matrix adhesion, thereby improving impact resistance and ductility.

- **Optimization of Fiber Morphology:** Investigating different particle sizes, aspect ratios, and orientations of CANA fibers could provide deeper insight into their reinforcing efficiency and effect on rheological and mechanical behavior.
- **Use of Alternative Plasticizers or Compatibilizers:** Other bio-based plasticizers, such as epoxidized linseed oil, citrate esters, or modified starches, may offer improved mechanical resilience and further enhance biodegradability.
- **Long-Term Biodegradation and Environmental Impact:** Additional studies focusing on long-term environmental performance, such as soil and compost degradation over extended periods ecotoxicity assessments, and life-cycle analyses (LCA), are essential for a more comprehensive evaluation. Biodegradation test according to ISO 14855 / ASTM D5338 to quantify mineralization and verify compliance with industrial composting standards.
- **Industrial Scale-Up and Validation:** Pilot-scale processing and field trials using real agricultural conditions must be conducted to validate the technical and economic viability of these biocomposites for commercial applications. To this end, durability and field performance studies (UV exposure, humidity, temperature) must be conducted, considering agricultural applications.
- **Multifunctional Additive Integration:** The incorporation of other natural functional additives (e.g., antimicrobial agents, UV stabilizers, or nutrient carriers) could further increase the applicability of the composites in smart or active packaging.

6.0 REFERENCES

- A. Nazrin, S.M.Saouan, M.Y.M. Zuhri, R.A.Ilyas, R.Syafiq, S.F.K. Sherwani, 2020. Nanocellulose Reinforced Thermoplastic Starch (TPS), Polylactic Acid (PLA), and Polybutylene Succinate (PBS) for Food Packaging Applications. *Front Chem.*
- Aaliya, B., Sunooj, K.V., Lackner, M., 2021. Biopolymer composites: a review. *International Journal of Biobased Plastics* 3, 40–84.
<https://doi.org/10.1080/24759651.2021.1881214>
- Abderrahim, B., Abderrahman, E., Mohamed, A., Fatima, T., Abdesselam, T., Krim, O., 2015. Kinetic Thermal Degradation of Cellulose, Polybutylene Succinate and a Green Composite: Comparative Study. *World Journal of Environmental Engineering*, Vol. 3, 2015, Pages 95-110 3, 95–110. <https://doi.org/10.12691/WJEE-3-4-1>
- Abu Ghalia, M., Dahman, Y., 2017. Synthesis and utilization of natural fiber-reinforced poly (lactic acid) bionanocomposites, *Lignocellulosic Fibre and Biomass-Based Composite Materials: Processing, Properties and Applications*. Elsevier Ltd.
<https://doi.org/10.1016/B978-0-08-100959-8.00015-9>
- Arabeche, K., Abdelmalek, F., Delbreilh, L., Zair, L., Berrayah, A., 2022. Physical and rheological properties of biodegradable poly(butylene succinate)/Alfa fiber composites. *Journal of Thermoplastic Composite Materials* 35, 1709–1727.
<https://doi.org/10.1177/0892705720904098>
- Ayu, R.S., Khalina, A., Harmaen, A.S., Zaman, K., Isma, T., Liu, Q., Ilyas, R.A., Lee, C.H., 2020. Fibers reinforcement in poly(Butylene) succinate (PBS)/starch/glycerol composite sheet. *Polymers (Basel)* 12, 1–13. <https://doi.org/10.3390/polym12071571>
- Bahrami, M., Abenojar, J., Martínez, M.Á., 2020. Recent progress in hybrid biocomposites: Mechanical properties, water absorption, and flame retardancy, *Materials*.
<https://doi.org/10.3390/ma13225145>
- Barletta, M., Aversa, C., Ayyoob, M., Gisario, A., Hamad, K., Mehrpouya, M., Vahabi, H., 2022. Poly(butylene succinate) (PBS): Materials, processing, and industrial applications. *Prog Polym Sci* 132, 101579.
<https://doi.org/10.1016/j.progpolymsci.2022.101579>
- Basbasan, A.J., Hararak, B., Winotapun, C., Wanmolee, W., Chinsirikul, W., Leelaphiwat, P., Chonhenchob, V., Boonruang, K., 2023. Lignin Nanoparticles for Enhancing Physicochemical and Antimicrobial Properties of Polybutylene Succinate/Thymol Composite Film for Active Packaging. *Polymers (Basel)* 15.
<https://doi.org/10.3390/polym15040989>
- Behera, D., Pattnaik, S.S., Sanjibani, S., Nayak, G.C., Das, N., Behera, A.K., 2024. Fabrication and characterization of eco-friendly biocomposites from waste coconut

- spathe fabric for sustainable progress. *New Journal of Chemistry*.
<https://doi.org/10.1039/d4nj03831b>
- Bozell, J.J., Petersen, G.R., 2010. Technology development for the production of biobased products from biorefinery carbohydrates—the US Department of Energy’s “top 10” revisited. *Green Chemistry* 12, 539–55. <https://doi.org/10.1039/b922014c>
- Braskem S.A., 2018. Polypropylene EP 440L datasheet.
- Chen, J., Xu, J., Xu, H., Li, Z., Zhong, G., Lei, J., 2015. The Crystallization Behavior of Biodegradable Poly(butylene succinate) in the Presence of Organically Modified Clay with a Wide Range of Loadings. *Chinese Journal of Polymer Science* 33, 576–586.
- Chidambara Kuttalam, K., Palaniappan, M., Santulli, C., Karuppiah, G., Palanisamy, S., 2021. Mechanical and Impact Strength of Nanoclay-Filled Composites: A Short Review.
- Chikh, A., Benhamida, A., Kaci, M., Pillin, I., Bruzaud, S., 2016. Synergistic effect of compatibilizer and sepiolite on the morphology of poly(3-hydroxybutyrate-co-3-hydroxyvalerate)/poly(butylene succinate) blends. *Polym Test* 53, 19–28.
<https://doi.org/10.1016/j.polymertesting.2016.05.008>
- Coradin, L., Siminski, A., Reis, A., 2011. Native species of Brazilian flora with current or potential economic value: plants for the future. *Brazilian Ministry of the Environment* 934.
- De Luca, S., Mueller, K., Tomei, L., Gallichi Nottiani, D., Milanese, D., Sciancalepore, C., 2025. Brewer’s Spent Grains as Alternative Ligno-Cellulosic Filler for the Preparation of Bio-Based Polymer Composites. *Advances in Polymer Technology* 2025.
<https://doi.org/10.1155/adv/5060184>
- De Oliveira Santos, R.P., Castro, D.O., Ruvoilo-Filho, A.C., Frollini, E., 2014. Processing and thermal properties of composites based on recycled PET, sisal fibers, and renewable plasticizers. *J Appl Polym Sci* 131. <https://doi.org/10.1002/app.40386>
- Dilsad, A.M., Ahuja, A., Gupta, N., Kumar Bachala, S., Kumar Rastogi, V., 2024. Analysing the impact of nanomaterials on the degradation behaviour of biopolymers: A comprehensive review. *Eur Polym J*. <https://doi.org/10.1016/j.eurpolymj.2024.113189>
- DIPA Química, 2022. oleo-de-soja-epoxidado-draipexyet_DIPA Quimica.
- Domínguez-Robles, J., Larrañeta, E., Fong, M.L., Martin, N.K., Irwin, N.J., Mutjé, P., Tarrés, Q., Delgado-Aguilar, M., 2020. Lignin/poly(butylene succinate) composites with antioxidant and antibacterial properties for potential biomedical applications. *Int J Biol Macromol* 145, 92–99. <https://doi.org/10.1016/j.ijbiomac.2019.12.146>
- Ewurum, N., McDonald, A.G., 2025. Lignin Reinforcement in Polybutylene Succinate Copolymers. *Polymers (Basel)* 17. <https://doi.org/10.3390/polym17020194>
- Farshchi, N., Ostad, Y.K., 2020. Sepiolite as a nanofiller to improve mechanical and thermal behavior of recycled high-density polyethylene. *Progress in Rubber, Plastics and Recycling Technology* 36, 185–195. <https://doi.org/10.1177/1477760620918596>

- Franca, A., Santos, P.M.; ; A Queiroz, A.P., Santos, K.K.A.;, Silva, ; A Mattedi, A.C.M., 2019. ADSORPTION OF CRUDE OIL IN AQUEOUS ENVIRONMENT USING WILD CANE FIBER: EQUILIBRIUM AND KINETIC STUDIES 13, 333–354. <https://doi.org/10.2019/Accepted>
- Frollini, E., Bartolucci, N., Sisti, L., Celli, A., 2013. Poly(butylene succinate) reinforced with different lignocellulosic fibers. *Ind Crops Prod* 45, 160–169. <https://doi.org/10.1016/j.indcrop.2012.12.013>
- Fukushima, K., Wu, M.H., Bocchini, S., Rasyida, A., Yang, M.C., 2012. PBAT based nanocomposites for medical and industrial applications. *Materials Science and Engineering C* 32, 1331–1351. <https://doi.org/10.1016/j.msec.2012.04.005>
- García-Quiles, L., Cuello, Á.F., Castell, P., 2019. Sustainable materials with enhanced mechanical properties based on industrial polyhydroxyalkanoates reinforced with organomodified sepiolite and montmorillonite. *Polymers (Basel)* 11. <https://doi.org/10.3390/polym11040696>
- García-Villén, F., Faccendini, A., Aguzzi, C., Cerezo, P., Bonferoni, M.C., Rossi, S., Grisoli, P., Ruggeri, M., Ferrari, F., Sandri, G., Viseras, C., 2019. Montmorillonite-norfloracin nanocomposite intended for healing of infected wounds. *Int J Nanomedicine* 14, 5051–5060. <https://doi.org/10.2147/IJN.S208713>
- García-Villén, F., Sánchez-Espejo, R., López-Galindo, A., Cerezo, P., Viseras, C., 2020. Design and characterization of spring water hydrogels with natural inorganic excipients. *Appl Clay Sci* 197, 105772. <https://doi.org/10.1016/j.clay.2020.105772>
- Huang, Z., Qian, L., Yin, Q., Yu, N., Liu, T., Tian, D., 2018. Biodegradability studies of poly(butylene succinate) composites filled with sugarcane rind fiber. *Polym Test* 66, 319–326. <https://doi.org/10.1016/j.polymertesting.2018.02.003>
- Huo, S., Wang, J., Wu, X., 2017. Morphology, thermal and mechanical performances of SR composites containing sepiolite and HGMs as binary fillers. *Journal of Polymer Engineering* 37, 197–204. <https://doi.org/10.1515/polyeng-2015-0442>
- IBF, 2023. Tubes for seedlings: lower cost and more productivity [WWW Document]. Instituto Brasileiro de Florestas. URL <https://www.ibflorestas.org.br/conteudo/o-uso-de-materiais-plasticos-confere-o-reducao-de-custo-operacional-e-aumento-de-produtividade>
- ISO 178, 2019. Plastics-Determination of flexural properties. ISO.
- ISO 180, 2019. Plastics-Determination of Izod impact strength.
- ISO 527-1, 2012. Plastics—Determination of Tensile Properties—Part 1: General Principles. ISO.
- ISO 1133-1, 2011. Plastics-Determination of the melt mass flow rate MFR and melt volumeflow rate-MVR of thermoplastics. ISO.
- Izzati Zulkifli, N., Samat, N., Anuar, H., Zainuddin, N., 2015. Mechanical properties and failure modes of recycled polypropylene/microcrystalline cellulose composites. *Mater Des* 69, 114–123. <https://doi.org/10.1016/j.matdes.2014.12.053>

- Jia, P., Xia, H., Tang, K., Zhou, Y., 2018. Plasticizers derived from biomass resources: A short review. *Polymers (Basel)*. <https://doi.org/10.3390/polym10121303>
- Joy, J., Jose, C., Yu, X., Mathew, L., Thomas, S., Pilla, S., 2017. The influence of nanocellulosic fiber, extracted from *Helicteres isora*, on thermal, wetting and viscoelastic properties of poly(butylene succinate) composites. *Cellulose* 24, 4313–4323. <https://doi.org/10.1007/s10570-017-1439-y>
- Kanemura, C., Nakashima, S., Hotta, A., 2012. Mechanical properties and chemical structures of biodegradable poly(butylene-succinate) for material reprocessing. *Polym Degrad Stab* 97, 972–980. <https://doi.org/10.1016/j.polymdegradstab.2012.03.015>
- Kim, H.S., Kim, H.J., Lee, J.W., Choi, I.G., 2006. Biodegradability of bio-flour filled biodegradable poly(butylene succinate) bio-composites in natural and compost soil. *Polym Degrad Stab* 91, 1117–1127. <https://doi.org/10.1016/j.polymdegradstab.2005.07.002>
- Kuenz, A., Hoffmann, L., Goy, K., Bromann, S., Prübe, U., 2020. High-level production of succinic acid from crude glycerol by a wild type organism. *Catalysts* 10. <https://doi.org/10.3390/catal10050470>
- Li, J., Wang, X., Li, Y., Hu, H., Liang, X., 2024. Rheological, thermal, and mechanical properties of poly(butylene succinate) (PBS)/poly(L-lactide) (PLA) fiber biodegradable green composites. *Colloid Polym Sci* 302, 1053–1066. <https://doi.org/10.1007/s00396-024-05243-0>
- Li, Y.-D., Fu, Q.-Q., Wang, M., Zeng, J.-B., 2017. Morphological, crystallization and rheological behavior in poly(butylenesuccinate)/cellulose nanocrystal nanocomposites fabricated by solution coagulation. *Carbohydr Polym* 164, 75–82.
- Liang, Z., Pan, P., Zhu, B., Dong, T., Inoue, Y., 2009. Mechanical and Thermal Properties of Poly (butylene succinate)/ Plant Fiber Biodegradable Composite. <https://doi.org/10.1002/app>
- Liminana, P., Garcia-Sanoguera, D., Quiles-Carrillo, L., Balart, R., Montanes, N., 2018. Development and characterization of environmentally friendly composites from poly(butylene succinate) (PBS) and almond shell flour with different compatibilizers. *Compos B Eng* 144, 153–162. <https://doi.org/10.1016/j.compositesb.2018.02.031>
- Liu, L., Yu, J., Cheng, L., Yang, X., 2009. Biodegradability of poly(butylene succinate) (PBS) composite reinforced with jute fibre. *Polym Degrad Stab* 94, 90–94. <https://doi.org/10.1016/j.polymdegradstab.2008.10.013>
- Lopez, Y.C.O., Vergara, J.F.P., Alvarez, A.H., Guzmán, J.D.C., Hernández, H.M., Guzmán, J.F.C., 2025. Standardized Production of Artisanal Paper from *Gynerium sagittatum* Residues as a Sustainable Strategy for Zenú Handicrafts. *Journal of Hunan University Natural Sciences*. <https://doi.org/10.55463/issn.1674-2974.52.3.4>
- Lule, Z., Shiferaw, E.W., Kim, J., 2020. Thermomechanical Properties of SiC-Filled Polybutylene Succinate Composite Fabricated via Melt Extrusion. *Polymers (Basel)* 12, 1–9. <https://doi.org/10.3390/polym12020418>

- Mcc Biochem Company Limited, P., 2025. GREEN LIVING REDEFINED.
- Miao, C., Hamad, W.Y., 2019. Critical insights into the reinforcement potential of cellulose nanocrystals in polymer nanocomposites. *Curr Opin Solid State Mater Sci* 23, 100761. <https://doi.org/10.1016/j.cossms.2019.06.005>
- Miao, C., Hamad, W.Y., 2013. Cellulose reinforced polymer composites and nanocomposites: A critical review. *Cellulose* 20, 2221–2262. <https://doi.org/10.1007/s10570-013-0007-3>
- Mizuno, S., Maeda, T., Kanemura, C., Hotta, A., 2015. Biodegradability, reprocessability, and mechanical properties of polybutylene succinate (PBS) photografted by hydrophilic or hydrophobic membranes. *Polym Degrad Stab*. <https://doi.org/10.1016/j.polymdegradstab.2015.03.015>
- Mochane, M.J., Magagula, S.I., Sefadi, J.S., Mokhena, T.C., 2021. A review on green composites based on natural fiber-reinforced polybutylene succinate (PBS). *Polymers (Basel)* 13, 1–38. <https://doi.org/10.3390/polym13081200>
- Moon, R.J., Martini, A., Nairn, J., Simonsen, J., Youngblood, J., 2011. Cellulose nanomaterials review: Structure, properties and nanocomposites, Chemical Society Reviews. <https://doi.org/10.1039/c0cs00108b>
- Muniyasamy, S., Anstey, A., Reddy, M.M., Misra, M., Mohanty, A., 2013. Biodegradability and compostability of lignocellulosic based composite materials. *J Renew Mater* 1, 253–272. <https://doi.org/10.7569/JRM.2013.634117>
- Muranaka, Y., Koike, T., Osuga, T., Maki, T., 2025. Degradation behavior of polybutylene succinate with fillers. *Polym Degrad Stab* 235. <https://doi.org/10.1016/j.polymdegradstab.2025.111266>
- Muthuraj, R., Misra, M., Mohanty, A.K., 2015. Hydrolytic degradation of biodegradable polyesters under simulated environmental conditions. *J Appl Polym Sci* 132, 1–13. <https://doi.org/10.1002/app.42189>
- Nabels-Sneiders, M., Barkane, A., Platnieks, O., Orlova, L., Gaidukovs, S., 2023. Biodegradable Poly(butylene succinate) Laminate with Nanocellulose Interphase Layer for High-Barrier Packaging Film Application. *Foods* 12. <https://doi.org/10.3390/foods12224136>
- Nascimento, J. dos S., Santos, A.B. dos, Bulhões, E., Maziero, R., Campos Rubio, J.C., 2020. Incorporação da borra de café ao polipropileno para aplicação em tubetes utilizados no cultivo de plantas, in: 3º Congresso Sul Americano de Resíduos Sólidos e Sustentabilidade. Gramado-RS Brasil, pp. 1–6.
- Nikolic, M.S., Petrovic, R., Veljovic, D., Cosovic, V., Stankovic, N., Djonlagic, J., 2017. Effect of sepiolite organomodification on the performance of PCL/sepiolite nanocomposites. *Eur Polym J* 97, 198–209. <https://doi.org/10.1016/j.eurpolymj.2017.10.010>
- OECD, 2022. OECD Global Plastics Outlook: Economic Drivers, Environmental Impacts and Policy Options. <https://doi.org/https://doi.org/10.1787/de747aef-en>

- Ojijo, V., Ray, S.S., 2014. Nano-biocomposites based on synthetic aliphatic polyesters and nanoclay. *Prog Mater Sci* 62, 1–57. <https://doi.org/10.1016/j.pmatsci.2014.01.001>
- Olivato, J.B., Marini, J., Yamashita, F., Pollet, E., Grossmann, M.V.E., Avérous, L., 2017. Sepiolite as a promising nanoclay for nano-biocomposites based on starch and biodegradable polyester. *Materials Science and Engineering C* 70, 296–302. <https://doi.org/10.1016/j.msec.2016.08.077>
- Osorio, P.A.M., Landim, P. da C., Barata, T.Q.F., 2018. Handcraft process for sustainable production of Arrow cane particle boards flecha (*Gynerium sagittatum*).
- Pattnaik, S.S., Behera, D., Das, N., Dash, A.K., Behera, A.K., 2024a. Fabrication and characterization of natural fiber reinforced cowpea resin-based green composites: an approach towards agro-waste valorization. *RSC Adv* 14, 25728–25739. <https://doi.org/10.1039/d4ra03546a>
- Pattnaik, S.S., Behera, D., Nanda, D., Das, N., Behera, A.K., 2025. Green chemistry approaches in materials science: physico-mechanical properties and sustainable applications of grass fiber-reinforced composites. *Green Chemistry*. <https://doi.org/10.1039/d4gc05569a>
- Pattnaik, S.S., Behera, D., Pani, Y., Das, N., Misra, M., Mohanty, A.K., Behera, A.K., 2024b. Fabrication and characterizations of screw pine root fiber reinforced soy composite as sustainable green composite. *Polym Eng Sci* 64, 3048–3058. <https://doi.org/10.1002/pen.26746>
- Phua, Y.J., Chow, W.S., Mohd Ishak, Z.A., 2011. Mechanical properties and structure development in poly(butylene succinate)/organo-montmorillonite nanocomposites under uniaxial cold rolling. *Express Polym Lett* 5, 93–103. <https://doi.org/10.3144/expresspolymlett.2011.11>
- Phua, Y.J., Lau, N.S., Sudesh, K., Chow, W.S., Mohd Ishak, Z.A., 2012. Biodegradability studies of poly(butylene succinate)/organo-montmorillonite nanocomposites under controlled compost soil conditions: Effects of clay loading and compatibiliser. *Polym Degrad Stab* 97, 1345–1354. <https://doi.org/10.1016/j.polymdegradstab.2012.05.024>
- Platnieks, O., Gaidukovs, S., Barkane, A., Gaidukova, G., Grase, L., Thakur, V.K., Filipova, I., Fridrihsone, V., Skute, M., Laka, M., 2020. Highly loaded cellulose/poly (butylene succinate) sustainable composites for woody-like advanced materials application. *Molecules* 25. <https://doi.org/10.3390/molecules25010121>
- Platnieks, O., Sereda, A., Gaidukovs, S., Thakur, V.K., Barkane, A., Gaidukova, G., Filipova, I., Ogurcovs, A., Fridrihsone, V., 2021. Adding value to poly (butylene succinate) and nanofibrillated cellulose-based sustainable nanocomposites by applying masterbatch process. *Ind Crops Prod* 169. <https://doi.org/10.1016/j.indcrop.2021.113669>
- Possari, L.T., Bretas, R.E.S., Rigolin, T.R., Bettini, S.H.P., 2021. Dualistic effect of Kraft lignin on the viscoelastic behavior of biodegradable biobased PBSA. *Mater Today Commun* 29, 102847. <https://doi.org/10.1016/j.mtcomm.2021.102847>
- PTT MCC Biochem, 2023. BioPBS™ FZ71PM / FZ71PB Technical Data Sheet Injection molding for general purpose.

- Qi, J., Wu, J., Chen, J., Wang, H., 2019. An investigation of the thermal and (bio)degradability of PBS copolyesters based on isosorbide. *Polym Degrad Stab.* <https://doi.org/10.1016/j.polymdegradstab.2018.12.031>
- Rafiqah, S.A., Khalina, A., Harmaen, A.S., Tawakkal, I.A., Zaman, K., Asim, M., Nurrazi, M.N., Lee, C.H., 2021. A review on properties and application of bio-based poly(Butylene succinate). *Polymers (Basel)* 13, 1–28. <https://doi.org/10.3390/polym13091436>
- Rashid, M., Chetehouna, K., Cablé, A., Gascoin, N., 2021. Analysing Flammability Characteristics of Green Biocomposites: An Overview, *Fire Technology.* <https://doi.org/10.1007/s10694-020-01001-0>
- Rosa, M.F., Medeiros, E.S., Malmonge, J.A., Wood, D.F., Mattoso, L.H.C., Orts, W., Imam, S.H., 2008. Extração e caracterização de whiskers de celulose de fibra de coco, in: 18° CBECiMat. Porto de Galinhas - PE - Brazil, pp. 4050–4058.
- Sahoo, S., Misra, M., Mohanty, A.K., 2013. Effect of compatibilizer and fillers on the properties of injection molded lignin-based hybrid green composites. *J Appl Polym Sci* 127, 4110–4121. <https://doi.org/10.1002/app.37667>
- Shah, T.A., Zhihe, L., Zhiyu, L., Andong, Z., 2023. Lignin: Chemistry, Structure, and Application, in: *Aleph*. pp. 149–200. <https://doi.org/10.5772/intechopen.106527>
- Sharma, A., Zafar, S., Nirala, C.K., 2025. Mechanical, Viscoelastic and Soil Degradation Performance of Hemp Fiber Reinforced Bio-PBS Composites Developed via Microwave Processing. *Fibers and Polymers.* <https://doi.org/10.1007/s12221-025-00944-x>
- Silva, M. de L., Silva, W.J. dos S., Pereira, A.K.L.S., 2020. APROVEITAMENTO DE RESÍDUOS VEGETAIS COMO ALTERNATIVA NA FABRICAÇÃO DE EMBALAGENS BIODEGRADÁVEIS / USE OF VEGETABLE WASTE AS AN ALTERNATIVE IN THE MANUFACTURE OF BIODEGRADABLE PACKAGING. *Brazilian Journal of Development* 6, 86238–86250. <https://doi.org/10.34117/bjdv6n11-155>
- Sisti, L., Totaro, G., Marchese, P., 2016. PBS Makes its Entrance into the Family of Biobased Plastics, in: Kalia, Susheel; Avérous, L. (Ed.), *Biodegradable and Biobased Polymers for Environmental and Biomedical Applications.* Scrivener Publishing LLC, pp. 225–285.
- Soares, D.Q.P., Souza Jr, F.G., Freitas, R.B.V., Soares, V.P., Ferreira, L.P., Ramon, J.A., Oliveira, G.E., 2017. Praziquantel Release Systems Based on Poly(Butylene Succinate)/Polyethylene Glycol Nanocomposites. *Current Applied Polymer Science* 1, 45–51. <https://doi.org/10.2174/2452271601666160922163508>
- Someya, Y., Nakazato, T., Teramoto, N., Shibata, M., 2003. Thermal and Mechanical Properties of Poly(butylene succinate) Nanocomposites with Various Organo-Modified Montmorillonites. *J Appl Polym Sci* 91, 1463–1475.
- Sun, X., Wu, Q., Zhang, X., Ren, S., Lei, T., Li, W., Xu, G., Zhang, Q., 2018. Nanocellulose films with combined cellulose nanofibers and nanocrystals: tailored thermal, optical and mechanical properties. *Cellulose* 25, 1103–1115. <https://doi.org/10.1007/s10570-017-1627-9>

- Tian, Q., Qin, S., Long, L., Jiang, Y., Zhou, Rongfeng, Zhou, Rong, He, W., Xu, G., 2016. Effect of reaction media on clay dispersion and mechanical properties in poly(butylene succinate)/organoclay nanocomposites. *Journal of Vinyl and Additive Technology* 22, 423–432. <https://doi.org/10.1002/vnl.21461>
- Turco, R., Mallardo, S., Zannini, D., Moeini, A., Serio, M. Di, Tesser, R., Cerruti, P., Santagata, G., 2024. Dual role of epoxidized soybean oil (ESO) as plasticizer and chain extender for biodegradable polybutylene succinate (PBS) formulations. *Giant* 20. <https://doi.org/10.1016/j.giant.2024.100328>
- Wang, H., Gao, Z., Yang, X., Liu, K., Zhang, M., Qiang, X., Wang, X., 2018. Epitaxial crystallization behavior of poly(butylene adipate) on orientated poly(butylene succinate) substrate. *Polymers (Basel)* 10. <https://doi.org/10.3390/polym10020110>
- Wang, L., Miao, Z., Song, J., Zhang, M., 2019. Effects of quaternization on properties of biodegradable Poly(butylene succinate) with low crystallinity. *Mater Res Express* 6.
- Wu, F., Misra, M., Mohanty, A.K., 2019. Rheological monitoring of chemical gelation of biodegradable poly(butylene succinate): importance of peroxide concentration and temperature in reactive extrusion. *Applied Polymer Materials* 1, 1604–1612.
- Xiao, F., Fontaine, G., Bourbigot, S., 2021. Recent developments in fire retardancy of polybutylene succinate. *Polym Degrad Stab* 183, 109466. <https://doi.org/10.1016/j.polymdegradstab.2020.109466>
- Yan, Q., Arango, R., Li, J., Cai, Z., 2021. Fabrication and characterization of carbon foams using 100% Kraft lignin. *Mater Des* 201, 109460. <https://doi.org/10.1016/j.matdes.2021.109460>
- Yan, Q., Xue, B., Zhao, Q., Wang, W., Li, X., Zhao, Y., Wen, J., Meng, X., Zhao, W., 2025. Fully biobased, ultra-tough lignin/polybutylene succinate composites through reactive extrusion. *Ind Crops Prod* 226. <https://doi.org/10.1016/j.indcrop.2025.120638>
- Zakharova, E., Alla, A., Martínez De Ilarduya, A., Muñoz-Guerra, S., 2015. Bio-based PBS copolyesters derived from a bicyclic d-glucitol. *RSC Adv* 5, 46395–46404. <https://doi.org/10.1039/c5ra03844h>
- Zhang, S., He, Y., Yin, Y., Jiang, G., 2019. Fabrication of innovative thermoplastic starch bio-elastomer to achieve high toughness poly(butylene succinate) composites. *Carbohydr Polym* 206, 827–836. <https://doi.org/10.1016/j.carbpol.2018.11.036>
- Zhang, X., Zhang, Y., 2016. Reinforcement effect of poly(butylene succinate) (PBS)-grafted cellulose nanocrystal on toughened PBS/polylactic acid blends. *Carbohydr Polym* 140, 374–382.
- Zhao, Y., Qu, J., Feng, Y., Wu, Z., Chen, F., Tang, H., 2012. Mechanical and thermal properties of epoxidized soybean oil plasticized polybutylene succinate blends. *Polym Adv Technol* 23, 632–638. <https://doi.org/10.1002/pat.1937>
- Zhong, J., Yuan, Z., Lu, C., 2016. Layered-nanomaterial-amplified chemiluminescence systems and their analytical applications. *Anal Bioanal Chem* 408, 8731–8746. <https://doi.org/10.1007/s00216-016-9449-4>

Zhu, N., Ye, M., Shi, D., Chen, M., 2017. Reactive compatibilization of biodegradable poly(butylene succinate)/Spirulina microalgae composites. *Macromol Res* 25, 165–171. <https://doi.org/10.1007/s13233-017-5025-9>

Appendix

A. Canabrava residue treatment



(a)



(b)



(c)



(d)

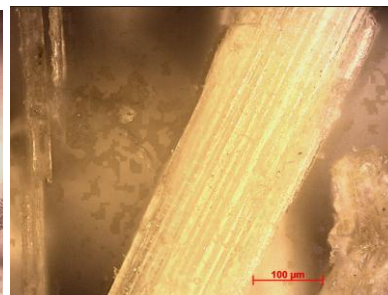
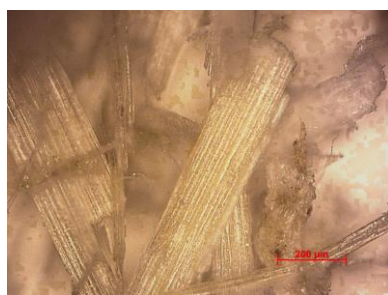


(e)



(f)

(a) Canabrava fiber residue as collected. (b) Crushing machine. (c) Cana fiber crushed. (d) Blender. (e) Sieve. (f) Cana fiber sieved.

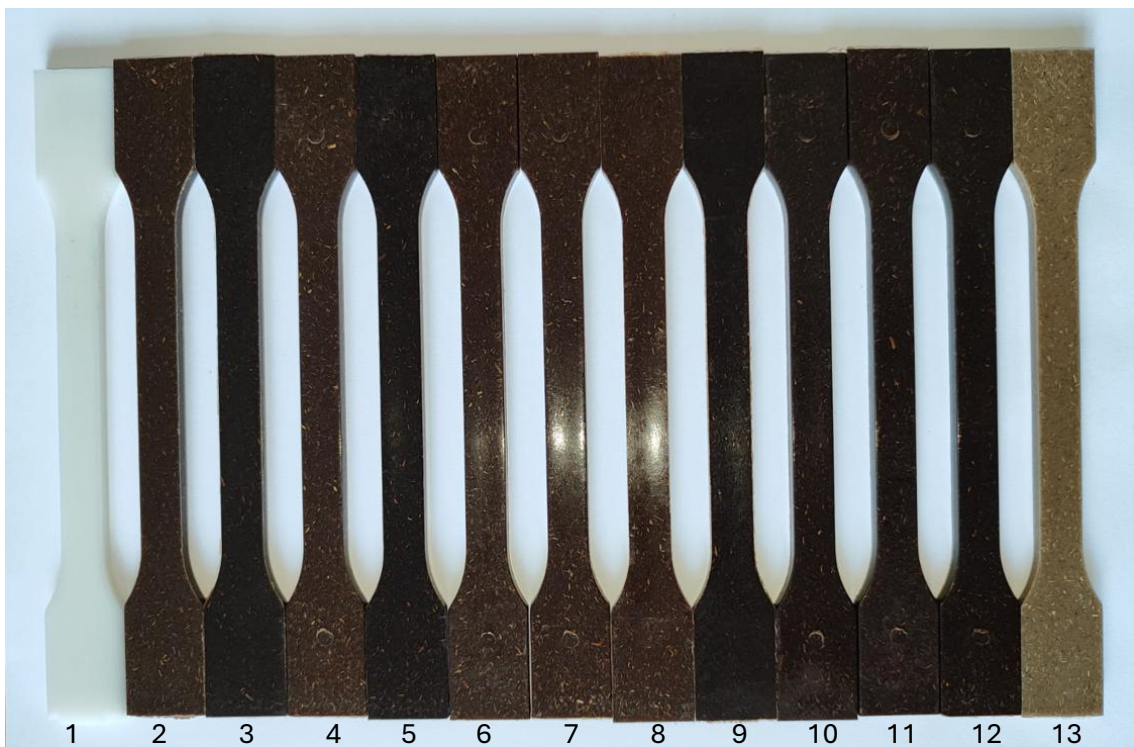


Final Cana fiber size: average length 3.18 ± 1.90 mm and average width 0.45 ± 0.23 mm measured by optical microscopy images and ImageJ (software image analysis), over 1000 measurements.

B. Twin-screw extruder co-rotating, AX.DR16.40 from AX Plásticos (UFBA).



C. Mechanical test specimens (injection molded)



Composite specimens (2nd article) produced by injection molding for tensile, flexural, impact, shore D, density test (before test). 1) Neat PBS. 2) 2PBS-01. 3) 2PBS-02. 4) 2PBS-03. 5) 2PBS-04. 6) 2PBS-05. 7) 2PBS-06. 8) 2PBS-07; 9) 2PBS-08. 10) 2PBS-09. 11) 2PBS-10. 12) 2PBS-11. 13) PBS-30%Caná.

D. Cost reduction estimation

Raw Material Cost Estimation

Exchange rate, 20/7/25	U\$ 1	R\$ 5.58
------------------------	-------	----------

Price	R\$/kg	U\$/kg	Source:
Bio-PBS, FZ-71	54.36	9.74	Mitsubishi Co, 2025
Canabrava	5	0.90	Estimation
Lignina kraft	2.12	0.38	https://www.researchgate.net/figure/Price-of-lignins-and-potential-products-a
Sepiolite Pangel S9	2.51	0.45	https://biotio.en.made-in-china.com/product/rZAGCOUHLbVN/China-High-Pur
Epoxydized Soy Bean	12.3	2.20	https://www.google.com/url?sa=t&source=web&rct=j&opi=89978449&url=http

Bio-composite	Formulation (phr)	Equivalent Weight (g)	Weight to produce 1kg of biocomposite	R\$/kg	U\$/kg
Bio-PBS, FZ-71	100.00	1000	0.65	35.07	6.29
Canabrava	30.00	300.00	0.19	0.97	0.17
Lignina kraft	7.50	75.00	0.05	0.10	0.02
Sepiolite Pangel S9	7.50	75.00	0.05	0.12	0.02
Epoxydized Soy Bean	10.00	100.00	0.06	0.79	0.14
phr: part per hundred of resin				Price per kg =>	
				37.06	6.64

Price comparison, 1kg	R\$/kg	U\$/kg
Bio PBS	54.36	R\$ 9.74
Bio-composite	37.06	R\$ 6.64
% difference	-31.8%	-31.8%

	R\$/kg	
Bio PBS	54.36	
Bio-composite	37.06	
HDPE Green	12.87	https://www.lojapiramidal.com.br/produtos/1385-gf4950-pead-polietileno-s25.aspx
PLA	72.00	https://3dlab.com.br/produto/graos-de-pla-virgem/

E. Canabrava supply

Regarding the viability of Canabrava supply:

Canabrava is a fast-growing grass that develops a dense plant mass. It is non-seasonal (growing continuously throughout the year), propagating both vegetatively through shoots and rhizomes, as well as by wind-dispersed seeds. It commonly grows in riparian zones, lakesides, and even coastal areas (<https://www.biodiversity4all.org/taxa/163471-Gynerium-sagittatum>).

Regarding logistics:

The most efficient approach is to supply Canabrava fiber residue in shredded form, which reduces transport volume, facilitates bagged packaging, and lowers transportation costs. This could be facilitated through the involvement of organizations such as ABECIM (Associação Beneficente Educacional e Cultural de Ilha de Maré), which currently has a basic shredding structure; however, additional equipment, such as a milling unit and a drying oven, may be required.

Regarding available volume:

No specific data on the quantity of Canabrava available in Brazil was found. However, Ferreira et al. (2011) report that the species is native to the Americas and occurs in abundance throughout Brazil—except in Rio Grande do Sul—primarily in humid ravines near rivers, where it forms dense vegetation. (<https://www.alice.cnptia.embrapa.br/alice/bitstream/doc/906725/1/6525.pdf>)

UFBA
UNIVERSIDADE FEDERAL DA BAHIA
ESCOLA POLITÉCNICA

PROGRAMA DE PÓS GRADUAÇÃO EM ENGENHARIA
INDUSTRIAL - PEI

Rua Aristides Novis, 02, 6º andar, Federação, Salvador
BA

CEP: 40.210-630

Telefone: (71) 3283-9800

E-mail: pei@ufba.br

Home page: <http://www.pei.ufba.br>

